WADD TECHNICAL REPORT 60-904

MEASUREMENT OF THERMAL PROPERTIES

I. B. FIELDHOUSE
J. I. LANG

ARMOUR RESEARCH FOUNDATION

JULY 1961

DIRECTORATE OF MATERIALS AND PROCESSES
CONTRACT No. AF 33(616)-6324
PROJECT No. 7381

WRIGHT AIR DEVELOPMENT DIVISION
AIR RESEARCH AND DEVELOPMENT COMMAND
UNITED STATES AIR FORCE
WRIGHT-PATTERSON AIR FORCE BASE, OHIO

McGregor & Werner, Inc., Dayton, O.
500 - November 1961 - 10-345 & 346

FOREWORD

This report was prepared by the Heat and Mass Transfer Section of the Fluid Dynamics and Systems Research Division of the Armour Research Foundation, Chicago, Illinois, under USAF Contract No. AF 33(616)-6324. This contract was initiated under Project No. 7381, "Materials Application", Task No. 73812, "Data Collection and Correlation". The program was administered by the Directorate of Materials and Processes, Deputy for Advanced Systems Technology, Aeronautical Systems Division, with Mr. Hyman Marcus acting as project engineer.

This report covers work carried out from 5 February 1959 to 15 December 1960.

ABSTRACT

The purpose of this investigation has been to measure the thermal conductivity, specific heat, and linear coefficient of thermal expansion of the following materials.

1.	Stainless Steel type 420	ρ = 7.71 g/cc
2.	Stainless Steel type 17-4 PH	ρ = 7.74 g/cc
3.	AM 355	ρ = 7.78 g/cc
4.	Crucible HNM	ρ = 7.67 g/cc
5.	Titanium C110M	ρ = 4.59 g/cc
6.	Inco 713C	ρ = 9.23 g/cc
7.	Haynes Stellite HE 1049	ρ = 8.85 g/cc
8.	Kennametal K161B	ρ = 5.66 g/cc
9.	M252 (GE-J1500) (Solutioned 1950°F, air cooled)	ρ = 8.22 g/cc
10.	Rene 41 (GE-J1610) (Solutioned 1975°F, water quenched)	ρ = 8.08 g/cc
11.	Vanadium Hot rolled, annealed	ρ = 6.05 g/cc
12.	Zirconium	ρ = 6.49 g/cc
13.	Molybdenum Disilicide (Slip cast)	ρ = 5.80 g/cc
14.	Magnesium Oxide	ρ = 2.98 g/cc
15.	Hafnium	ρ = 13.09 g/cc

PUBLICATION REVIEW

This report has been reviewed and is approved.

FOR THE COMMANDER:

Jules I. Wittebort

JULES I. WITTEBORT
Chief, Thermophysics Branch
Physics Laboratory
Materials Central

TABLE OF CONTENTS

		Page
I	INTRODUCTION	1
II	THERMAL CONDUCTIVITY	4
	Apparatus	4
	Test Procedure	4
	Experimental Accuracy	6
	Test Results	6
III	SPECIFIC HEAT	39
	Apparatus	39
	Operating Procedure	42
	Calculation of Enthalpy	43
	Calculation of Specific Heat	43
	Accuracy of Measurements	44
	Calibration of System	45
IV	LINEAR THERMAL EXPANSION	86
	Apparatus	86
	Operating Procedure	86
	Results	88
	Discussion of Experimental Errors	89

LIST OF FIGURES

Figure		Page
1	Stacked Disk Thermal Conductivity Apparatus	7
2	Thermal Conductivity of Stainless Steel 420	24
3	Thermal Conductivity of Stainless Steel 17-4 PH	25
4	Thermal Conductivity of AM 355	26
5	Thermal Conductivity of Crucible HNM	27
6	Thermal Conductivity of Titanium C110M	28
7	Thermal Conductivity of Inco 713C	29
8	Thermal Conductivity of HE 1049	30
9	Thermal Conductivity of Kennametal K161B	31
10	Thermal Conductivity of M252	32
11	Thermal Conductivity of Rene 41	33
12	Thermal Conductivity of Vanadium	34
13	Thermal Conductivity of Zirconium	35
14	Thermal Conductivity of Molybdenum Disilicide	36
15	Thermal Conductivity of Magnesium Oxide	37
16	Thermal Conductivity of Hafnium	38
17	Schematic Diagram of Apparatus for Measuring Specific Heat	40
18	Cross Sectional View of Specific Heat Furnace	41
19	Enthalpy of Stainless Steel Type 420	63
20	Enthalpy of Stainless Steel Type 17-4 PH	64
21	Enthalpy of AM 355	65

Figure		Page
22	Enthalpy of Crucible HNM	66
23	Enthalpy of Titanium C110M	67
24	Enthalpy of Inco 713C	68
25	Enthalpy of HE 1049	69
26	Enthalpy of Kennametal K161B	70
27	Enthalpy of M252	71
28	Enthalpy of Rene 41	72
29	Enthalpy of Vanadium	73
30	Enthalpy of Zirconium	74
31	Enthalpy of Molybdenum Disilicide	75
32	Enthalpy of Magnesium Oxide	76
33	Enthalpy of Hafnium	77
34	Specific Heats of Stainless Steel Types 420 and 17-4 PH	78
35	Specific Heats of AM 355 and Crucible HNM	79
36	Specific Heats of Kennametal K161B and Titanium C110M	80
37	Specific Heats of Inco 713C and Haynes Stellite HE 1049	81
38	Specific Heats of M252 and Rene 41	82
39	Specific Heats of Vanadium and Zirconium	83
40	Specific Heats of Molybdenum Disilicide and Magnesium Oxide	84
41	Specific Heat of Hafnium	85
42	Apparatus for Measuring Linear Thermal Expansion	87
43	Linear Thermal Expansion of Stainless Steel Type 420	105
44	Linear Thermal Expansion of Stainless Steel Type 17-4 PH	106

Figure		Page
45	Linear Thermal Expansion of AM 355	107
46	Linear Thermal Expansion of Crucible HNM	108
47	Linear Thermal Expansion of Titanium C110M	109
48	Linear Thermal Expansion of Inco 713C	110
49	Linear Thermal Expansion of HE 1049.	111
50	Linear Thermal Expansion of Kennametal K161B . . .	112
51	Linear Thermal Expansion of M252	113
52	Linear Thermal Expansion of Rene 41	114
53	Linear Thermal Expansion of Vanadium	115
54	Linear Thermal Expansion of Zirconium	116
55	Linear Thermal Expansion of Molybdenum Disilicide . .	117
56	Linear Thermal Expansion of Magnesium Oxide	118
57	Linear Thermal Expansion of Hafnium	119

LIST OF TABLES

Table		Page
1	Chemical Analyses	3
2	Thermal Conductivity of Armco Iron	8
3	Thermal Conductivity of Stainless Steel 420	9
4	Thermal Conductivity of Stainless Steel 17-4 PH (H900)	10
5	Thermal Conductivity of AM 355	11
6	Thermal Conductivity of Crucible HNM	12
7	Thermal Conductivity of Titanium C110M	13
8	Thermal Conductivity of Inco 713C	14
9	Thermal Conductivity of HE 1049	15
10	Thermal Conductivity of Kennametal K161B	16
11	Thermal Conductivity of M252 (GE-J1500)	17
12	Thermal Conductivity of Rene 41 (GE-J1610)	18
13	Thermal Conductivity of Vanadium	19
14	Thermal Conductivity of Zirconium	20
15	Thermal Conductivity of Molybdenum Disilicide	21
16	Thermal Conductivity of Magnesium Oxide	22
17	Thermal Conductivity of Hafnium	23
18	Enthalpy of Synthetic Sapphire	45
19	Enthalpy Coefficients	46
20	Specific Heat Coefficients	47
21	Enthalpy Values for Stainless Steel Type 420	48
22	Enthalpy Values for Stainless Steel Type 17-4 PH	49

Table		Page
23	Enthalpy Values for AM 355	50
24	Enthalpy Values for Crucible HNM	51
25	Enthalpy Values for Titanium C110M	52
26	Enthalpy Values for Inco 713C	53
27	Enthalpy Values for HE 1049	54
28	Enthalpy Values for Kennametal K161B	55
29	Enthalpy Values for M252 (GE-J1500)	56
30	Enthalpy Values for Rene 41 (GE-J1610)	57
31	Enthalpy Values for Vanadium	58
32	Enthalpy Values for Zirconium	59
33	Enthalpy Values for Molybdenum Disilicide	60
34	Enthalpy Values for Magnesium Oxide	61
35	Enthalpy Values for Hafnium	62
36	Calibration of Optical System	88
37	Linear Thermal Expansion Measurements for Stainless Steel Type 420	90
38	Linear Thermal Expansion Measurements for Stainless Steel Type 17-4 PH (H900)	91
39	Linear Thermal Expansion Measurements for AM 355	92
40	Linear Thermal Expansion Measurements for Crucible HNM	93
41	Linear Thermal Expansion Measurements for Titanium C110M	94
42	Linear Thermal Expansion Measurements for Inco 713C	95
43	Linear Thermal Expansion Measurements for HE 1049	96

Table		Page
44	Linear Thermal Expansion Measurements for Kennametal K161B	97
45	Linear Thermal Expansion Measurements for M252 . .	98
46	Linear Thermal Expansion Measurements for Rene 41 .	99
47	Linear Thermal Expansion Measurements for Vanadium .	100
48	Linear Thermal Expansion Measurements for Zirconium	101
49	Linear Thermal Expansion Measurements for Molybdenum Disilicide	102
50	Linear Thermal Expansion Measurements for Magnesium Oxide	103
51	Linear Thermal Expansion Measurements for Hafnium .	104

MEASUREMENT OF THERMAL PROPERTIES

INTRODUCTION

The purpose of this investigation has been to measure the thermal conductivity, specific heat and linear coefficient of thermal expansion of the following materials:

1. Stainless Steel type 420
2. Stainless Steel type 17-4 PH
3. AM 355
4. Crucible HNM
5. Titanium C110M
6. Inco 713C
7. Haynes Stellite HE 1049
8. Kennametal K161B
9. M252 (GE-J1500)
10. Rene 41 (GE-J1610)
11. Vanadium
12. Zirconium
13. Molybdenum Disilicide
14. Magnesium Oxide
15. Hafnium

The chemical analysis of these materials is given in Table 1.

The report is divided into three sections, and each section is devoted to the measurement of a particular thermal property.

Thermal conductivity was determined by using the radial heat flow method developed by R. W. Powell. This method consists of measuring, during steady state, the radial flow and radial temperature drop in a vertical stack of disks composed of the material whose thermal conductivity is to be measured. The equipment was calibrated by determining the thermal conductivity of Armco iron. The results agreed closely with accepted values.

Specific heat was measured by means of the method of mixtures. The sample in the form of a cylinder was suspended in a constant temperature furnace until it reached the temperature of the furnace. It was then dropped into a modified Parr adiabatic calorimeter. This resulted in data of enthalpy as a function of temperature. Specific heat, as a function of temperature, was then calculated by fitting an equation to this data and differentiating the equation.

Manuscript released by authors 15 November 1960 for publication as a WADD Technical Report.

Linear thermal expansion was determined by measuring the distance between two recrystallized alumina pins mounted in a rod of the material to be evaluated which was placed in a constant temperature furnace.

It is our hope that this work will help in filling the void in the literature on high temperature thermal properties.

Table 1

CHEMICAL ANALYSES

Material	Per cent of listed element								
	Fe	C	Ni	P	Cr	Mo	Si	Mn	Others
Stainless Steel 420		0.30	0.50	0.02	13.10	0.06	0.41	0.48	0.12 Cu, 0.011 S
Stainless Steel 17-4 PH	72.9*	0.07	4.2	0.04	16.4		1.00	1.00	4.1 Cu, 0.30 Cb + Ta
AM 355	75.5*	0.12	4.27	0.02	15.66	2.82	0.05	0.94	
Crucible HNM	68*	0.30	9.5	0.23	18.5	trace	0.05	3.50	trace of Al and W
Titanium C110M		0.03						7.9	91.81Ti, 0.01 W, 0.15 O
Inco 713C	5.0	0.20	71.53*		11.0	3.5	1.0	1.0	6.5 Al, 0.25 Ti, 1.0 Cb + Ta
HE 1049	3.0	0.40	10.0		26.0		0.8	0.8	15.0 W, 43.6 Cu*, 0.4 Boron
Kennametal K161B**			16.7			3.3			
M252	<0.30	0.12	57.15*		18.65	9.98	0.06	0.07	1.17 Al, 2.74 Ti, 9.75 Cu
Rene 41	1.54	0.11	54.60*		18.60	9.63	0.07	0.08	1.49 Al, 3.14 Ti, 10.73 Cu
Vanadium	0.048	0.042							99.74 Vanadium, 0.043 N, 0.073 O
Zirconium	0.029	0.017							99.95 Zirconium, 0.0045 Hafnium, all other elements < 0.031
Molybdenum Disilicide						61.5-63.5	35-37		
Magnesium Oxide							<0.5	<0.3	> 99 MgO
Crystal bar Hafnium									99 Hafnium, 1 max Zr, 0.1 max Ti & Si, 0.01 max Fe, V & Zn, 0.001 max Mn, Ni & Cu, 0.0001 max Mg

* By difference.

** TiC 72%, CbC 6% CbC added as a solid solution of CbC, TaC, TiC, 90% of added solid solution is CbC

THERMAL CONDUCTIVITY

APPARATUS

The radial heat flow method developed by R. W. Powell[1] was used to measure the thermal conductivity of the test specimens. With this method, the radial heat flow and radial temperature drop was measured in a vertical stack of disks composed of the material whose thermal conductivity was to be determined. More specifically, the disks were in the form of annular rings and radial heat flow through the disks was supplied by an electric heater centered in the axial hole of the stacked disks. In order to obtain high temperatures as well as to control the temperature gradient in the test specimens, the column of stacked disks was placed in an electrically heated furnace in which a helium atmosphere was maintained. The radial heat flow through a section of the stacked disks three inches long, 1.5 inches above and below the vertical center of the column, was derived from measurement of the current and voltage-drop along a three-inch length of the axial heater adjacent to the test section. The temperature gradient was measured by means of thermocouples inserted in small vertical holes, one near the axial hole containing the heater and the other near the outer edge of the disks. The thermal conductivity of the disk material was calculated under steady state conditions from the power input, the radial distance of the inner and outer thermocouples from the axis of the disks, and the temperature difference between these holes. A section through the apparatus which was used is shown in Figure 1.

TEST PROCEDURE

Each set of test specimens contained 5 one-inch diameter disks. As shown in Figure 1, four holes were located in each disk to permit insertion of thermocouples. Platinum, platinum-10% rhodium thermocouples protected by pure alumina tubing were used for measuring temperatures below 3000°F. Above 3000°F iridium, 60% iridium-40% rhodium thermocouples were used. The thermocouples were connected so that the temperature difference as well as the temperature level could be measured. With respect to the thermocouples, the accuracy of the final results depends primarily on the calibration accuracy of each couple relative to the others, and only reasonable accuracy is required as to absolute temperature measurement. The couples were calibrated relative to each other and checked within 0.1°F. The thermocouples were moved up and down so that a temperature traverse along the length of the samples would be made. It was necessary to measure the axial temperature distribution in order to determine if any heat was flowing in the axial direction. Axial heat flow would introduce an error since it was assumed in the calculations that the heat

* * * * * *

1. Powell, R. W. "Proceedings of the Physical Society", London. Vol. 46, pp 659-674, 1934.

flow in the three center disks was in the radial direction only. One reason for using disks rather than a single cylinder was that the poor thermal contact between disks offers considerable resistance to axial heat flow. In order to further insure that axial heat flow would not occur, molybdenum wound heaters were placed at both ends of the test specimens.

In performing the experimental measurements, the axial temperature gradient between the vertical center and the ends of the stack was less than 1°F. The radial temperature difference between the inner and outer thermocouples was maintained at 25°F over the entire mean temperature range at which the measurements were made. This radial temperature difference was identical on both sides of the axis.

The radial heat flow through the test specimens was accomplished by a molybdenum coil wound on a ceramic core and centered in the axial hole of the stacked disks. As shown in Figure 1, the stacked disks were placed in a ceramic tube which had a molybdenum coil wound around the outer surface. The outer heater provided the energy needed to raise the temperature of the sample, while the inner heater provided a means of varying the temperature drop through the sample. The 3 one-inch thick samples located in the center of the stack were considered as the test section, and the current and voltage-drop of the inner heater was measured over this three-inch length. The outer heater was surrounded by bubble alumina insulation and a water-cooled steel housing. The apparatus was purged with helium to provide an inert atmosphere.

The thermal conductivity was calculated by the following equation:

$$k = \frac{Q \ln r_2/r_1}{2\pi L (\Delta t)} \qquad (1)$$

where

k = thermal conductivity, Btu hr^{-1} ft^{-1} $°F^{-1}$

Q = radial heat flow, Btu hr^{-1}

L = length of test section, ft

r_1 = radial distance from axis to inner thermocouple, ft

r_2 = radial distance from axis to outer thermocouple, ft

Δt = temperature drop over the radial distance between thermocouples, °F

EXPERIMENTAL ACCURACY

The preliminary tests were made using Armco iron test specimens in order to confirm the accuracy of the apparatus. The results of these experiments are given in Table 2.[2] These results compare quite well with the results obtained by Powell [2] who felt that the error in his measurements was less than 2%.

Errors in measurement may result from misalignment of the inner and outer heaters, variation in the resistance of the inner heater wire, location of the thermocouples, etc. Because of the close agreement with Powell's data on Armco iron and the small spread in experimental data, it is felt that the accuracy of our results is within 5%.

TEST RESULTS

The experimental test results are shown in Tables 3 through 17, and in Figures 2 through 16.

* * * * * *

2. Powell, R.W. "Proceedings of the Physical Society", London. Vol. 50, p 407, 1938.

Furnace Details

1 Furnace shell

2 Insulation space

3 Current leads to end and main guard heaters

4 Zirconia or graphite support ring

5 End flanges, top & bottom

6 Thermocouple leads

7 Voltage tap leads

8 Central heater leads

9 End guard heaters, top & bottom

10 Main guard heater

11 Test samples

12 Central heater

13 Helium inlet

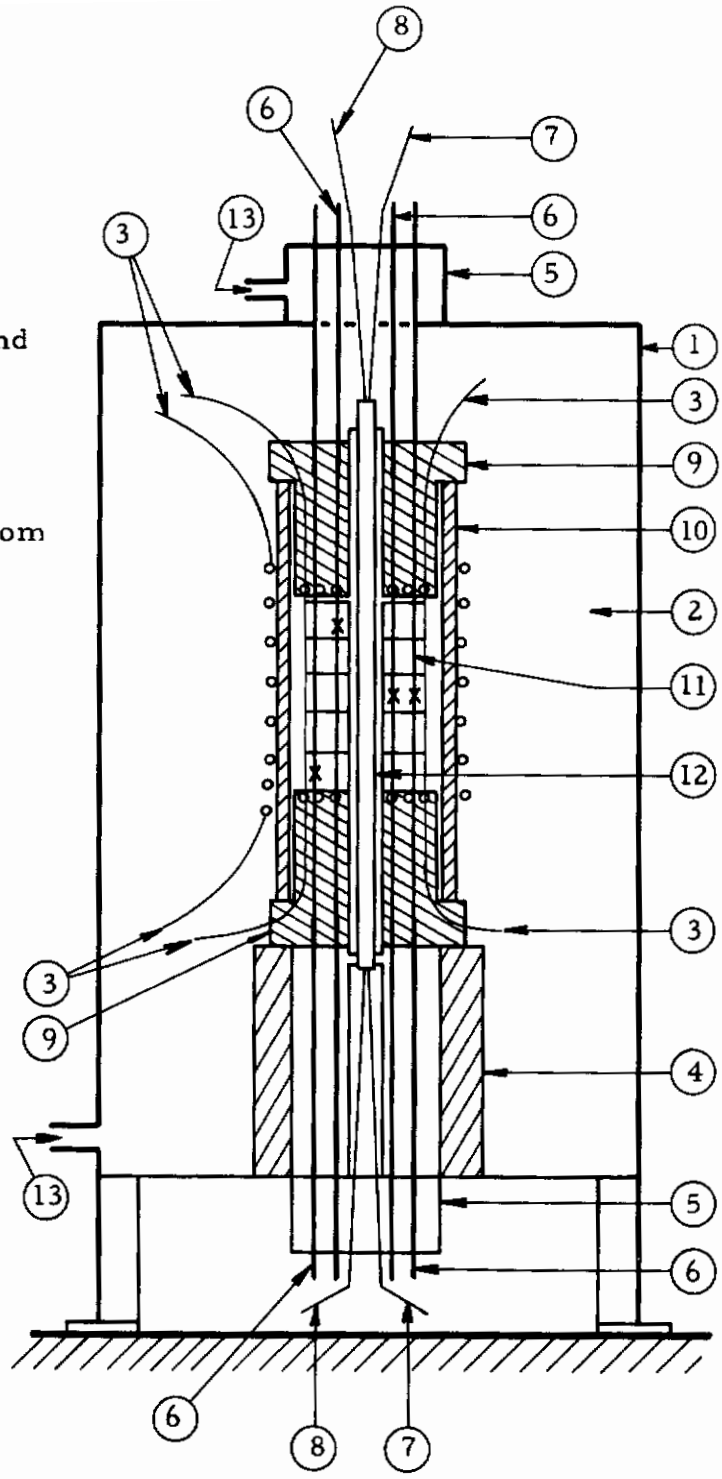

Figure 1 STACKED DISK THERMAL CONDUCTIVITY APPARATUS

Table 2

THERMAL CONDUCTIVITY OF ARMCO IRON

Mean temperature, °F	Thermal conductivity, Btu hr^{-1} ft^{-1} $°F^{-1}$	
	Armour Research	Powell*
141.0	40.1	--
212.0	--	39.5
351.6	36.1	--
392.0	--	35.6
572.0	--	32.0
664.6	29.6	--
752.0	--	28.1
932.0	--	25.0
973.7	24.2	--
995.0	--	24.0
1112.0	--	22.5
1235.8	19.8	--
1292.0	--	19.8
1472.0	--	17.2
1496.0	--	16.9
1562.3	17.0	--
1615.0	--	16.1
1652.0	--	16.0
1832.0	--	16.2
1870.0	17.2	--
2140.9	17.4	--
2398.1	17.8	--
2507.1	18.1	--

* Powell, R.W. "Proceedings of the Physical Society", London, Vol. 50, p 407, 1938.

Table 3

THERMAL CONDUCTIVITY OF STAINLESS STEEL 420

Mean temperature, °F	Thermal conductivity, Btu hr^{-1} ft^{-1} $°F^{-1}$
324	13.11
516	13.39
682	13.93
790	14.00
885	14.28
943	14.19
1037	14.40
1291	15.21
1407	15.33
1692	15.68
1915	16.50
2087	16.72
2250	16.76
2477	17.58

Table 4

THERMAL CONDUCTIVITY OF PH 17-4 (H900)

Mean temperature °F	Thermal conductivity Btu hr^{-1} ft^{-1} $°F^{-1}$
216	6.51
491	8.00
654	9.14
918	11.02
1215	12.66
1411	13.63
1633	14.61
1779	15.20
2071	16.45
2246	17.17
2543	18.20

Table 5

THERMAL CONDUCTIVITY OF AM355

Mean temperature °F	Thermal conductivity Btu hr^{-1} ft^{-1} $°F^{-1}$
110	8.91
273	9.64
466	10.30
681	11.02
972	12.11
1282	13.74
1577	14.86
1651	15.20
1946	16.15
2253	17.11
2462	17.63

Table 6

THERMAL CONDUCTIVITY OF CRUCIBLE HNM

Mean temperature °F	Thermal conductivity Btu hr^{-1} ft^{-1} $°F^{-1}$
211	8.78
437	9.92
669	11.58
987	13.26
1266	15.19
1407	16.06
1647	16.95
1951	18.83
2163	19.81
2237	20.09

Table 7

THERMAL CONDUCTIVITY OF TITANIUM - C110M

Mean temperature °F	Thermal conductivity Btu hr^{-1} ft^{-1} $°F^{-1}$
501	4.94
550	5.13
755	5.30
1005	5.72
1211	6.00
1340	6.26
1432	6.57
1496	6.80
1641	7.75
1740	8.60
1798	9.13
1962	10.56
2143	12.20

Table 8

THERMAL CONDUCTIVITY OF INCO 713C

Mean temperature °F	Thermal conductivity Btu hr^{-1} ft^{-1} $°F^{-1}$
415	7.00
512	7.34
771	8.92
982	10.00
1342	12.35
1601	13.91
1830	14.98
2062	16.51
2242	17.54

Table 9

THERMAL CONDUCTIVITY OF HE 1049

Mean temperature, °F	Thermal conductivity Btu hr^{-1} ft^{-1} $°F^{-1}$
327	8.09
562	9.39
749	11.00
917	12.03
1090	12.96
1233	14.03
1467	15.51
1682	17.00
1947	19.03

Table 10

THERMAL CONDUCTIVITY OF KENNAMETAL K161B

Mean temperature, °F	Thermal conductivity, Btu hr^{-1} ft^{-1} $°F^{-1}$
296	12.82
415	11.73
737	9.03
984	7.14
1116	5.78
1398	4.25
1583	3.91
1806	3.44
2251	3.10
2509	2.75
2794	2.40
2960	2.38
3251	2.22

Table 11

THERMAL CONDUCTIVITY OF M252
(GE-J 1500)

Mean temperature °F	Thermal conductivity Btu hr^{-1} ft^{-1} $°F^{-1}$
235	5.75
624	8.20
784	9.17
919	10.00
1111	11.20
1326	12.55
1532	13.90
1801	15.40
2109	17.60

Table 12

THERMAL CONDUCTIVITY OF RENE 41
(GE-J 1610)

Mean temperature °F	Thermal conductivity Btu hr^{-1} ft^{-1} $°F^{-1}$
271	7.03
594	8.49
896	9.68
1174	11.30
1330	12.15
1449	12.73
1722	13.90
2046	15.45
2303	16.20
2451	17.33

Table 13

THERMAL CONDUCTIVITY OF VANADIUM

Mean temperature °F	Thermal conductivity Btu hr^{-1} ft^{-1} $°F^{-1}$
302	18.70
516	19.62
698	20.00
845	20.63
1013	21.12
1065	21.34
1194	21.80
1329	22.23
1500	22.90
1633	23.35
1721	23.94
1835	24.31
2046	25.06
2312	26.14
2630	27.45
2916	28.61

Table 14

THERMAL CONDUCTIVITY OF ZIRCONIUM

Mean temperature °F	Thermal conductivity Btu hr^{-1} ft^{-1} $°F^{-1}$
411	12.62
571	11.93
666	11.70
863	11.67
1002	12.45
1191	12.96
1542	14.62
1800	15.50
2038	16.33
2163	16.58
2506	17.42
2749	17.80
3006	18.41

Table 15

THERMAL CONDUCTIVITY
OF MOLYBDENUM DISILICIDE

Mean temperature °F	Thermal conductivity Btu hr^{-1} ft^{-1} $°F^{-1}$
327	23.51
516	21.64
793	18.73
1015	15.89
1282	13.57
1528	11.74
1801	10.02
2135	8.82
2462	6.83
2803	6.32
3021	6.63
3245	6.97

Table 16

THERMAL CONDUCTIVITY OF MAGNESIUM OXIDE

Mean temperature °F	Thermal conductivity Btu hr^{-1} ft^{-1} $°F^{-1}$
400	14.30
602	11.32
806	8.93
972	7.75
1197	6.42
1603	4.63
1991	3.86
2409	3.25
2810	3.97
3217	5.21
3615	8.06

Table 17

THERMAL CONDUCTIVITY OF HAFNIUM

Mean temperature, °F	Thermal conductivity, Btu hr^{-1} ft^{-1} $°F^{-1}$
262	13.05
867	12.25
1062	11.93
1683	11.44
2290	11.04
2920	10.90

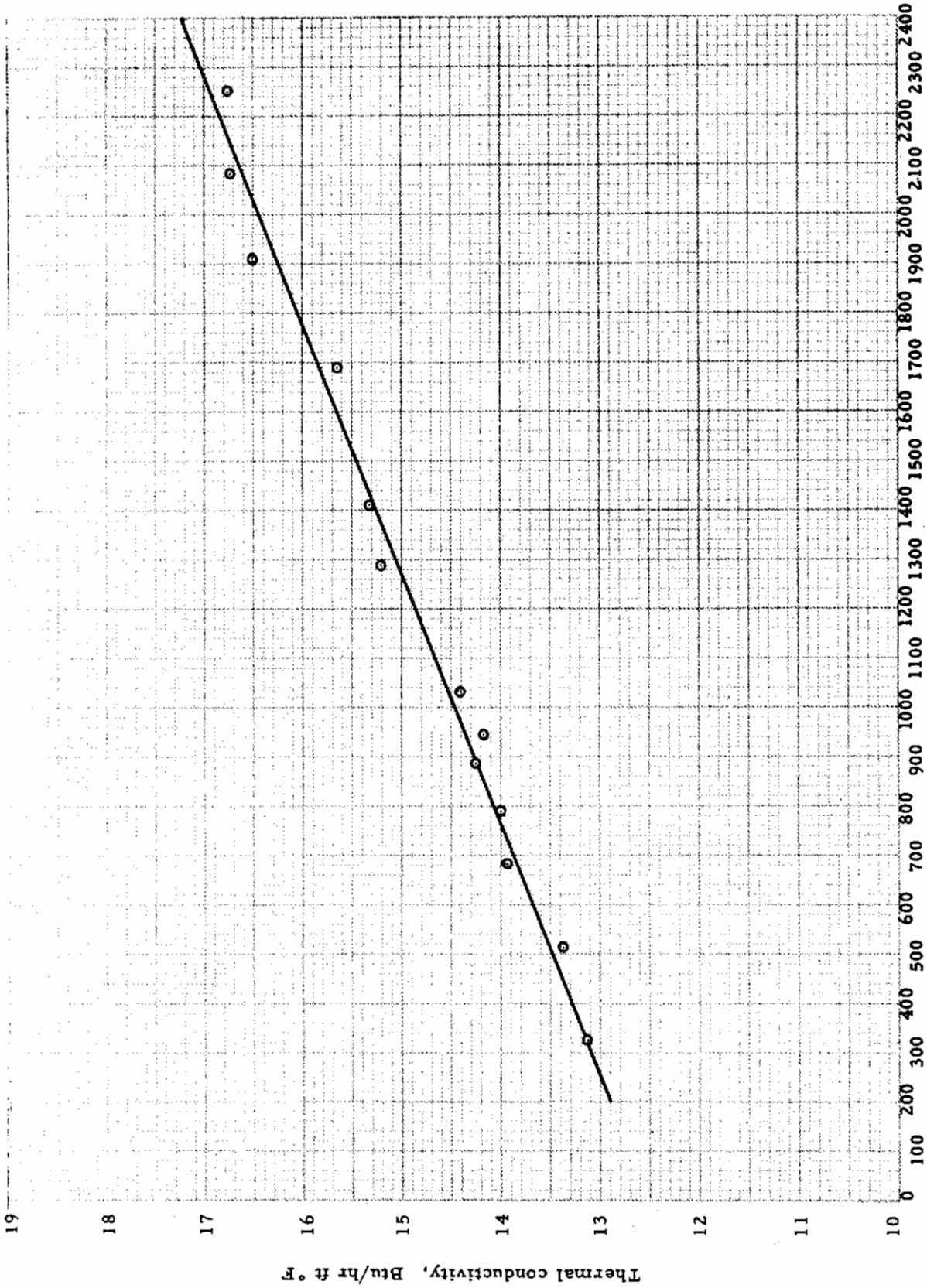

Figure 2 THERMAL CONDUCTIVITY OF STAINLESS STEEL 420

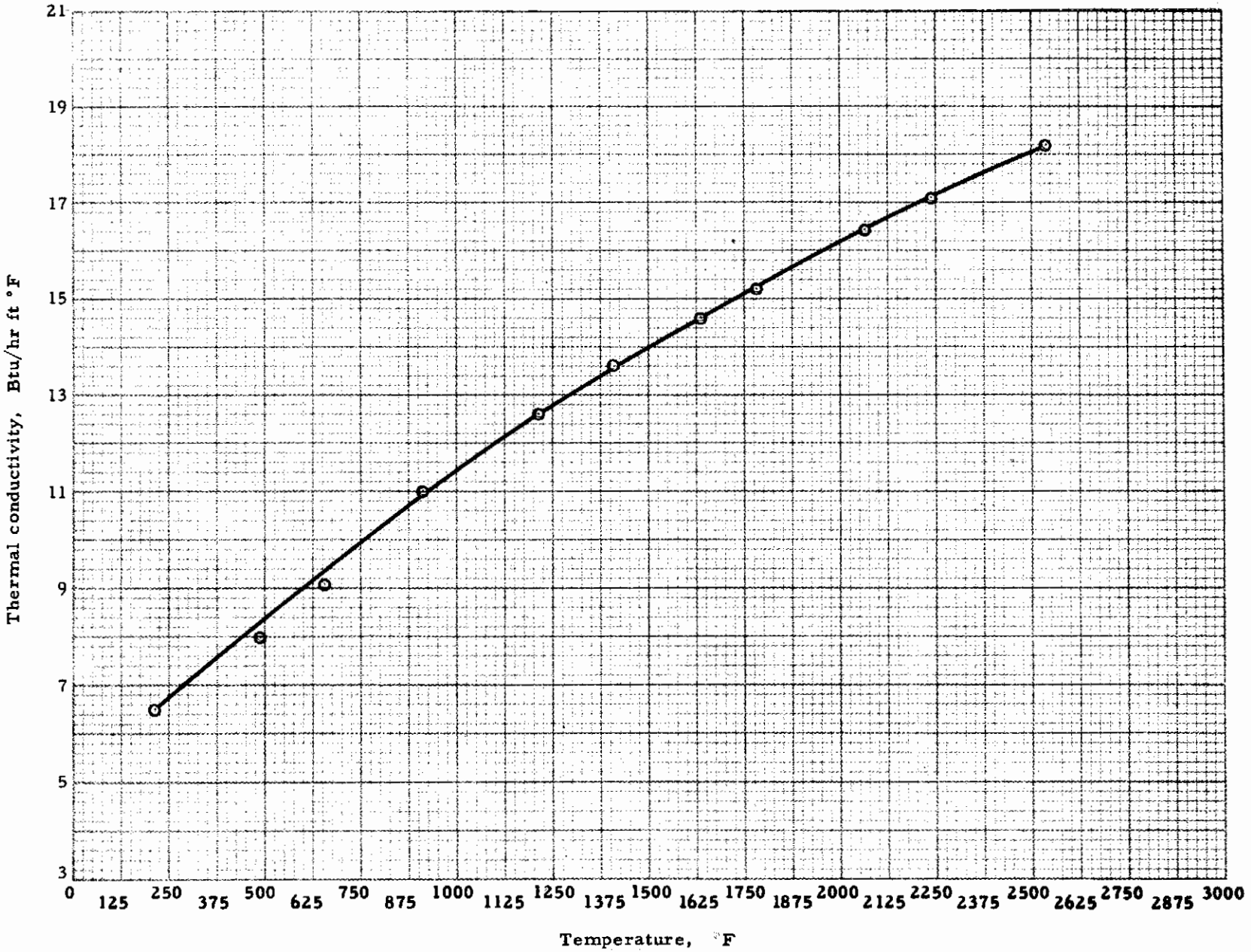

Figure 3 THERMAL CONDUCTIVITY OF STAINLESS STEEL 17-4 PH

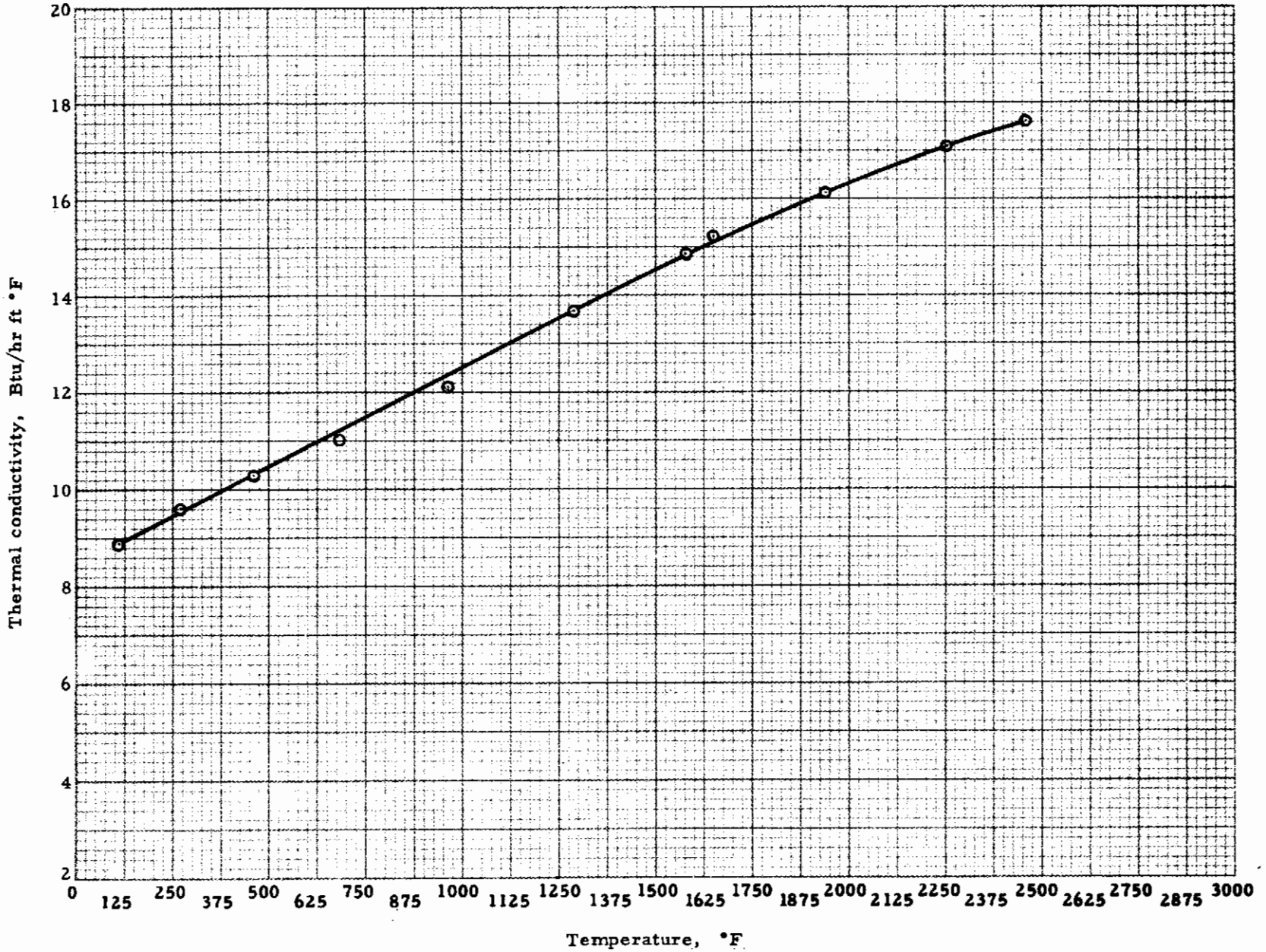

Figure 4 THERMAL CONDUCTIVITY OF AM 355

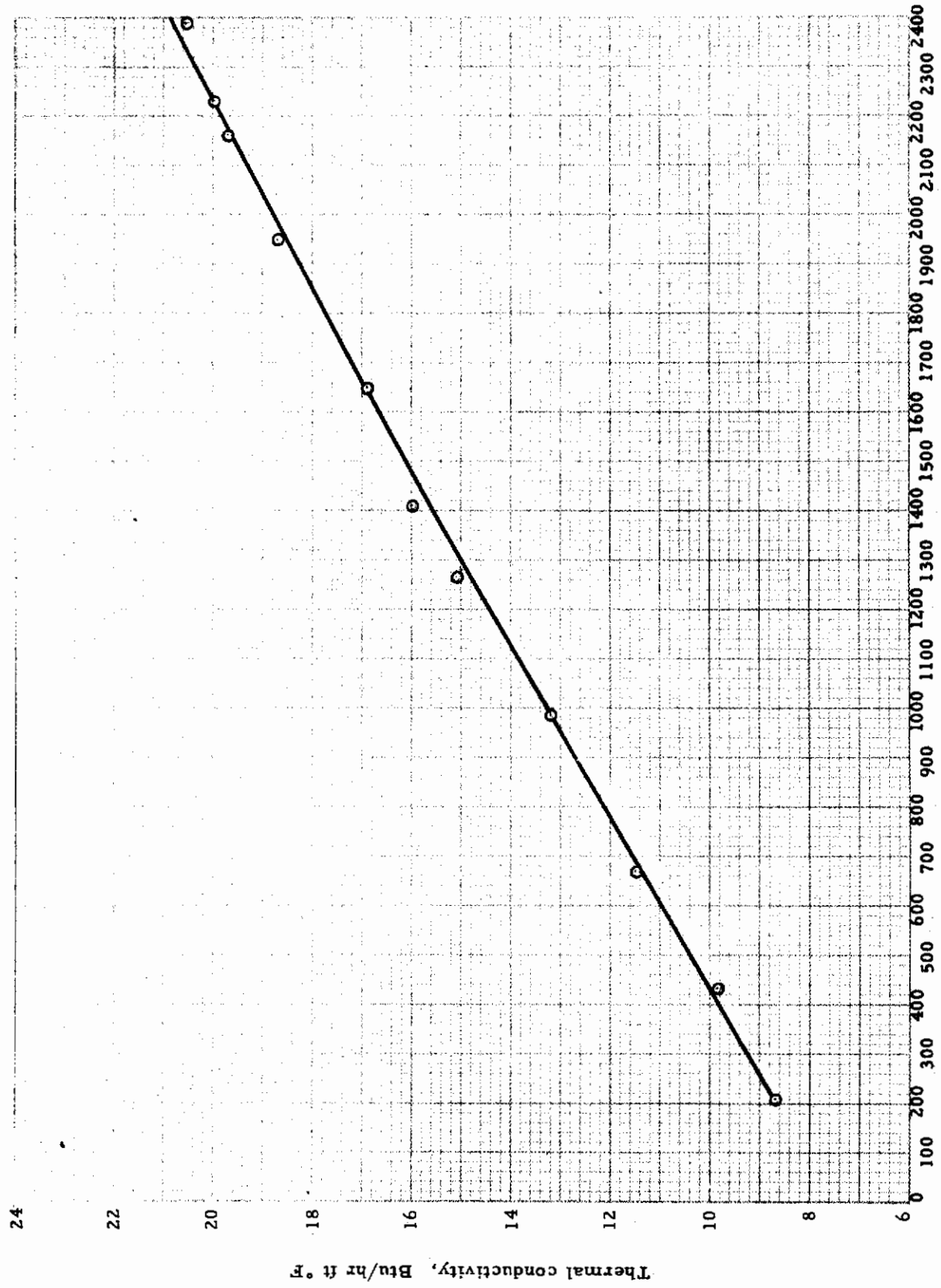

Figure 5 THERMAL CONDUCTIVITY OF CRUCIBLE HNM

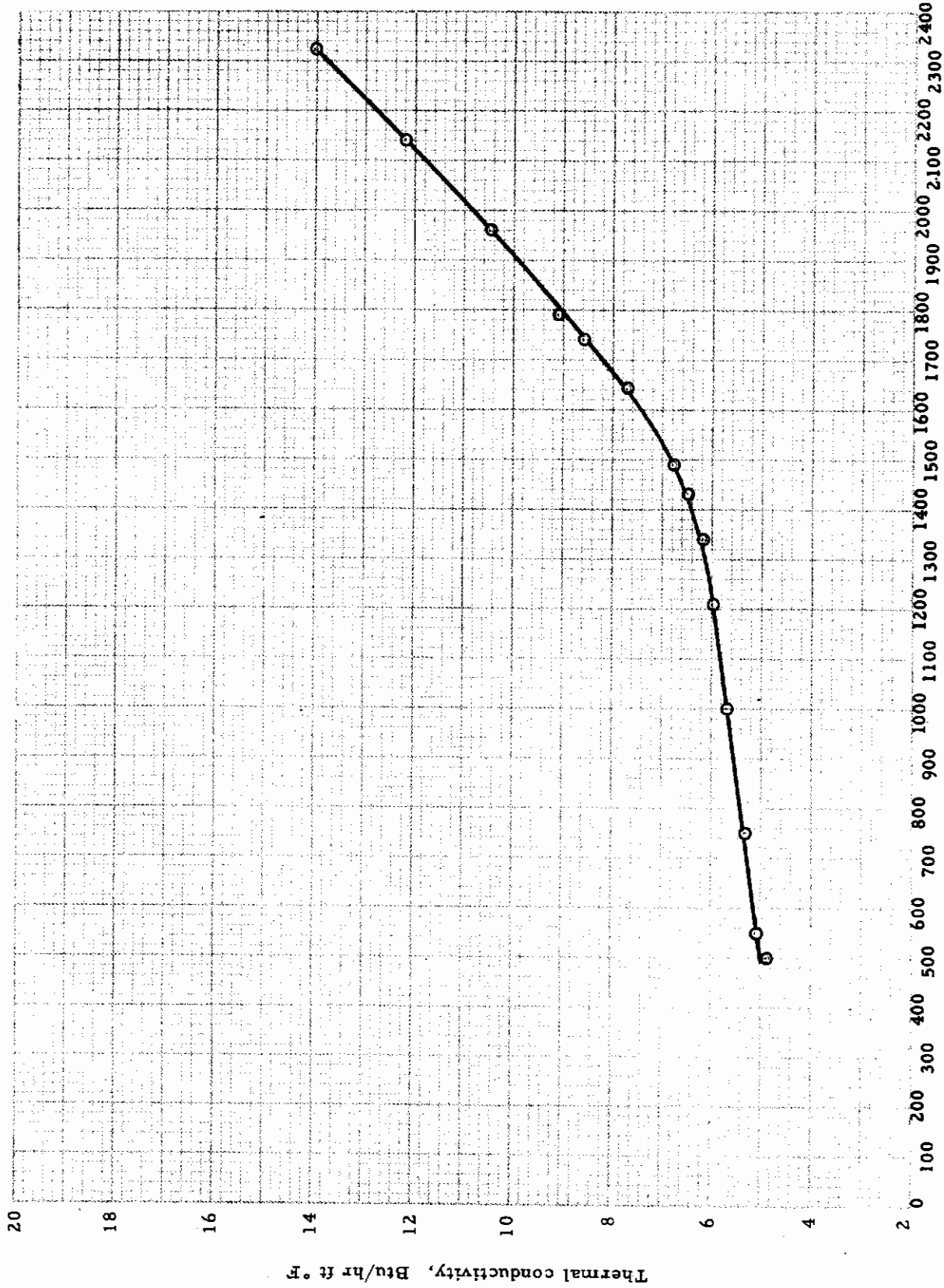

Figure 6 THERMAL CONDUCTIVITY OF TITANIUM C110M

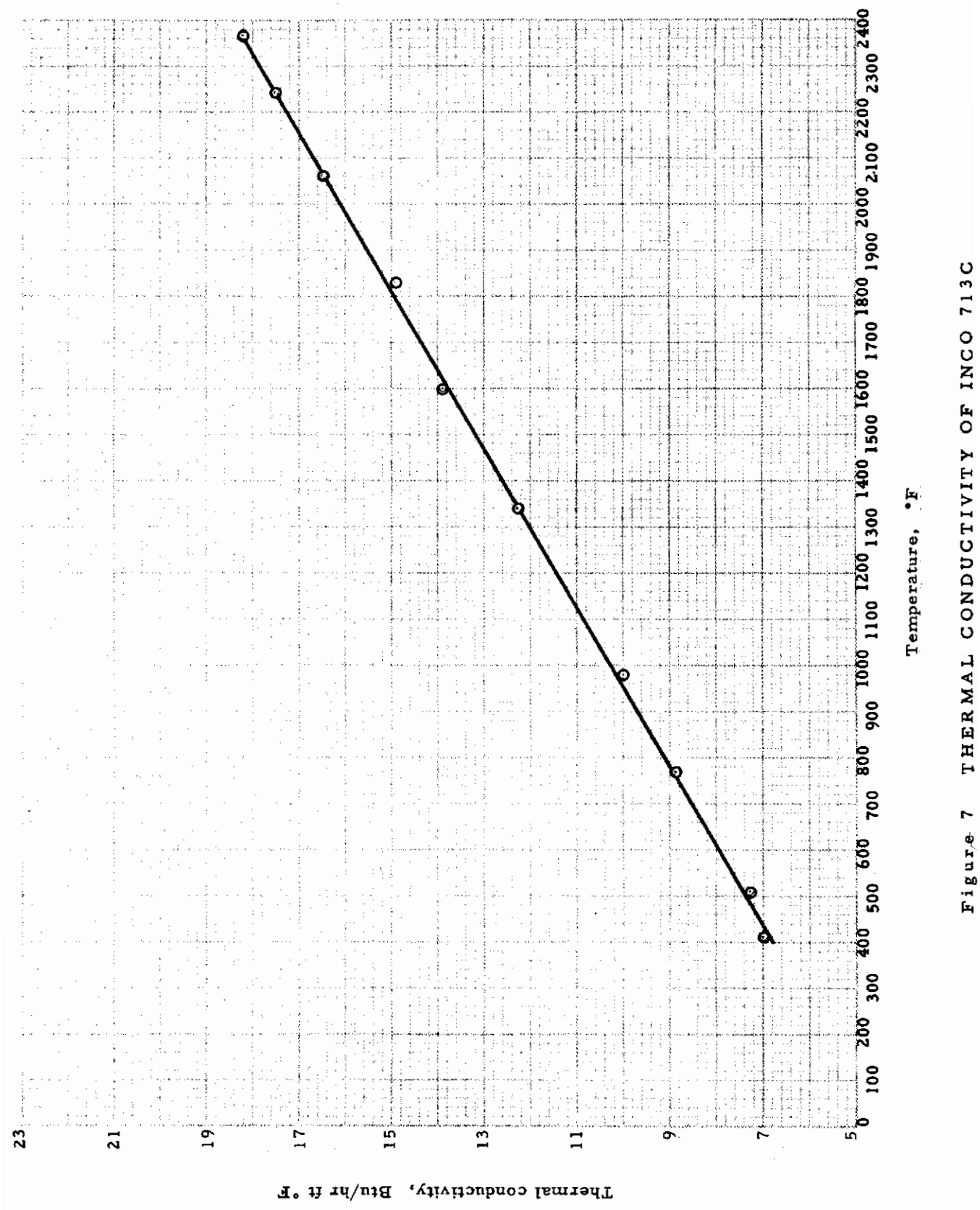

Figure 7 THERMAL CONDUCTIVITY OF INCO 713C

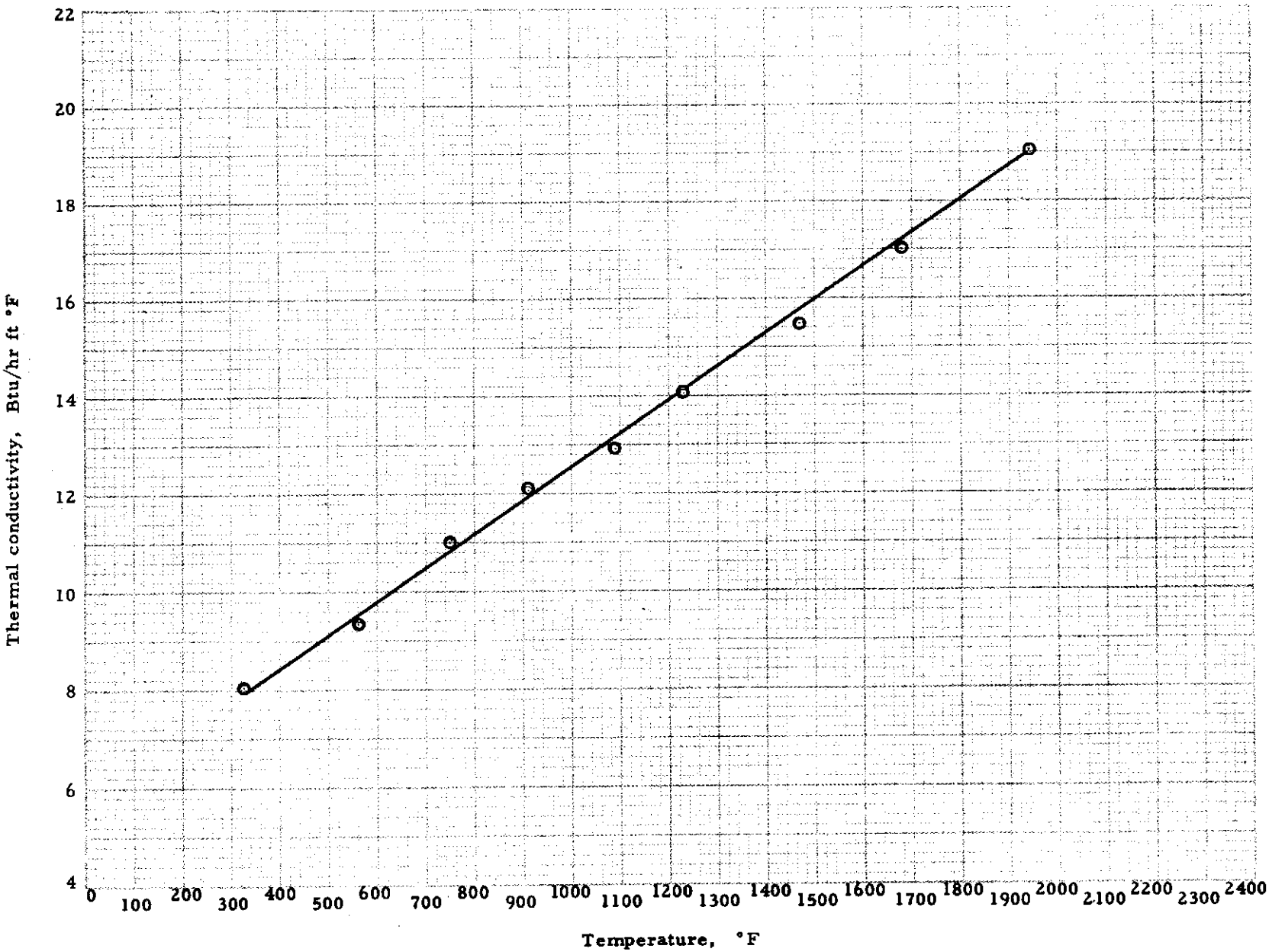

Figure 8 THERMAL CONDUCTIVITY OF HE 1049

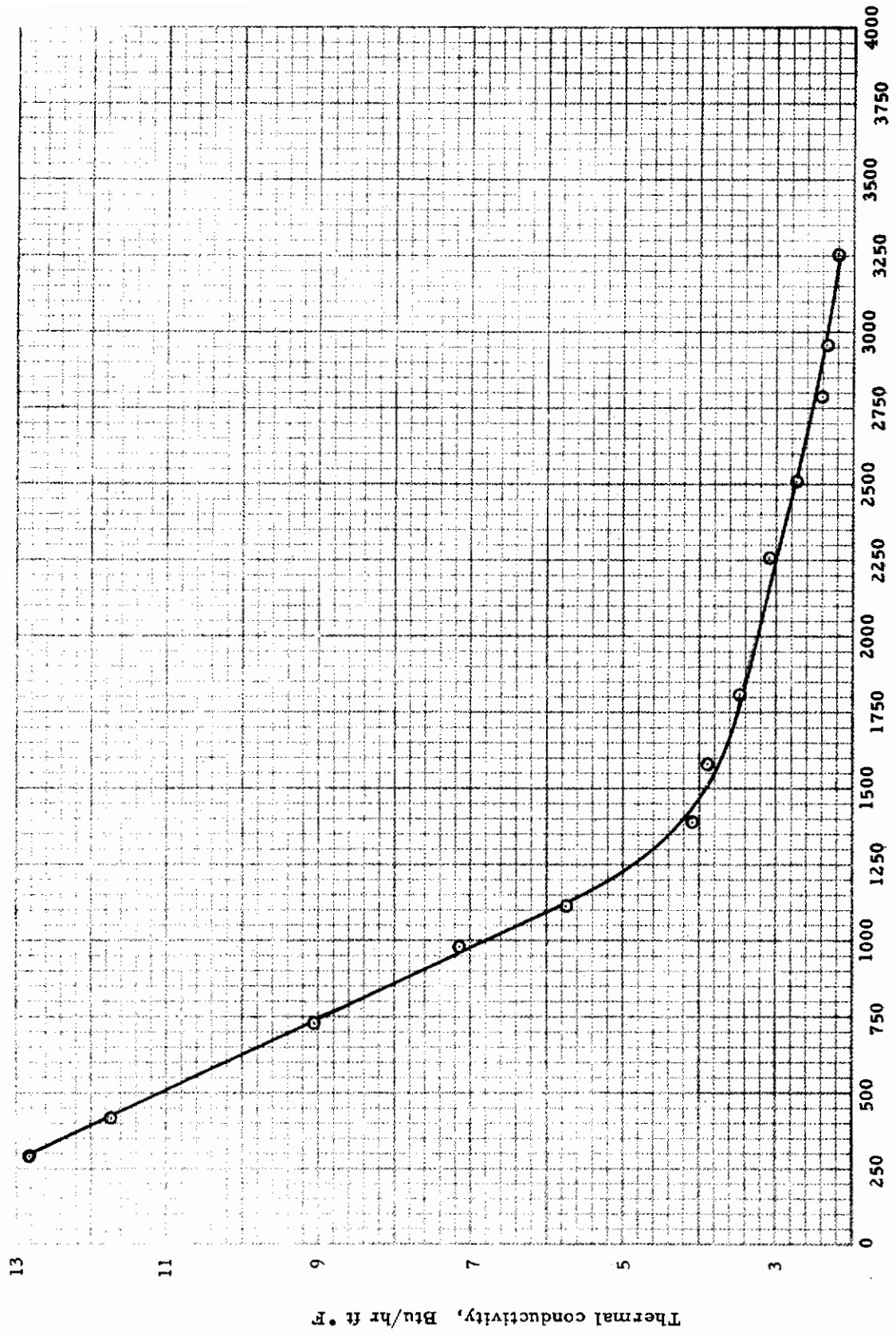

Figure 9 THERMAL CONDUCTIVITY OF KENNAMETAL K161B

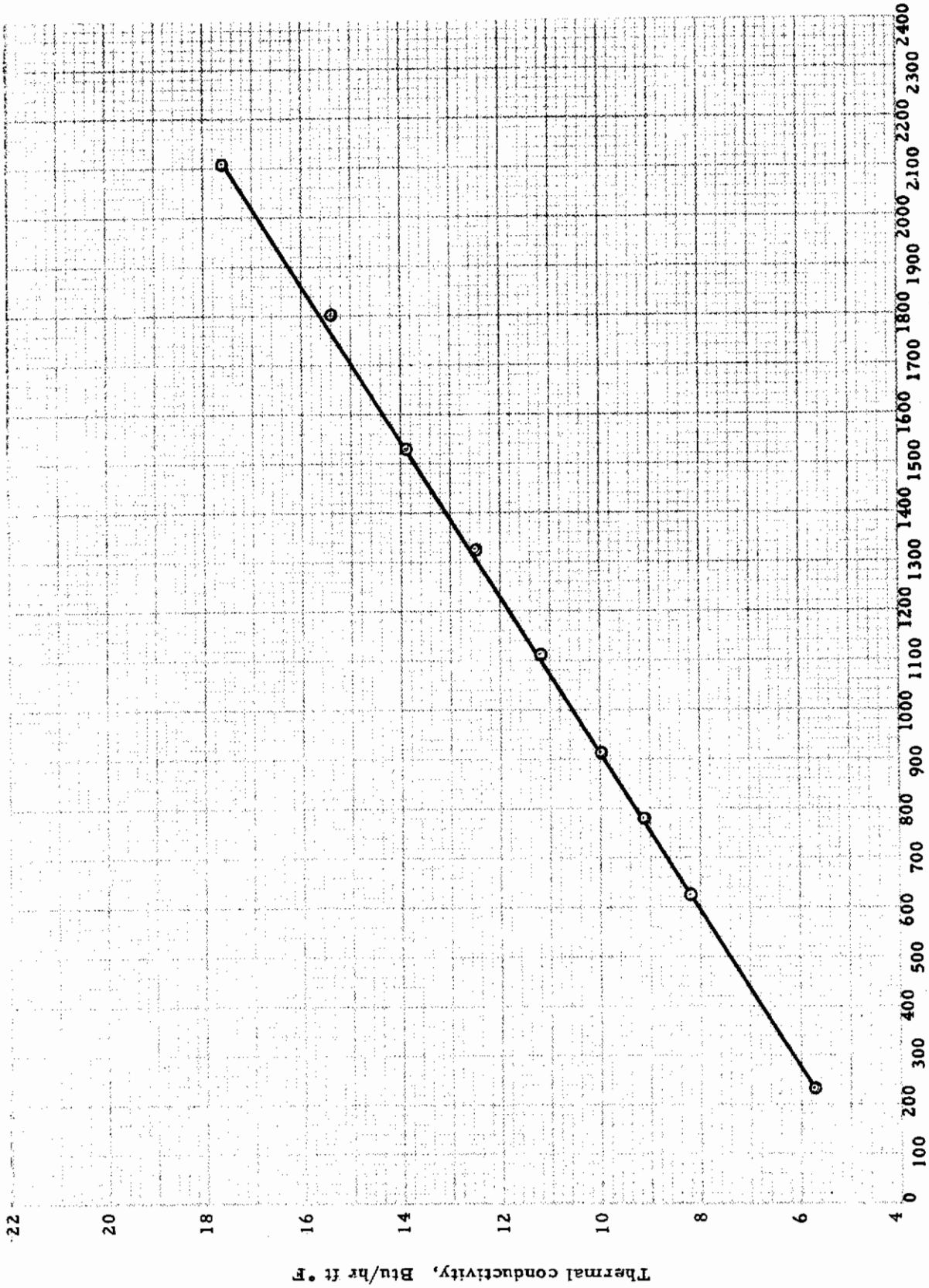

Figure 10 THERMAL CONDUCTIVITY OF M252

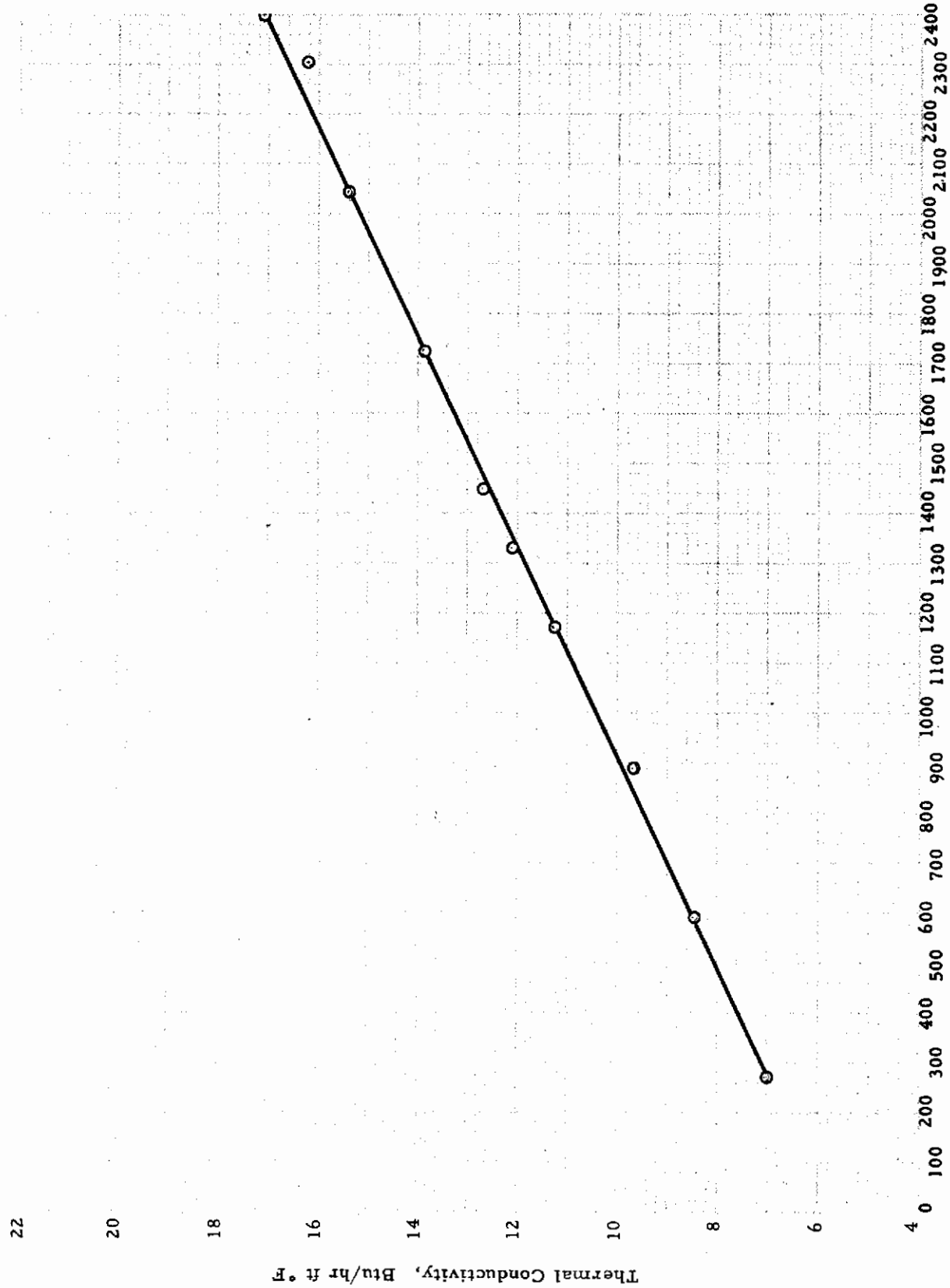

Figure 11 THERMAL CONDUCTIVITY OF RENE 41

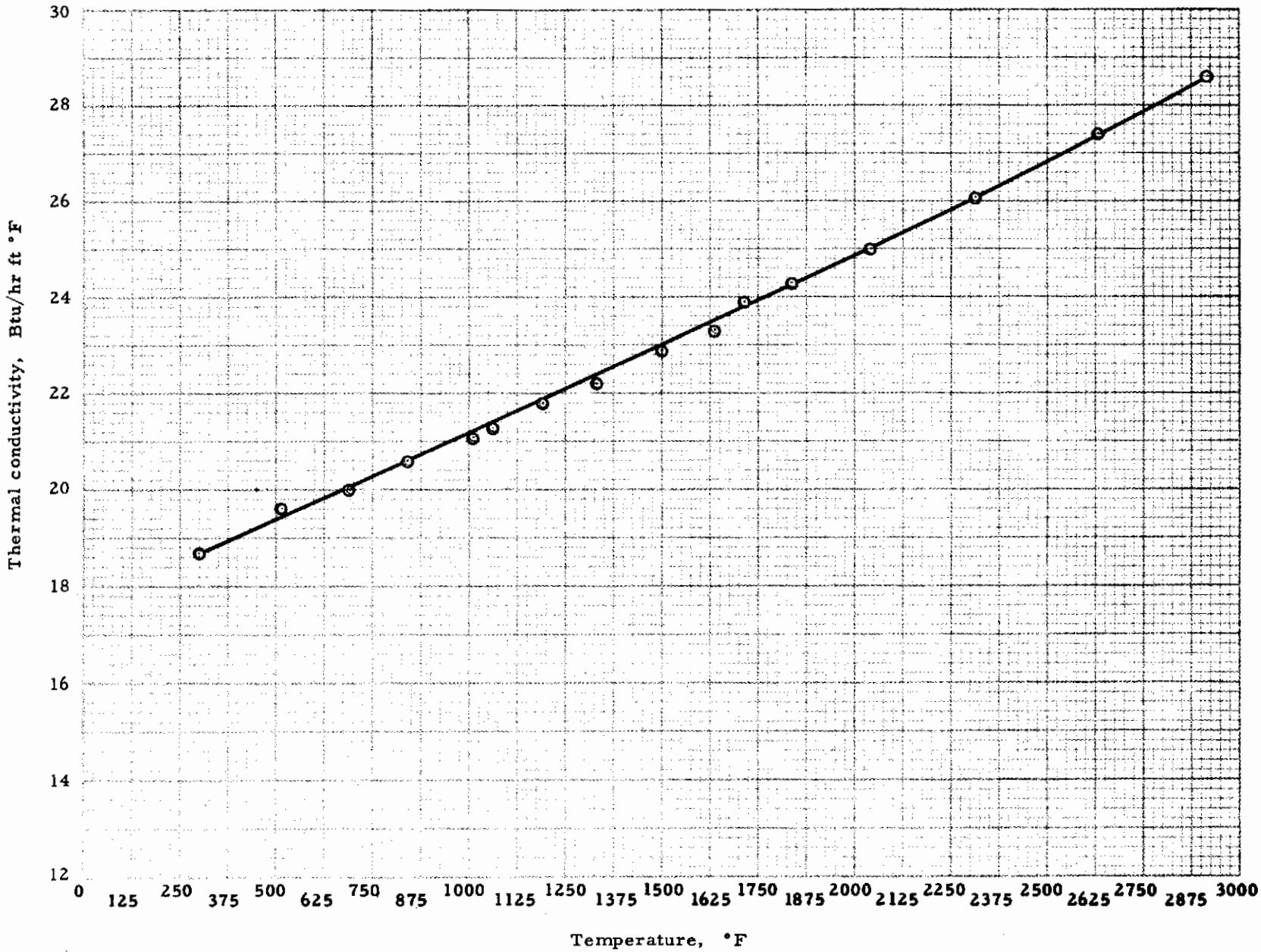

Figure 12 THERMAL CONDUCTIVITY OF VANADIUM

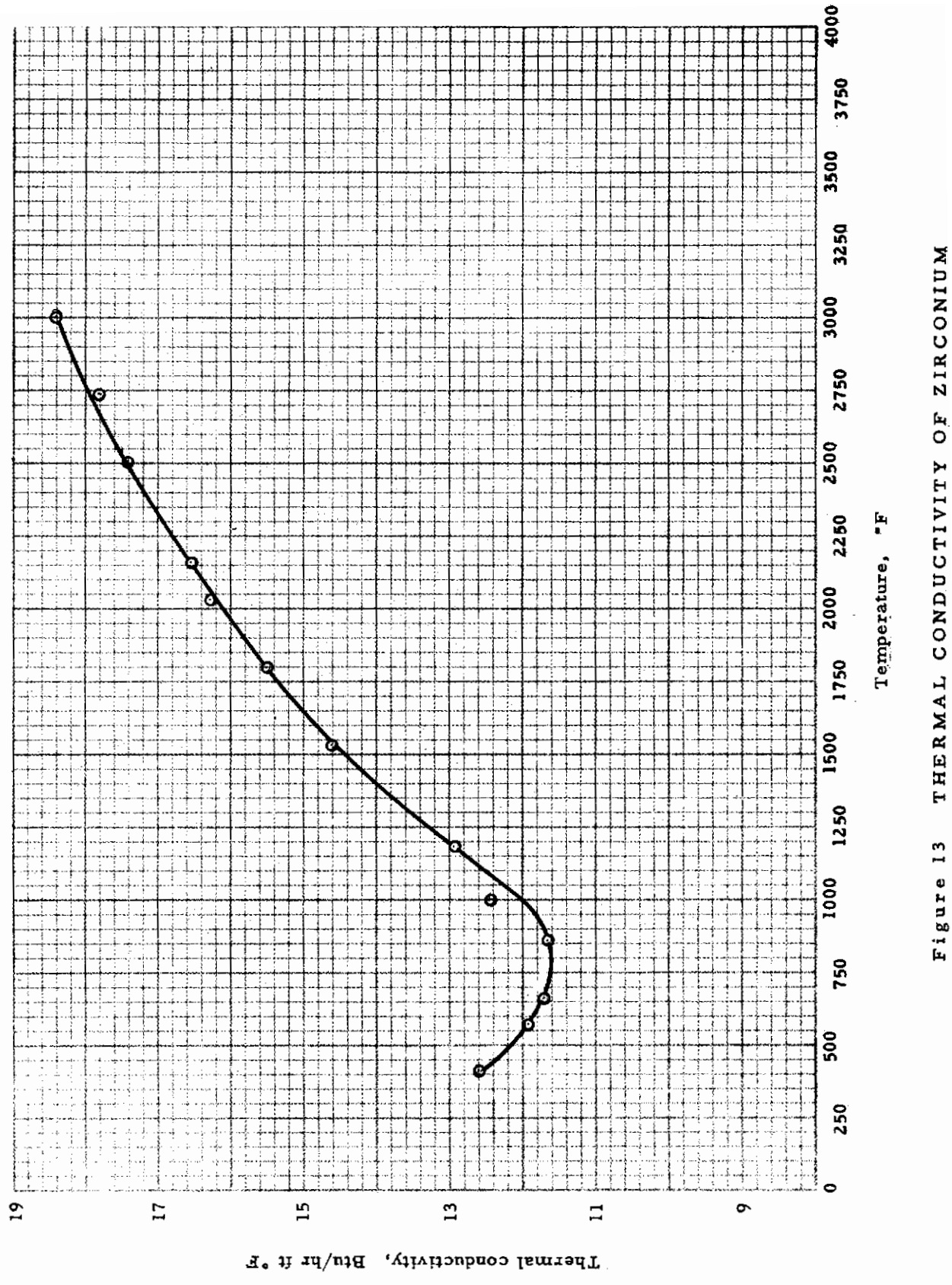

Figure 13 THERMAL CONDUCTIVITY OF ZIRCONIUM

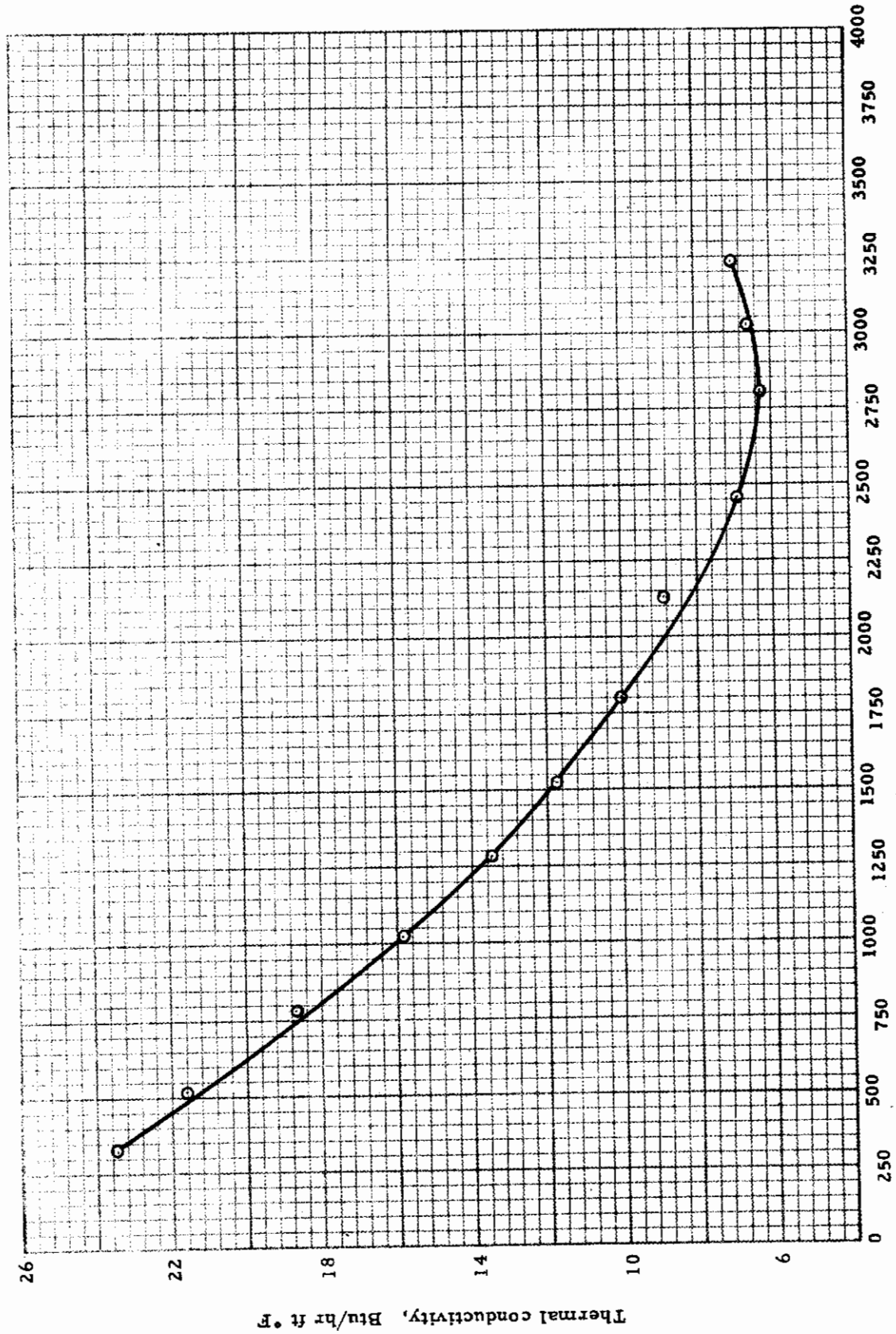

Figure 14 THERMAL CONDUCTIVITY OF MOLYBDENUM DISILICIDE

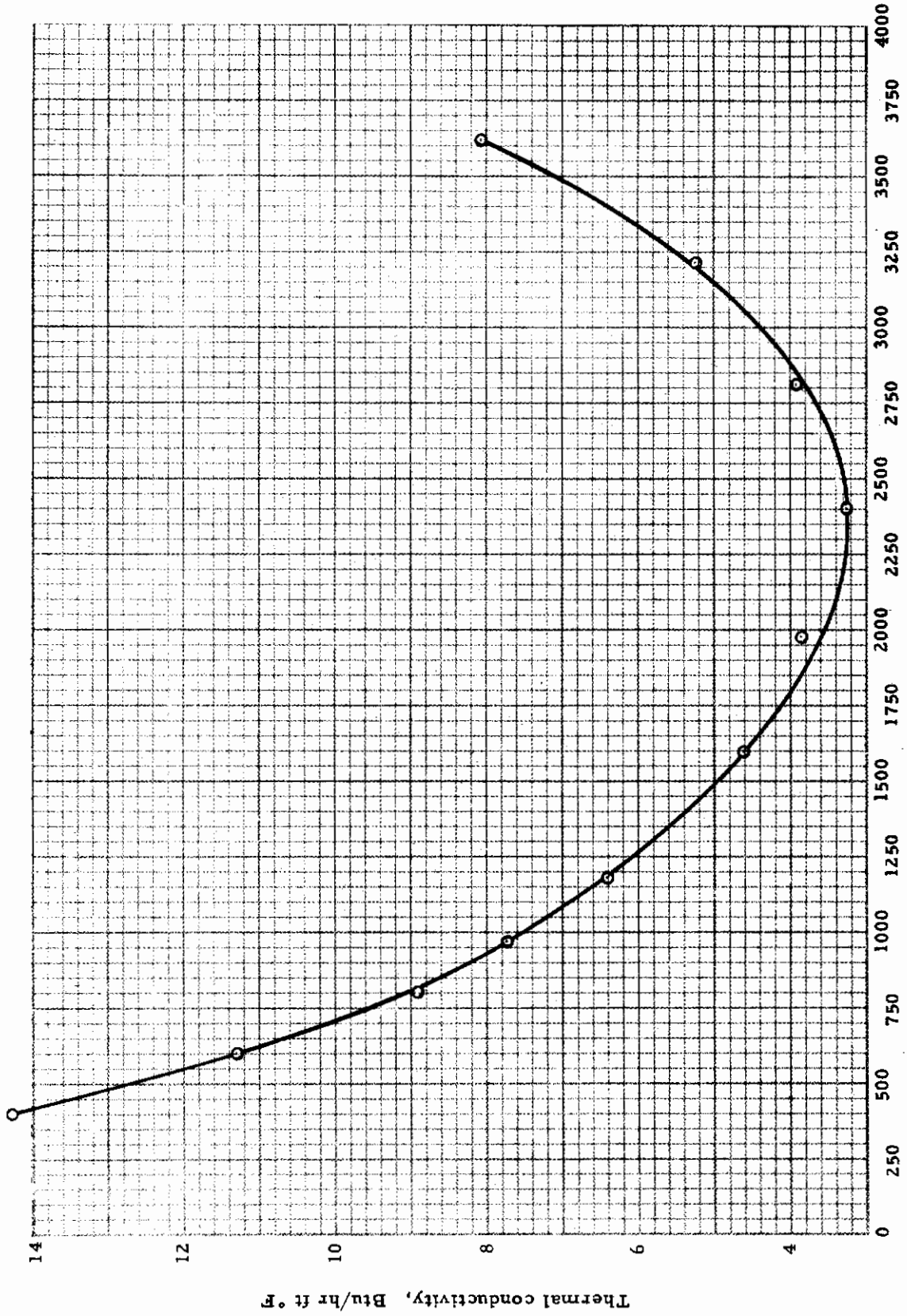

Figure 15 THERMAL CONDUCTIVITY OF MAGNESIUM OXIDE

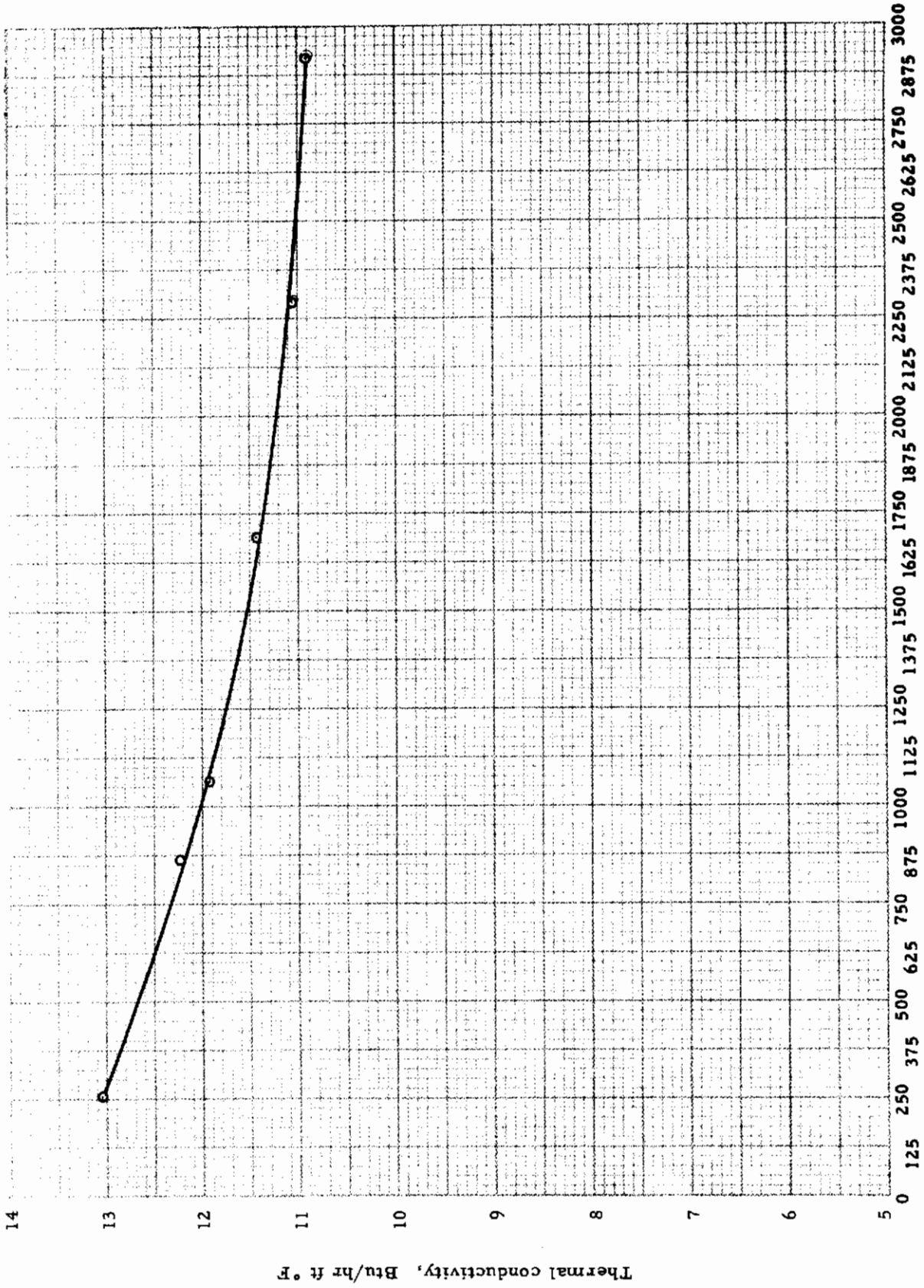

Figure 16 THERMAL CONDUCTIVITY OF HAFNIUM

SPECIFIC HEAT

APPARATUS

A diagram of the apparatus used is shown in Figure 17. The furnace is a vertical tube type purchased from the Harper Electric Company. The interior of the furnace contains an alundum tube, 1-1/2 inches inside diameter, 44 inches in length. The tube length and diameter was specified to assure a uniform temperature region surrounding the sample.

The furnace was heated electrically by a globar tube, exterior and concentric with the alundum tube. Power input to the globar element was controlled by a 3-step 6-position transformer. An inert atmosphere for the furnace interior was assured by constant purging with helium. Sealing at the top of the tube was attained by a pipe flange; bottom sealing was provided by a gate valve.

The temperature of the furnace at the point where the sample was suspended was measured by two platinum, platinum-10% rhodium thermocouples contained in protection tubes and suspended from the furnace top. The thermocouple signals were circuited to a Leeds and Northrup portable precision potentiometer. The thermocouple location, and in-furnace sample position are shown in the furnace elevation view of Figure 18. An axial temperature survey at the in-furnace sample position indicated a temperature gradient of less than 1°F/inch, at a mean furnace temperature of 2500°F.

As indicated in Figure 17, the furnace tube is connected to the calorimeter by means of a 1-1/2 inch stainless steel pipe. Immediately above the calorimeter, the 1-1/2 inch pipe was reduced by a convergent section to a one inch pipe. The one inch pipe was inserted into the receiver for a length of one inch. The receiver is indicated in Figure 17, and is based on a design described by D. C. Ginnings*. The eccentric opening in the receiver gate was shaped to allow passage of the wire on which the sample was suspended, and yet reduce heat loss from the sample by natural convection. Normal position of the receiver in the calorimeter was such that the gate was submerged in the water. A pipe tap in the receiver allowed helium purging of both receiver and pipe connecting the receiver to the furnace.

Heat content of the sample was measured by a Parr adiabatic calorimeter. The calorimeter cover was modified to provide entrance to the receiver, inert gas tubes and gate shaft.

The temperatures in the calorimeter and the calorimeter jacket were measured with calibrated thermometers supplied by the Parr Instrument Company. Water to the calorimeter jacket was heated by means of a 500 watt heater.

---

* Ginnings, D. C. and R. J. Corruccini, J. of Research NBS 38, Research Paper 1797, 1947.

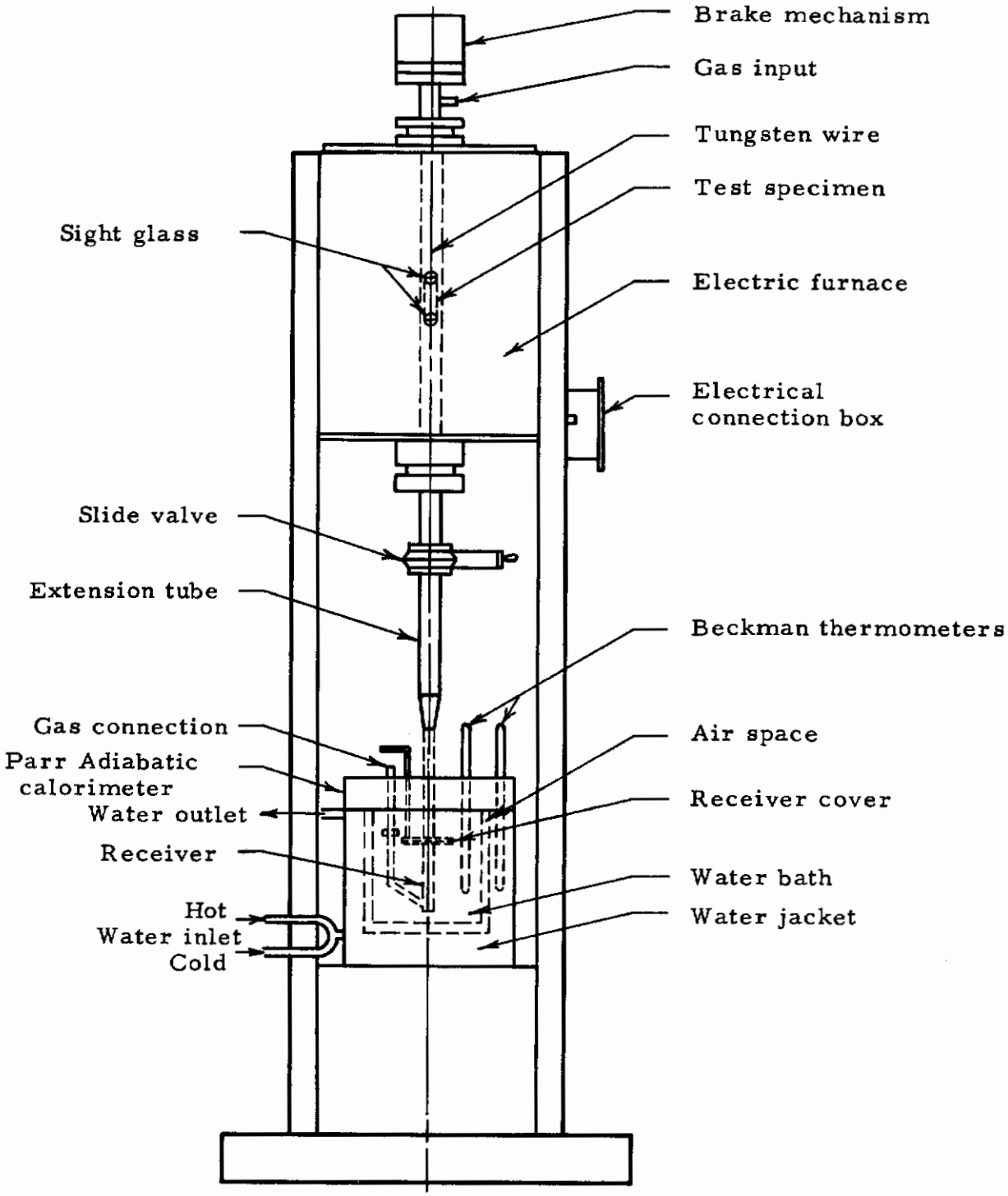

Figure 17 SCHEMATIC DIAGRAM OF APPARATUS FOR MEASURING SPECIFIC HEAT

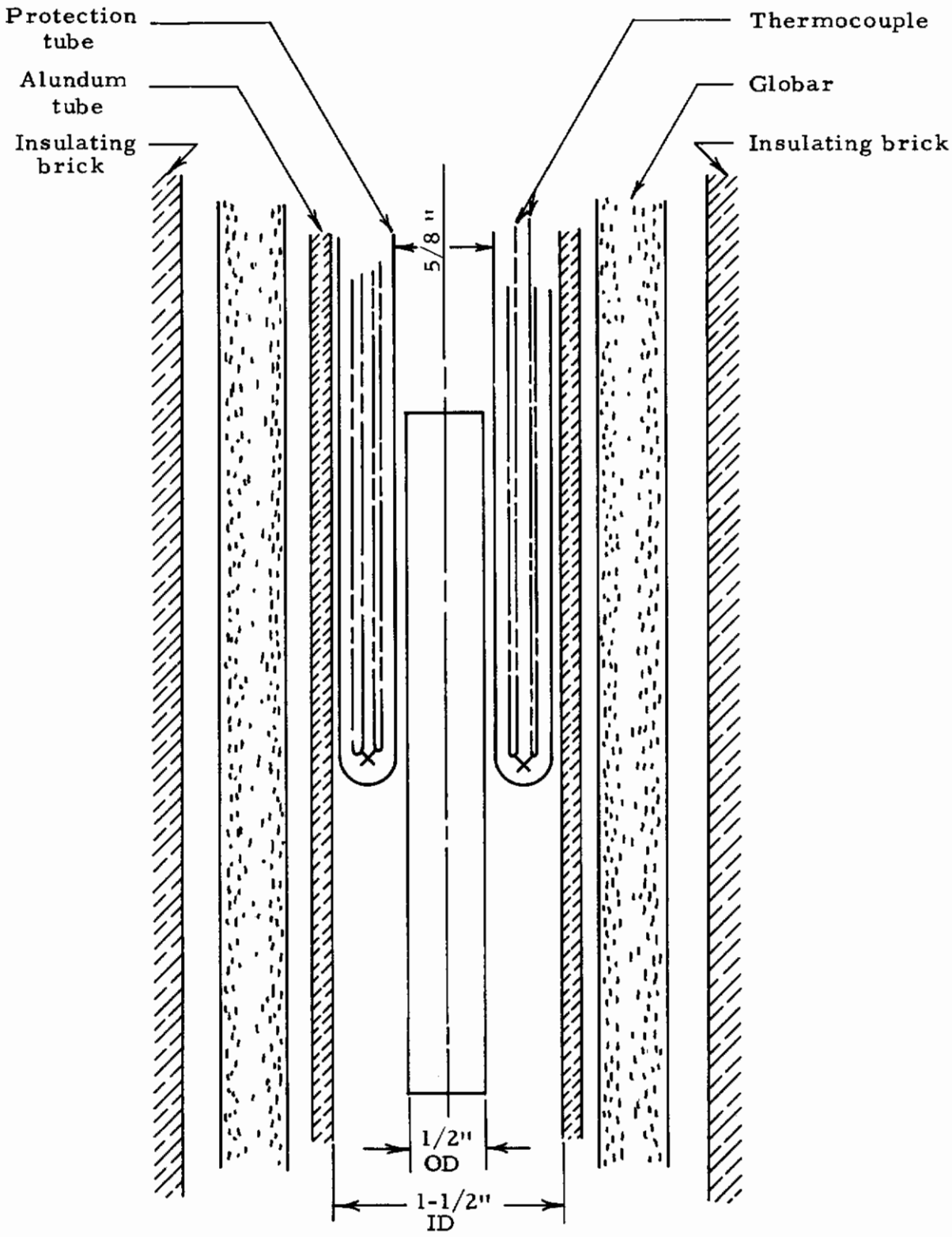

Figure 18 CROSS SECTIONAL VIEW OF SPECIFIC HEAT FURNACE

OPERATING PROCEDURE

The procedure for operation of the system is outlined below. The outline is presented in chronological order:

1. The sample weight was measured using an analytical balance precise to 0.1 milligram. The sample weight was determined prior to each test.

2. The sample was then suspended in the furnace by means of a wire. The length of the wire was carefully measured before attaching the sample to assure that the sample was correctly positioned in the furnace, respective to the monitor thermocouples.

3. The sample was maintained in the furnace for 25 minutes. This time period was considered sufficient for the sample to attain thermal equilibrium. The period of time required for the sample to attain 0.95 of the difference between room temperature and furnace temperature was calculated. For a sample emissivity of 0.7 and assuming infinite sample thermal diffusivity, the period of time for 0.95 temperature rise was 3 minutes.

4. The weight of water contained in the bucket was measured using a pan balance precise to 0.1 gram. The bucket was then placed in the calorimeter jacket, the calorimeter cover set in position, and the calorimeter elevated to the connecting tube. The calorimeter was then brought to thermal equilibrium by equalizing the temperature level in the jacket and bucket. The receiver and connecting tube were then purged with helium.

5. The system was then in readiness for the sample drop. During the preparatory stages of this operation, the furnace thermocouple signals were recorded on a Leeds and Northrup Speedomax, which provided visual observation of in-furnace temperature behavior. Injection of the sample into the furnace caused the furnace temperature to decrease; this behavior and the subsequent rise in temperature to a non-varying level was also noted. At this point in the operation the furnace thermocouple signals were circuited to a Leeds and Northrup portable precision potentiometer; emf output of each thermocouple was determined to a precision of approximately 1°F.

6. The helium purging of receiver and connecting tube was stopped immediately before sample drop. Then the gate valve at the furnace bottom was opened, the sample dropped, and the receiver gate closed. The operation from this point consisted simply of regulating the hot water input to the calorimeter jacket to maintain equal temperature level with the rising temperature level of the water in the bucket. The calorimeter attained thermal equilibrium after a period of 15 to 20 minutes, then the final temperatures were recorded.

The procedure listed above was used for all samples through the complete temperature range of operation. Overall procedure was to obtain heat content of all samples at one specified temperature level, then the power input to the furnace was increased, and the above procedure was repeated at the new temperature level.

CALCULATION OF ENTHALPY

The results of the measurements are presented in both tabular and graphical form. The test data are presented in Tables 21 through 35, and enthalpy change of each material, and measured sample temperatures are presented in Figures 19 through 33. The specific heat values obtained from Figures 19 through 33 are presented in analytical form, and are also presented in graphical form in Figures 34 through 41. A discussion of the accuracy of the results is also presented.

CALCULATION OF SPECIFIC HEAT

Specific heat at constant pressure is defined by the equation:

$$C_p = \left[\frac{\partial (\Delta H)}{\partial T}\right]_P \tag{2}$$

where

ΔH = enthalpy change relative to a specified datum

T = temperature

P subscript indicates the partial derivative at constant pressure.

The experimental method described here yields measurements of enthalpy change and corresponding temperature level. The relation between specific heat and the measured quantities is given by integration of Eq. 2 with respect to temperature.

$$\Delta H = C_p \, dT = \frac{\partial (\Delta H)}{\partial T}_P \, dT \tag{3}$$

The enthalpy change may be expressed in terms of a temperature function:

$$\Delta H = \phi(T) \tag{4}$$

Simple differentiation of $\phi(T)$ then gives C_p. The expression $\phi(T)$ used here was a quadratic of the form:

$$\Delta H = a + bT + cT^2 \tag{5}$$

So:

$$C_p = b + 2cT \tag{6}$$

The enthalpy equation $\phi(T)$ was obtained from the experimental data by a least squares method. The specific heat function was determined as indicated above. Table 20 presents specific heat coefficients in the temperature range investigated. The enthalpy temperature coefficients are listed in Table 19.

ACCURACY OF MEASUREMENTS

The accuracy of the results is limited only by the accuracy of in-furnace sample temperature measurement. The measurement of heat content of the sample by the calorimeter is very precise. The temperature rise of the calorimeter was always more than 3°F; the temperature level of the calorimeter could be determined to 0.01°F. The magnitude of error from the calorimeter is probably no more than 1%. This conclusion is difficult to check experimentally because it was not possible to maintain furnace temperatures constant to less than 5°F. Furnace temperature variation was caused by fluctuation in voltage input to the furnace transformers.

Measurement of in-furnace sample temperature was accomplished by two platinum, platinum-10% rhodium thermocouples inserted in protection tubes as shown in Figure 18. The protection tubes were necessary to prevent contamination of the thermocouples, and also to allow diffusion of oxygen down the interior of the protection tube. The validity of this measurement method was checked in the following manner: a graphite sample was axially bored to accommodate an insulated platinum, platinum-10% rhodium thermocouple. The sample was placed in the normal in-furnace position, and the temperatures sensed by the thermocouples enclosed in the protection tubes were compared with the thermocouple enclosed in the sample. The results of this test indicated that the temperature sensed by the sample thermocouples agreed with the arithmetic average of the temperatures sensed by protected thermocouples to 4°F. This test also served to check the contamination of the protected thermocouple: one of the protected thermocouples used in this test was new; the other had been used extensively for the previous tests. Agreement between the new and old thermocouples was excellent.

The above test was repeated with a nickel sample, and the results were essentially the same.

The representativeness of the thermocouple measurements then was very good. However, fluctuations in furnace temperatures due to line voltage variations were quite severe, especially at high furnace temperatures. Superposition of unsteady state behavior on the thermocouples and sample was probably the chief source of error. An estimate of this effect was made by comparing readings of a thermocouple enclosed in a protection tube and an unprotected thermocouple. A test of this nature was made, the data obtained from this test indicated that at temperatures higher than 2400°F the unsteady state behavior may cause an error of 15°F. The error introduced from this source is probably about 1%.

The combined accuracy of the specific heat measurements is, then, about 3%.

CALIBRATION OF SYSTEM

The system was calibrated by measurement of the enthalpy content of synthetic sapphire. The measurements were compared with the accurate data of D. C. Ginnings, done at the National Bureau of Standards (NBS) loc cit. Several test drops were made in the temperature range 400° to 1200°F. The enthalpy measurements obtained at ARF are compared with the data by Ginnings in the table below.

Table 18

ENTHALPY OF SYNTHETIC SAPPHIRE

Temperature, °F	Enthalpy Content, Btu/lb		
	NBS	ARF	Difference, %
423	78.4	79.9	-0.64
713	154.5	155.5	+0.65
971	225.6	223.7	-0.84
1169	281.2	282.0	+0.28

Table 19

ENTHALPY COEFFICIENTS

$$\Delta H = a + b \cdot 10^{-2} T + c \cdot 10^{-4} T^2$$

Material	Coefficients a	b	c	Temperature range, °F
Stainless Steel type 420	1.8	7.4	0.478	427 - 1610
	24.3	13.6	---	1610 - 2188
Stainless Steel type 17-4 PH	6.8	5.53	0.641	390 - 1317
	61.3	6.08	0.263	1317 - 2193
AM 355	-23.1	12.6	0.182	420 - 1650
	222.6	-8.7	0.568	1650 - 2220
Crucible HNM	-7.9	11.1	0.159	425 - 1400
	-90.3	19.2	---	1400 - 1600
	26.7	9.6	0.144	1600 - 2169
Titanium C110M	-10.	11.7	0.215	435 - 2809
Inco 713C	2.8	6.6	0.346	464 - 2192
Haynes Stellite HE 1049	23.8	7.3	0.167	339 - 2081
Kennametal K161B	-19.	14.6	0.141	346 - 2320
	-782.	50.7	---	2320 - 2390
	-34.	19.4	---	2390 - 2759
M 252 (GE-J1500)	9.3	5.4	0.381	403 - 2215
Rene 41 (GE-J1610)	10.2	5.5	0.371	402 - 2210
Vanadium	-6.4	11.0	0.140	403 - 2950
Zirconium	-2.4	5.5	0.171	391 - 1600
	-142.	17.0	---	1600 - 1760
	-14.3	10.7	-0.058	1760 - 2793
Molybdenum Disilicide	7.9	7.5	0.202	443 - 2200
	-84.4	16.2	---	2200 - 2775
Magnesium Oxide	2.0	20.4	0.325	395 - 2801
Hafnium	-5.8	37.8	2.64	501 - 2931

Table 20

SPECIFIC HEAT COEFFICIENTS

$$C_p = b' + 2c' \cdot 10^{-2} T$$

Material	Coefficients b'	Coefficients 2c'	Temperature range, °F
Stainless Steel type 420	0.0736	0.00956	427 - 1610
	0.136	---	1610 - 2188
Stainless Steel type 17-4 PH	0.0553	0.0128	390 - 1317
	0.0608	0.00526	1317 - 2193
AM 355	0.126	0.00364	420 - 1650
	-0.0868	0.0114	1650 - 2220
Crucible HNM	0.111	0.0318	425 - 1400
	0.192	---	1400 - 1600
	0.0960	0.00288	1600 - 2169
Titanium C110M	0.117	0.00430	435 - 2809
Inco 713C	0.0661	0.00692	464 - 2192
Haynes Stellite HE 1049	0.0734	0.00334	339 - 2081
Kennametal 161B	0.146	0.00282	346 - 2320
	0.507	---	2320 - 2390
	0.194	---	2390 - 2759
M 252 (GE-J1500)	0.0545	0.00762	403 - 2215
Rene 41 (GE-J1610)	0.0548	0.00742	402 - 2210
Vanadium	0.110	0.00280	403 - 2950
Zirconium	0.0555	0.00342	391 - 1600
	0.170	---	1600 - 1760
	0.107	-0.00116	1760 - 2793
Molybdenum Disilicide	0.0746	0.00404	443 - 2200
	0.162	---	2200 - 2775
Magnesium Oxide	0.204	0.00650	395 - 2801
Hafnium	0.0378	0.00528	501 - 2931

Table 21

ENTHALPY VALUES FOR STAINLESS STEEL TYPE 420

Datum Temperature: 80°F

Temperature, °F	ΔH_c, Btu/lb
427	39.9
497	50.8
755	84.7
619	67.5
898	109
983	120
1176	156
1210	159
1349	188
1424	204
1425	205
1549	231
1608	244
1652	248
1793	270
1830	273
1962	289
2183	320
2188	324

Table 22

ENTHALPY VALUES FOR
STAINLESS STEEL TYPE PH 17-4 (H900)

Datum Temperature: 80°F

Temperature, °F	ΔH_c, Btu/lb
390	36.6
460	46.3
590	62.7
666	72.1
785	88.8
859	103
978	121
1082	144
1143	155
1176	160
1257	175
1333	190
1384	195
1485	209
1598	224
1690	238
1777	253
1786	255
1884	270
2010	292
2102	303
2193	322

Table 23

ENTHALPY VALUES FOR AM 355

Datum Temperature: 80°F

Temperature, °F	ΔH_c, Btu/lb
427	33.5
547	49.5
751	81.7
874	100
1009	120
1194	153
1250	165
1339	179
1466	201
1538	213
1604	226
1648	234
1713	240
1786	248
1930	268
2174	300
2001	275
2186	304
2220	309

Table 24

ENTHALPY VALUES FOR
CRUCIBLE HNM

Datum Temperature: 80°F

Temperature, °F	ΔH_c, Btu/lb
425	40.1
558	60.0
753	84.9
1008	120
1164	144
1377	174
1497	197
1614	219
1756	240
1865	257
1971	271
2169	303

Table 25

ENTHALPY VALUES FOR
TITANIUM-C110M

Datum Temperature: 80°F

Temperature, °F	ΔH_c, Btu/lb
435	44.7
625	74.6
711	84.0
888	112
1002	132
1102	147
1432	205
1657	243
1783	270
1998	312
2181	349
2398	399
2608	440
2809	490

Table 26

ENTHALPY VALUES FOR
INCO 713C

Datum Temperature: 80°F

Temperature, °F	ΔH_c, Btu/lb
464	39.4
627	60.0
828	83.7
869	90.4
1040	111
1162	129
1403	161
1588	190
1593	191
1781	226
1798	227
1975	265
1983	266
2192	317

Table 27

ENTHALPY VALUES FOR HE 1049

Datum Temperature: 80°F

Temperature, °F	ΔH_c, Btu/lb
339	39.6
562	63.2
812	77.8
997	110
1210	137
1406	161
1594	185
1808	212
2015	241
2081	248

Table 28

ENTHALPY VALUES FOR KENNEMETAL K161 B

Datum Temperature: 80°F

Temperature, °F	ΔH_c, Btu/lb
346	33.2
649	81.5
826	109
1028	146
1234	187
1606	250
1428	218
1818	293
1981	321
2184	368
2320	396
2385	430
2400	431
2609	471
2759	503

Table 29

ENTHALPY VALUES FOR

M 252 (GE-J1500)

Datum Temperature: 80°F

Temperature, °F	ΔH_c, Btu/lb
403	34.6
806	78.8
991	103
1187	128
1359	154
1421	160
1455	169
1643	200
1796	228
1883	246
1988	266
2011	273
2215	311

Table 30

ENTHALPY VALUES FOR
RENE 41 (GE-J 1610)

Datum Temperature: 80°F

Temperature, °F	ΔH_c, Btu/lb
402	34.4
588	54.8
664	64.6
822	83.7
888	91.4
971	102
1056	112
1182	130
1296	145
1397	160
1529	178
1662	203
1794	227
1889	250
2018	274
2081	283
2210	313

Table 31

ENTHALPY VALUES FOR
VANADIUM

Datum Temperature: 80°F

Temperature, °F	ΔH_c, Btu/lb
403	42.5
596	62.9
793	88.8
1022	118
1154	137
1403	171
1493	191
1670	213
1782	231
1980	266
2212	308
2388	340
2591	374
2602	379
2784	405
2950	444

Table 32

ENTHALPY VALUES FOR ZIRCONIUM

Datum Temperature: 80°F

Temperature, °F	ΔH_c, Btu/lb
391	21.3
566	35.8
598	36.8
790	52.6
846	56.4
1032	71.0
1257	93.8
1394	104
1398	105
1517	120
1599	129
1719	146
1760	157
1820	162
1974	174
2190	194
2394	208
2574	224
2793	240

Table 33

ENTHALPY VALUES FOR MOLYBDENUM DISILICIDE

Datum Temperature: 80°F

Temperature, °F	ΔH_c, Btu/lb
443	47.4
614	60.1
853	83.5
1001	100
1260	135
1425	155
1598	178
1790	211
1995	236
2011	244
2188	270
2381	301
2583	329
2775	361

Table 34

ENTHALPY VALUES FOR
MAGNESIUM OXIDE

Datum Temperature: 80°F

Temperature, °F	ΔH_c, Btu/lb
395	89.9
642	142
761	171
818	184
875	212
984	233
1016	235
1205	295
1435	351
1584	407
1828	487
2006	548
2193	610
2384	677
2582	747
2607	753
2801	825

Table 35

ENTHALPY VALUES FOR HAFNIUM

Datum Temperature: 80°F

Temperature, °F	ΔH_c, Btu/lb
501	14.3
622	18.0
780	23.2
978	34.0
1105	36.8
1286	47.1
1635	63.1
1768	68.2
1917	77.0
2190	90.0
2335	96.2
2471	104.1
2779	119.1
2931	128.6

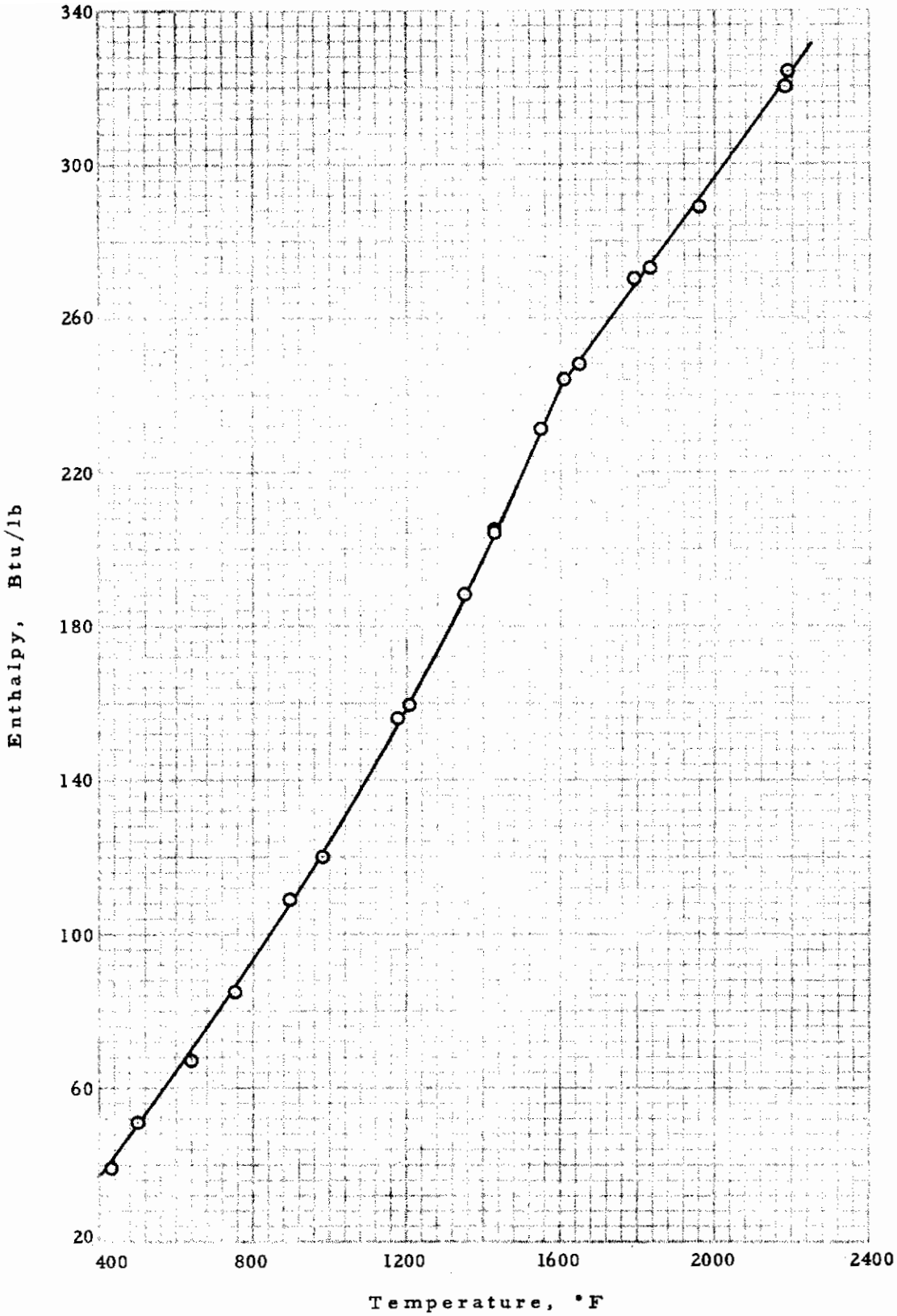

Figure 19 ENTHALPY OF STAINLESS STEEL TYPE 420

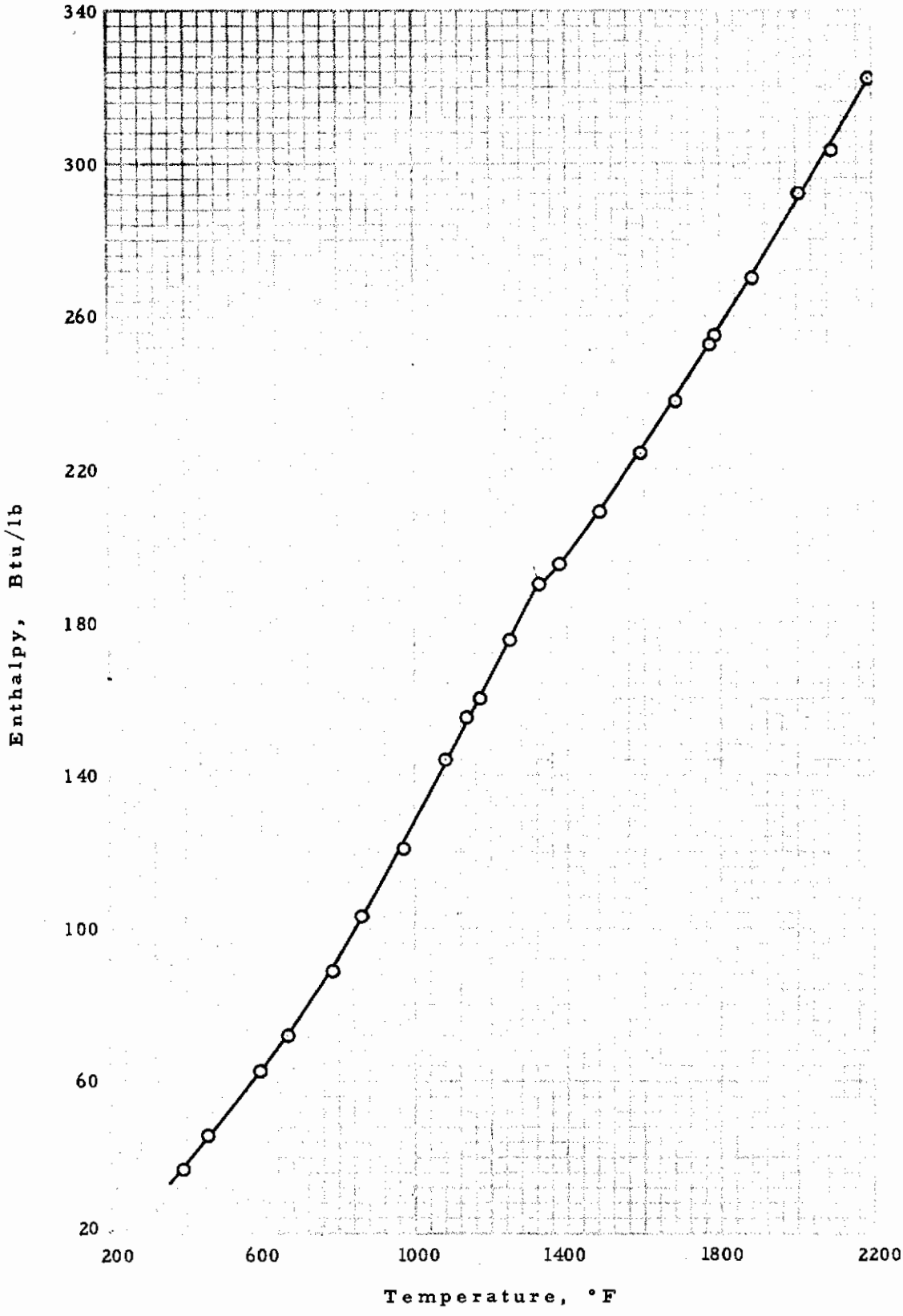

Figure 20 ENTHALPY OF STAINLESS STEEL TYPE PH 17-4

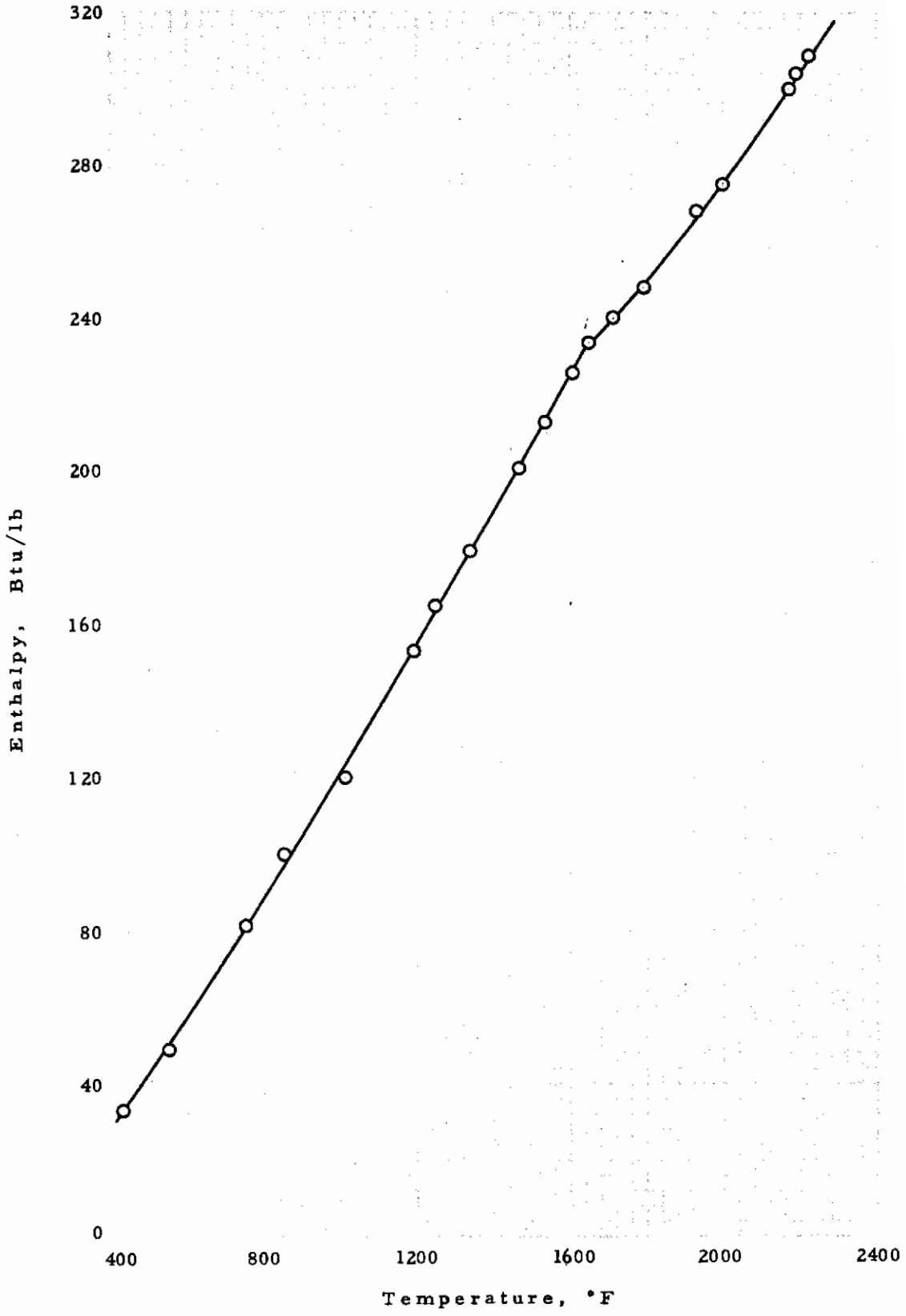

Figure 21 ENTHALPY OF AM 355

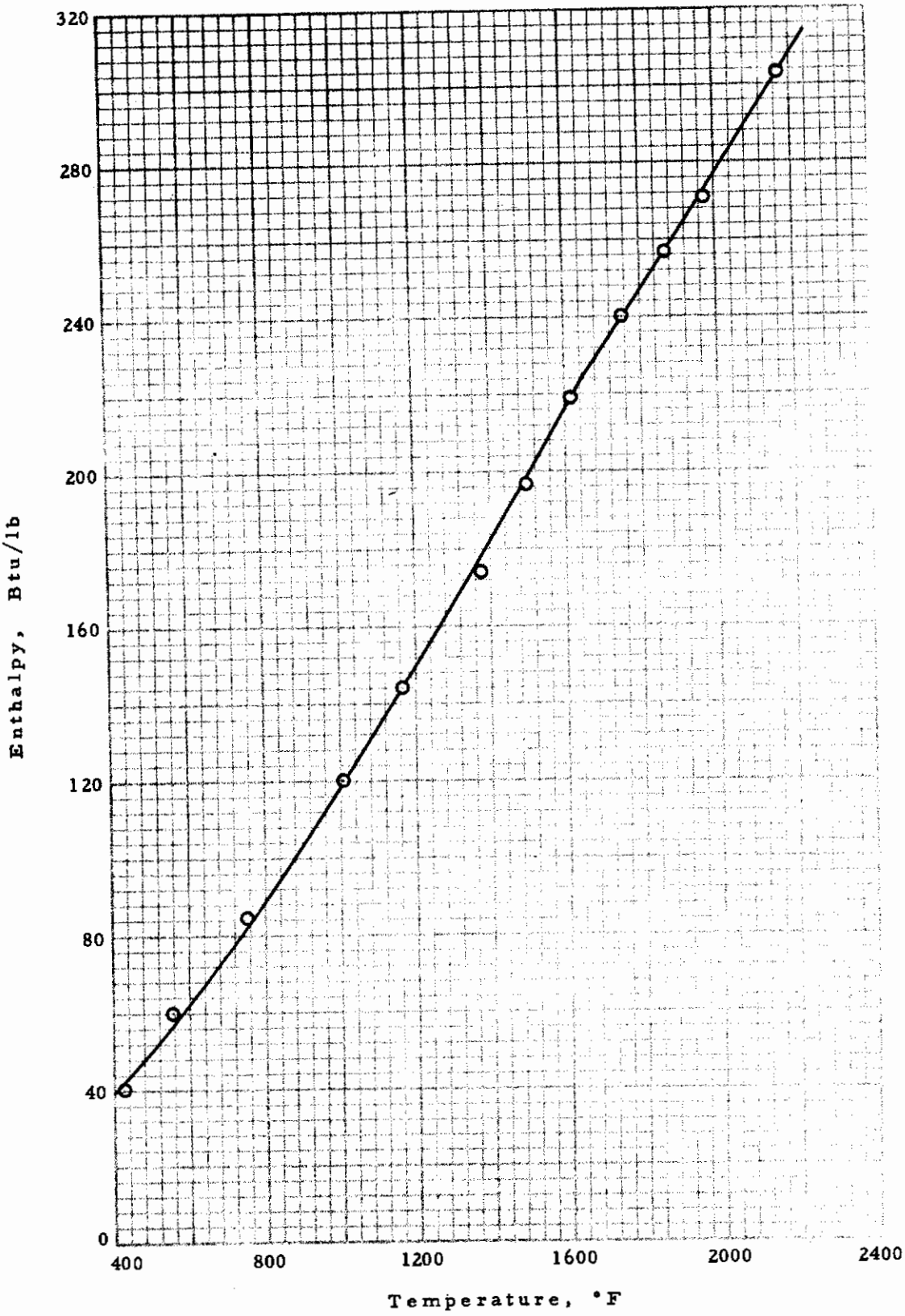

Figure 22 ENTHALPY OF CRUCIBLE HNM

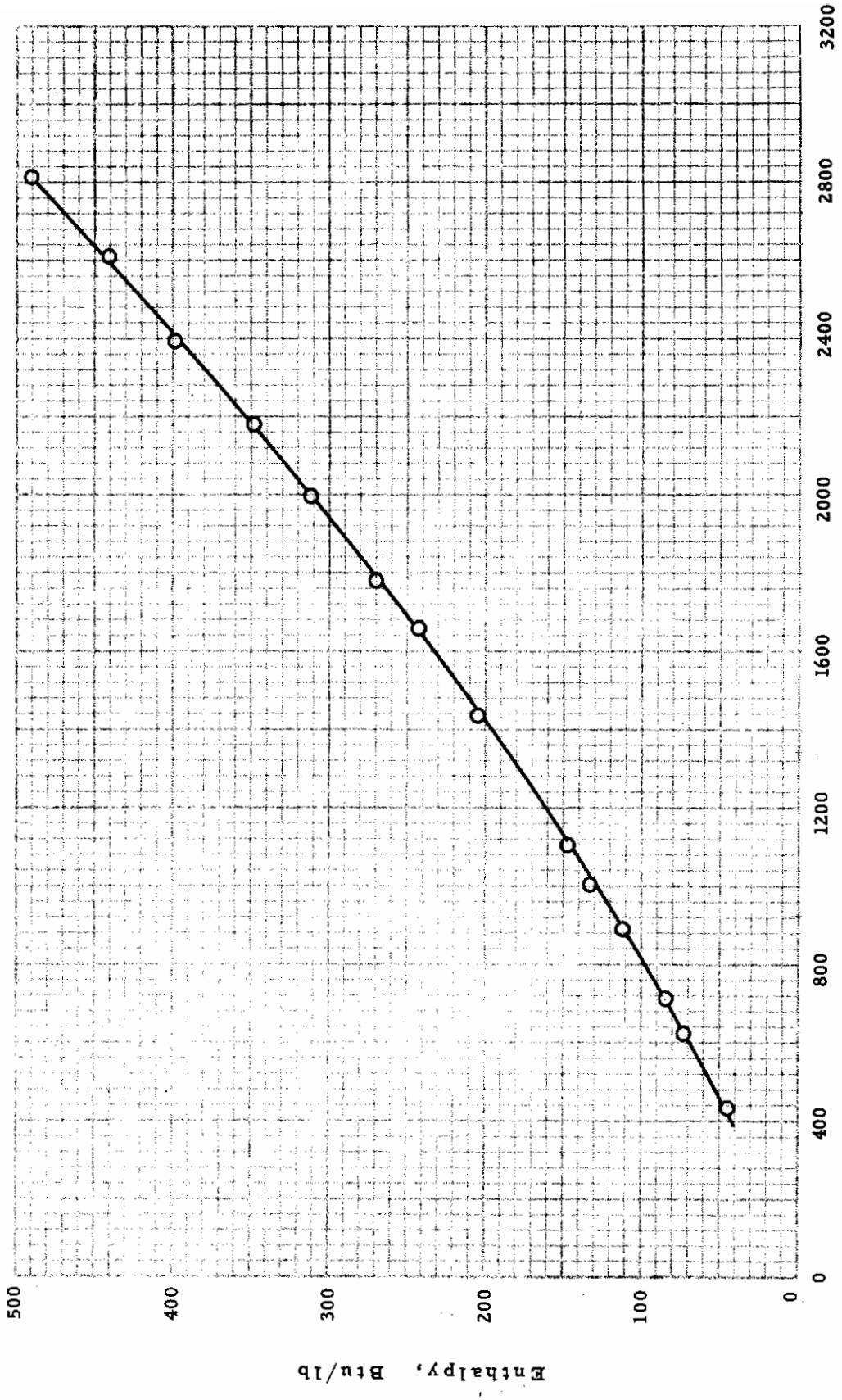

Figure 23 ENTHALPY OF TITANIUM C110M

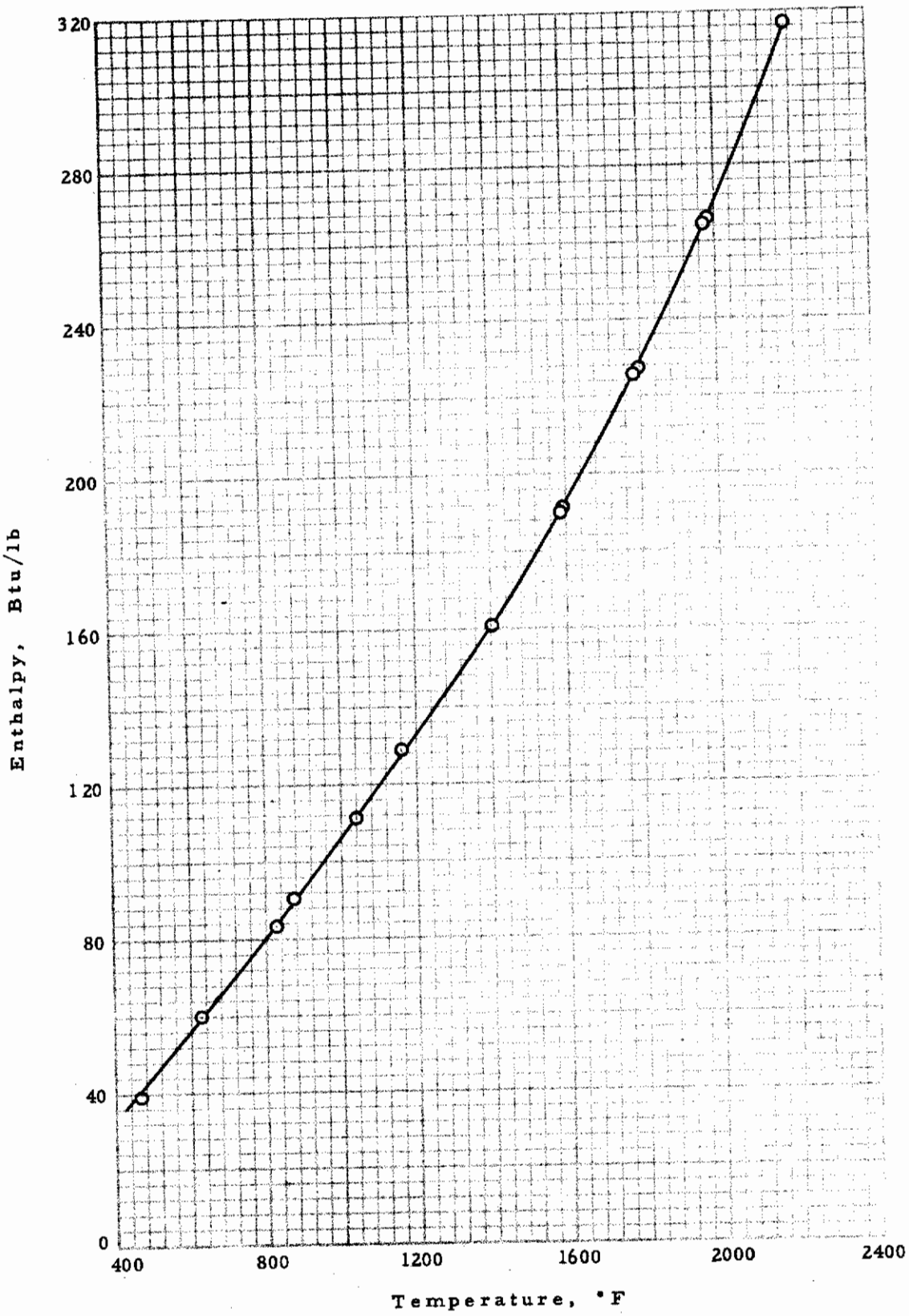

Figure 24 ENTHALPY OF INCO 713C

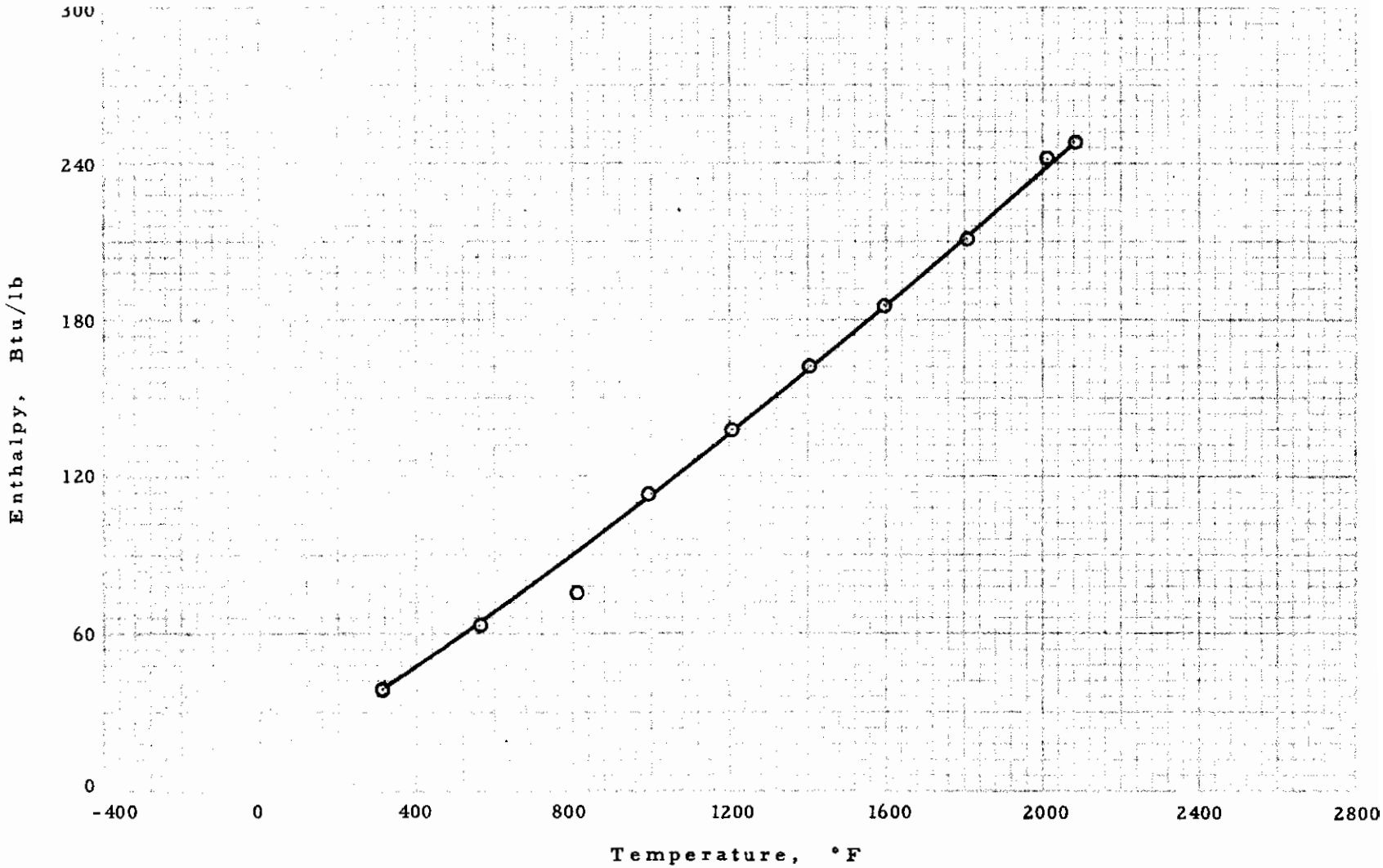

Figure 25 ENTHALPY OF HE 1049

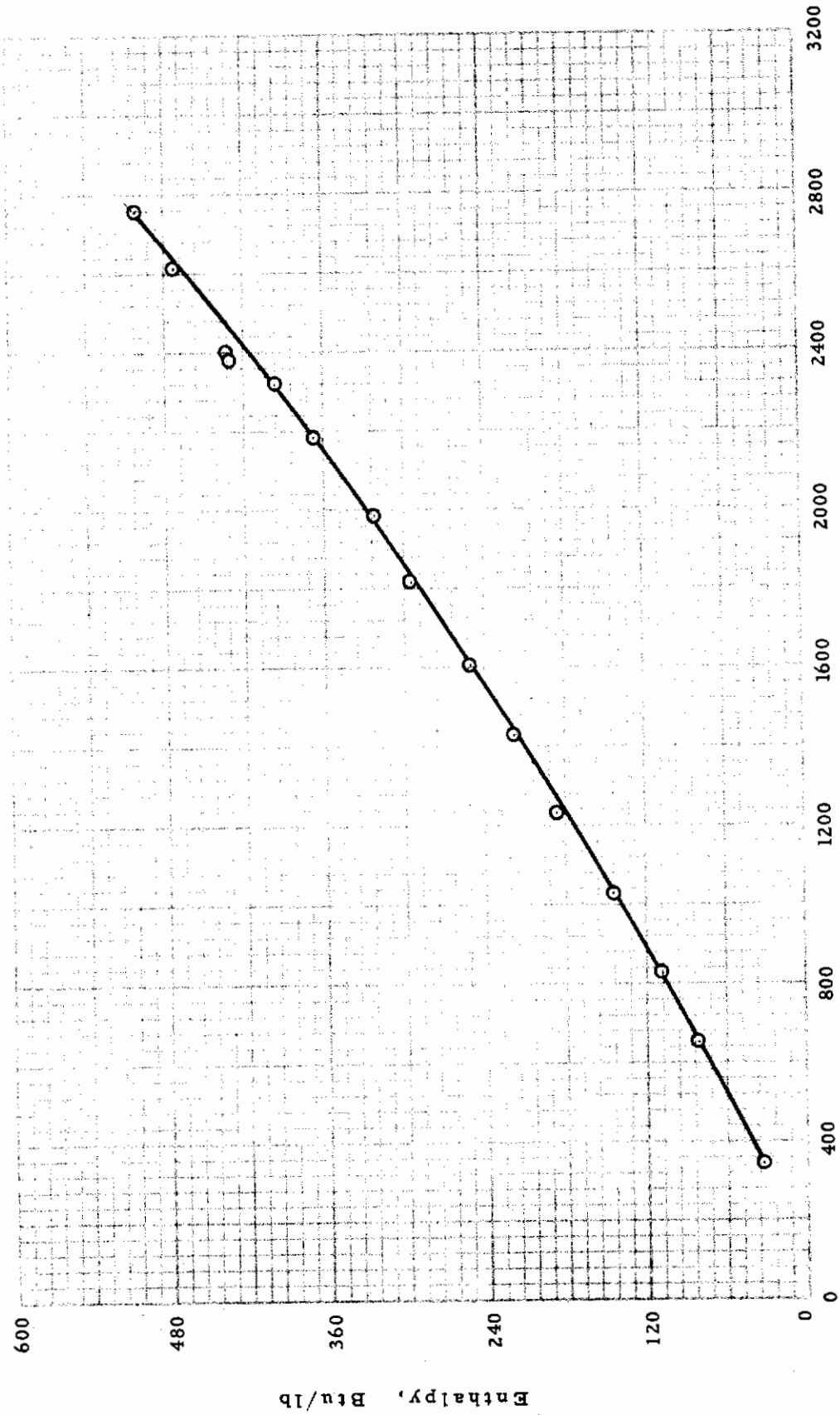

Figure 26 ENTHALPY OF KENNAMETAL K161B

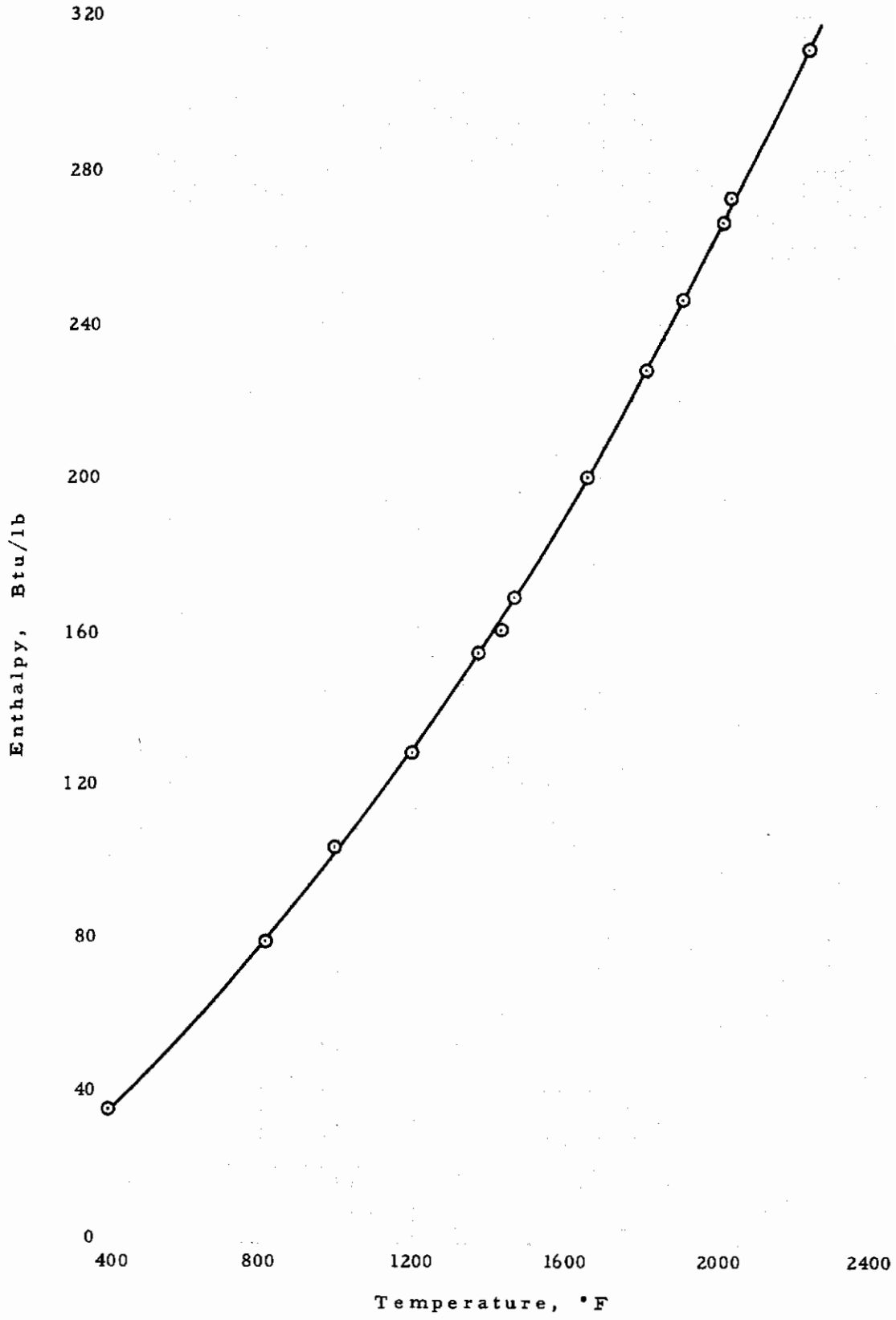

Figure 27 ENTHALPY OF M 252

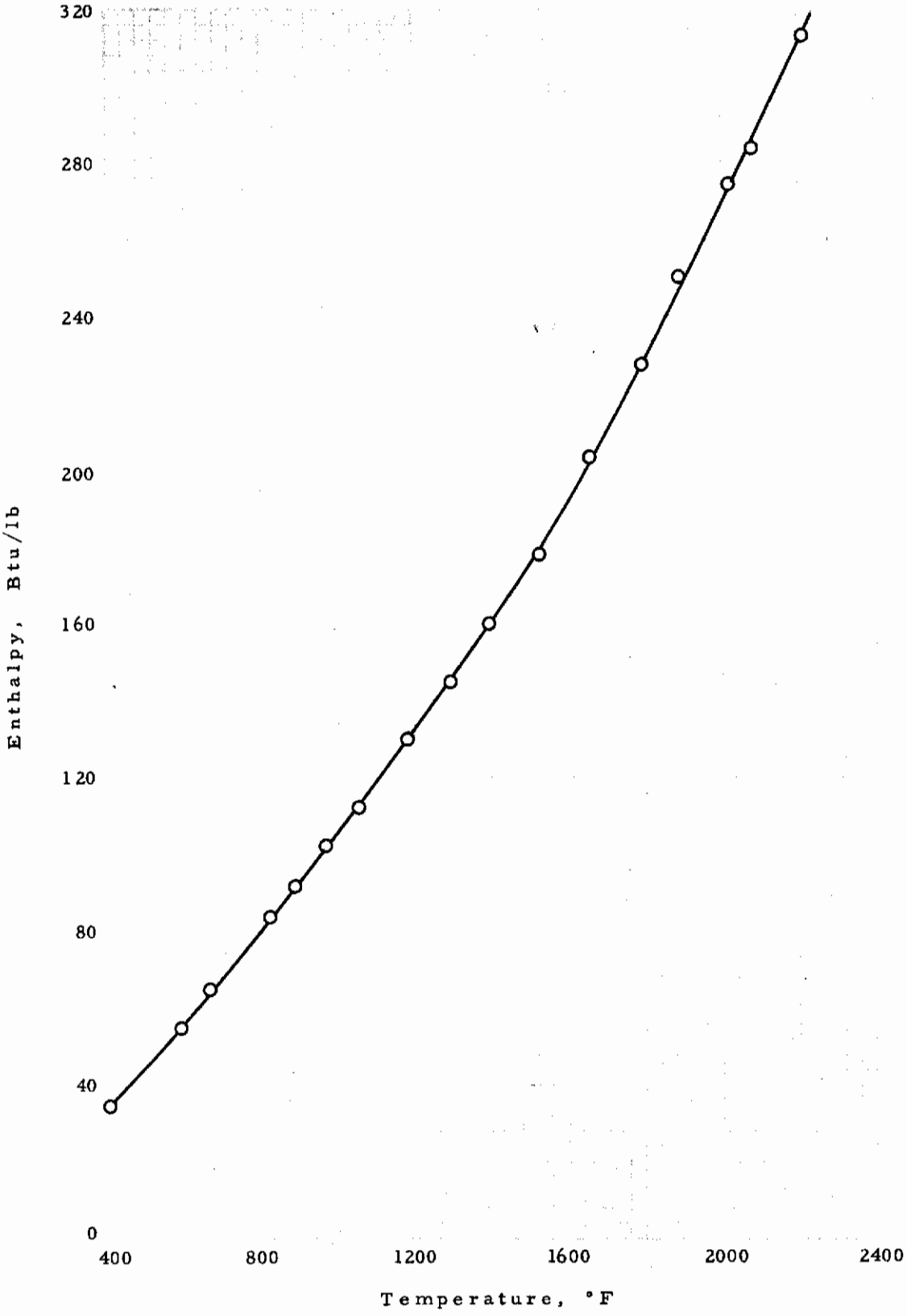

Figure 28 ENTHALPY OF RENE 41

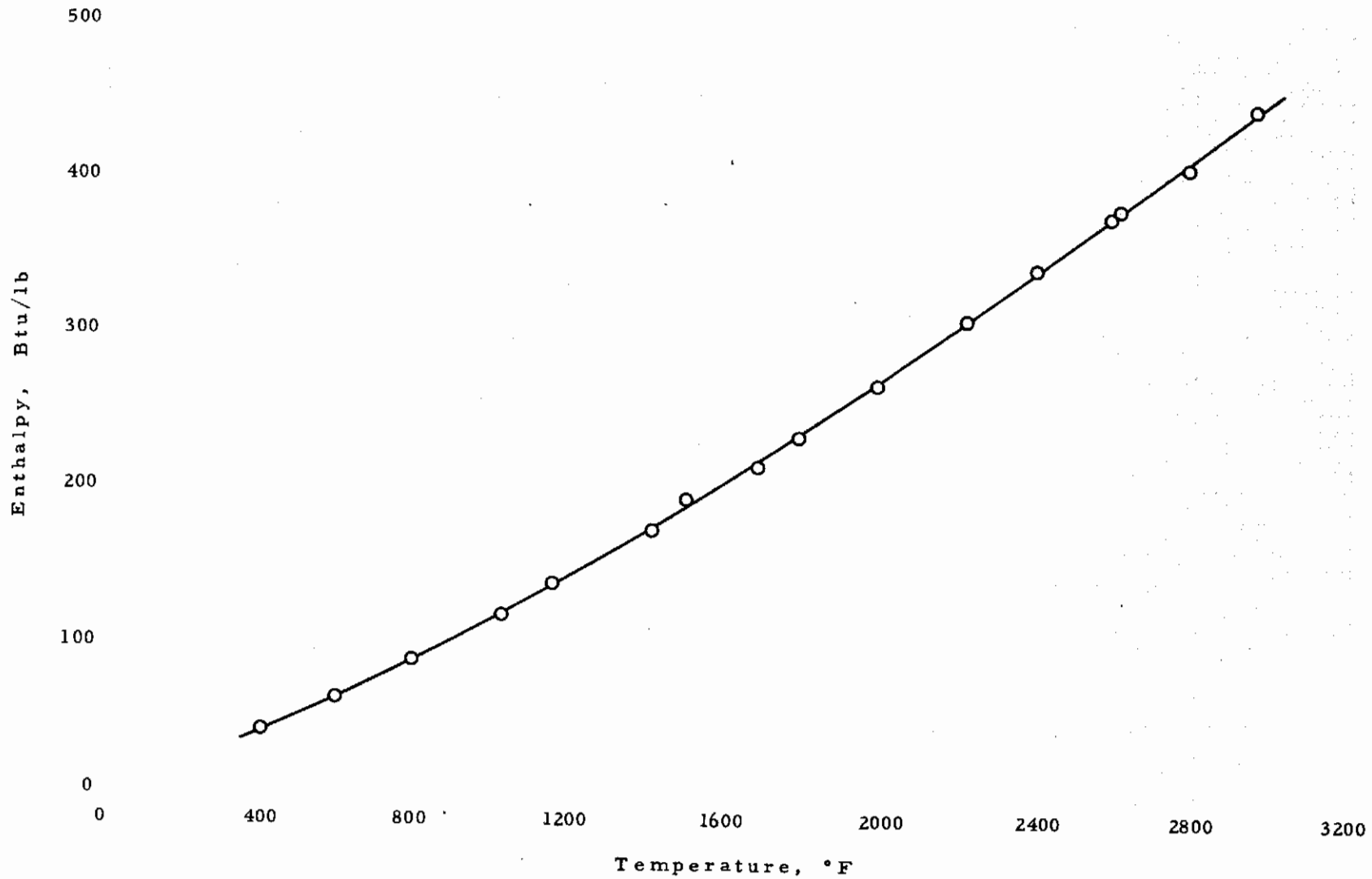

Figure 29 ENTHALPY OF VANADIUM

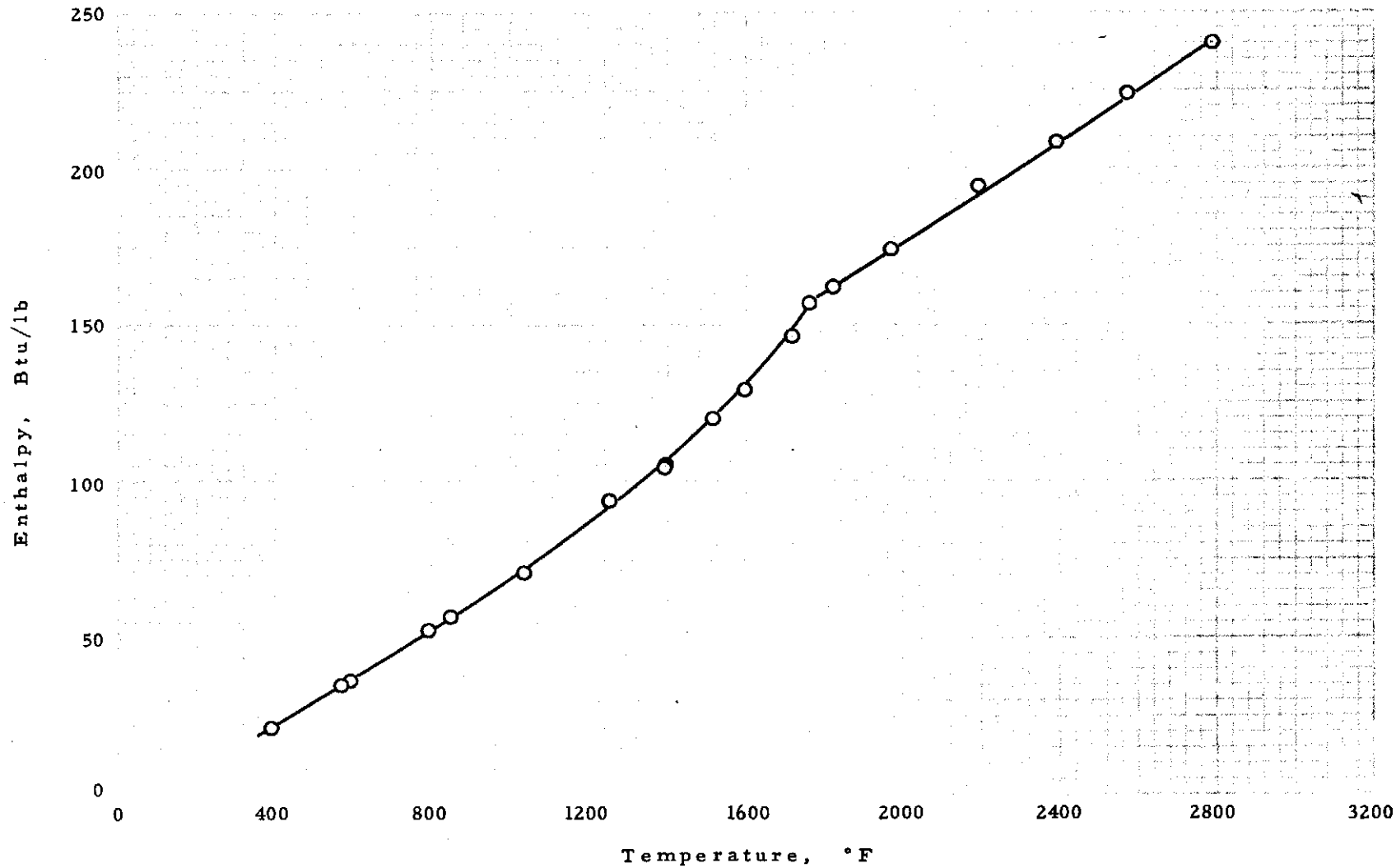

Figure 30 ENTHALPY OF ZIRCONIUM

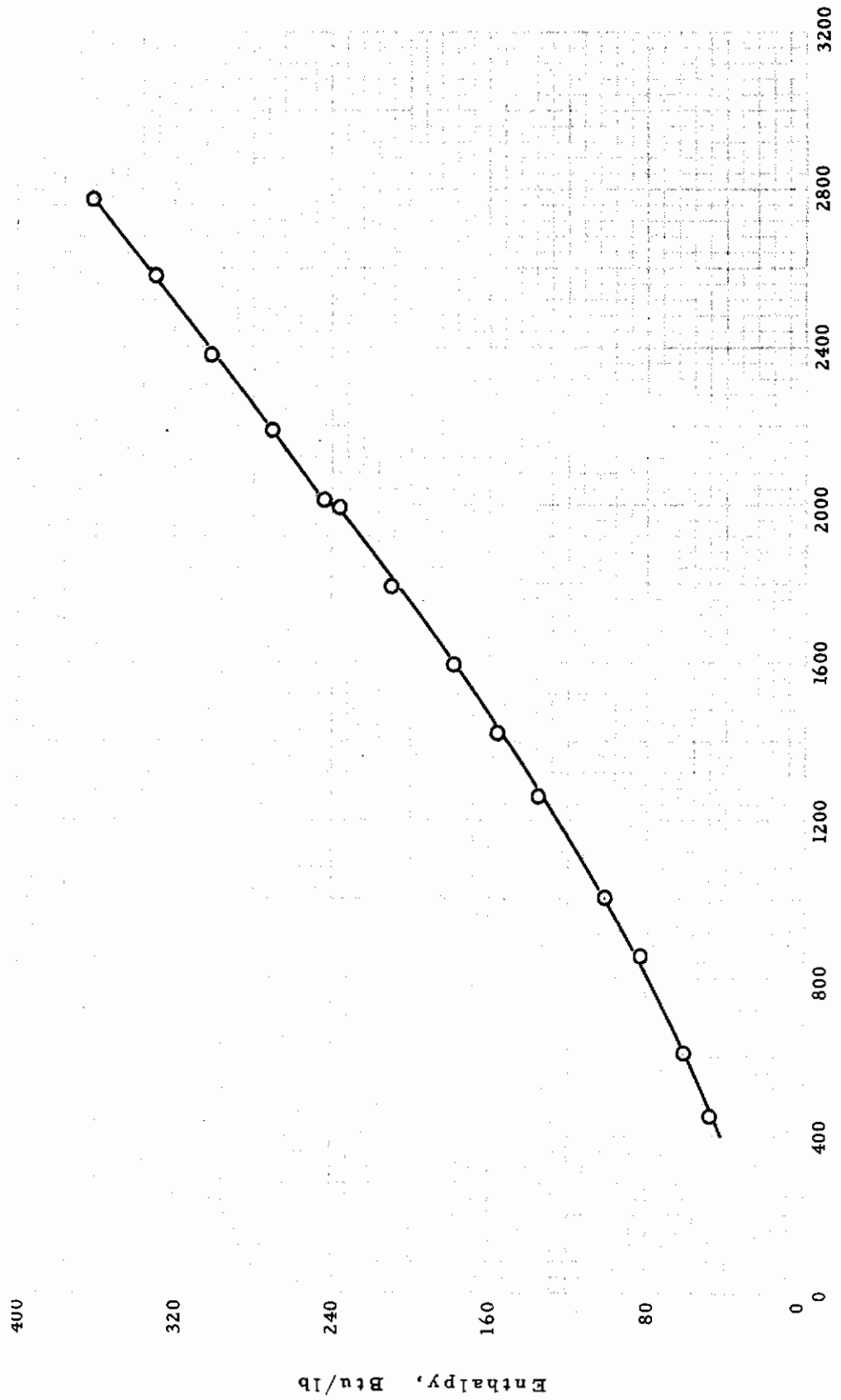

Figure 31 ENTHALPY OF MOLYBDENUM DISILICIDE

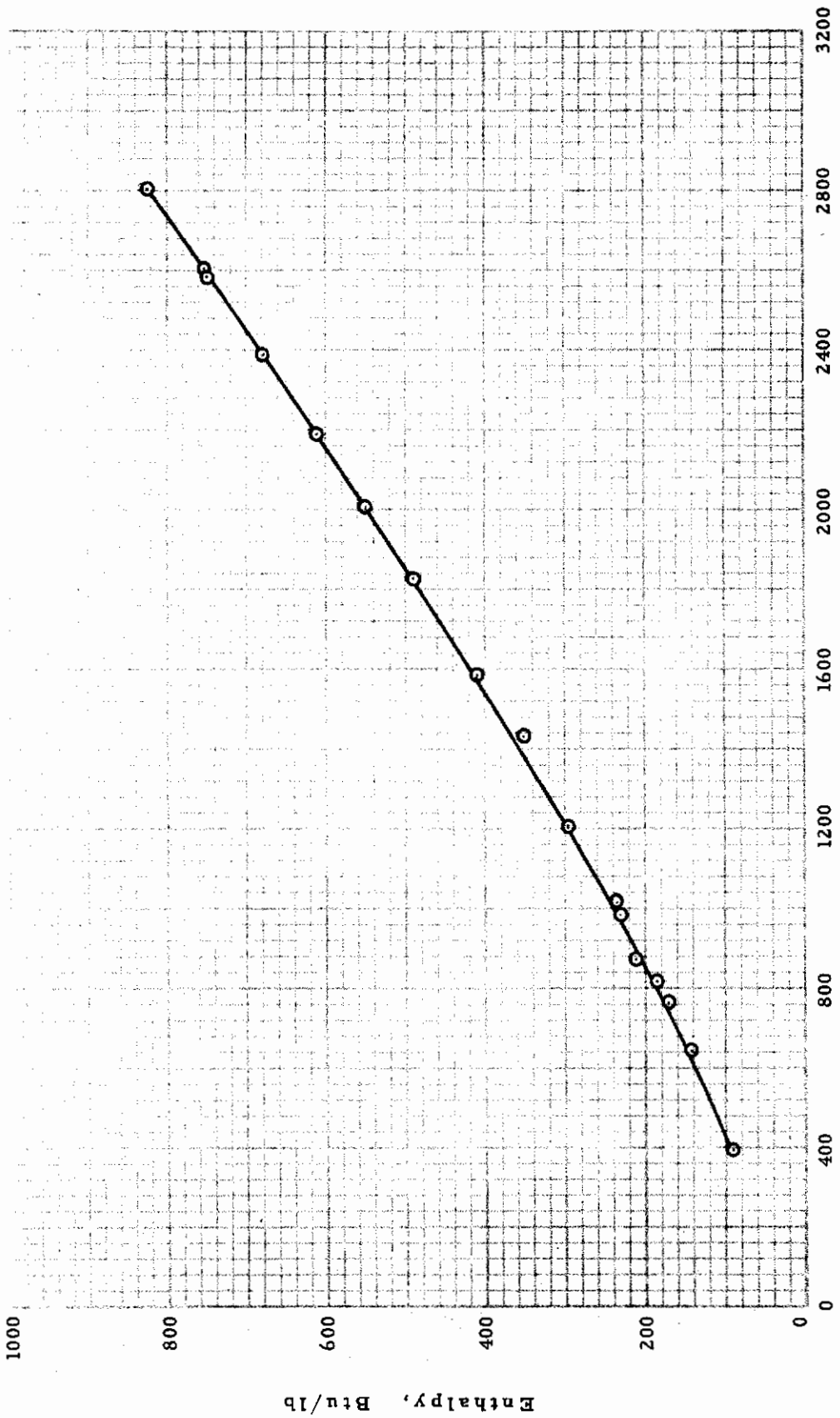

Figure 32 ENTHALPY OF MAGNESIUM OXIDE

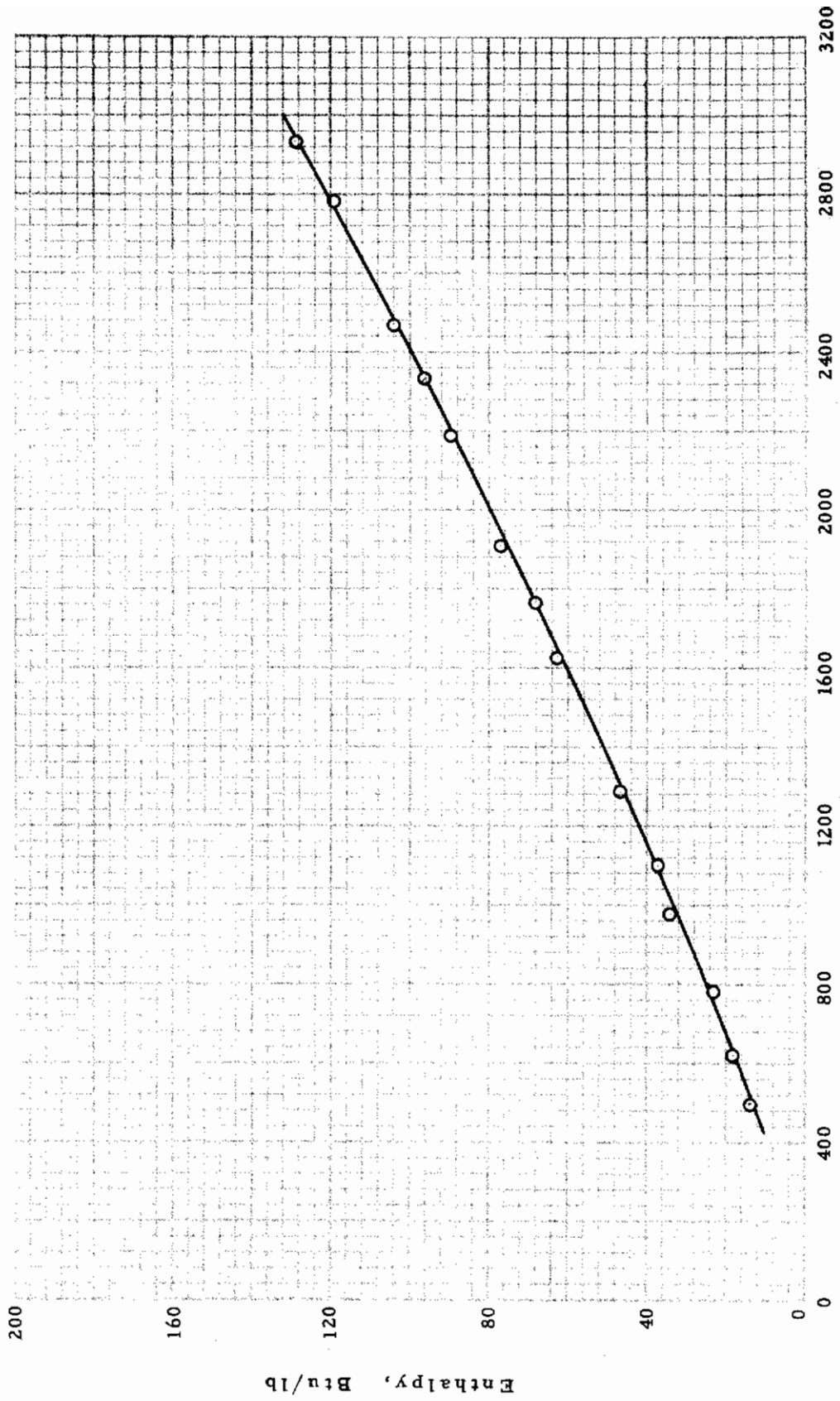

Figure 33 ENTHALPY OF HAFNIUM

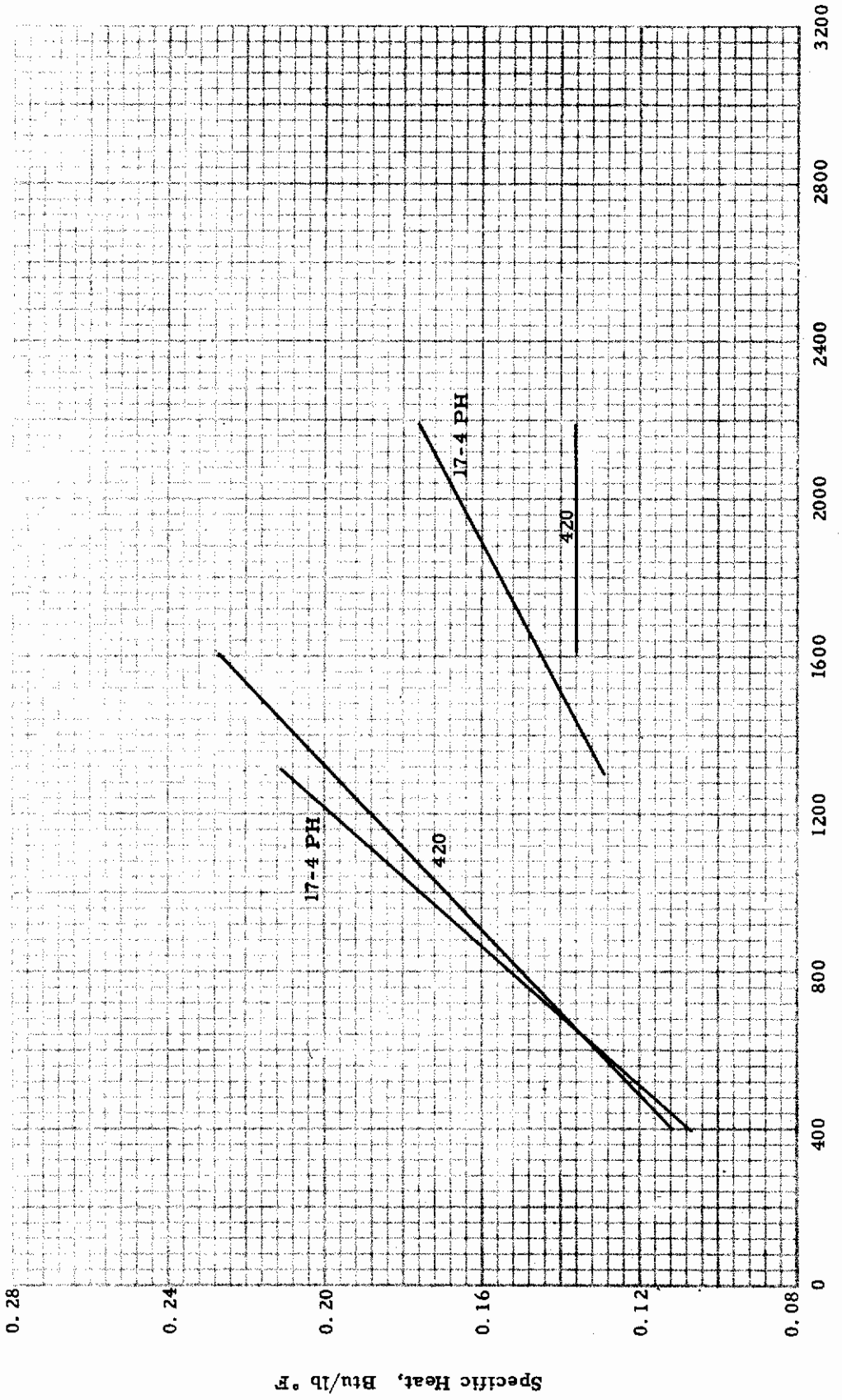

Figure 34 SPECIFIC HEATS OF STAINLESS STEEL TYPES 420 AND 17-4 PH

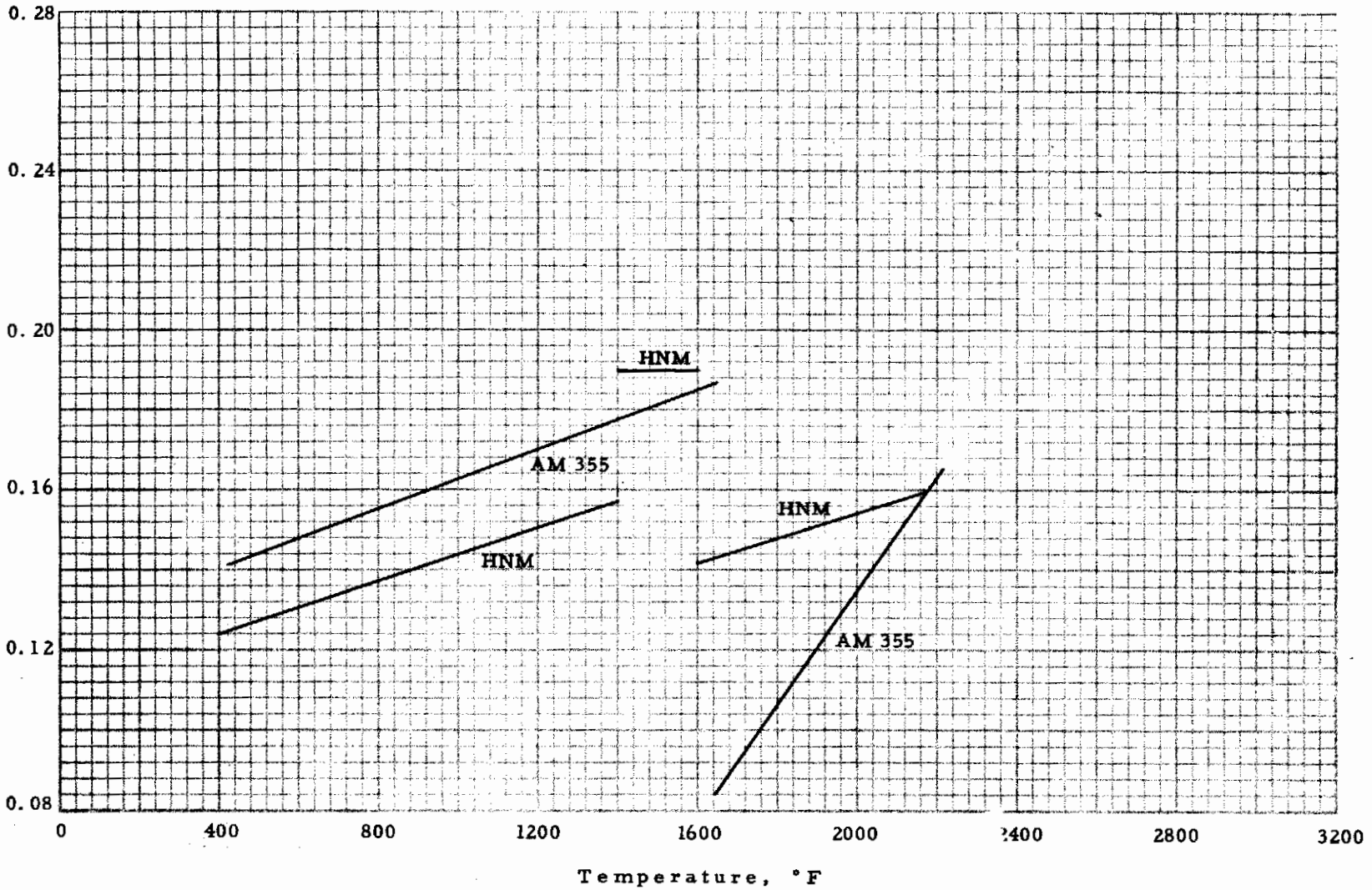

Figure 35 SPECIFIC HEATS OF AM 355 AND CRUCIBLE HNM

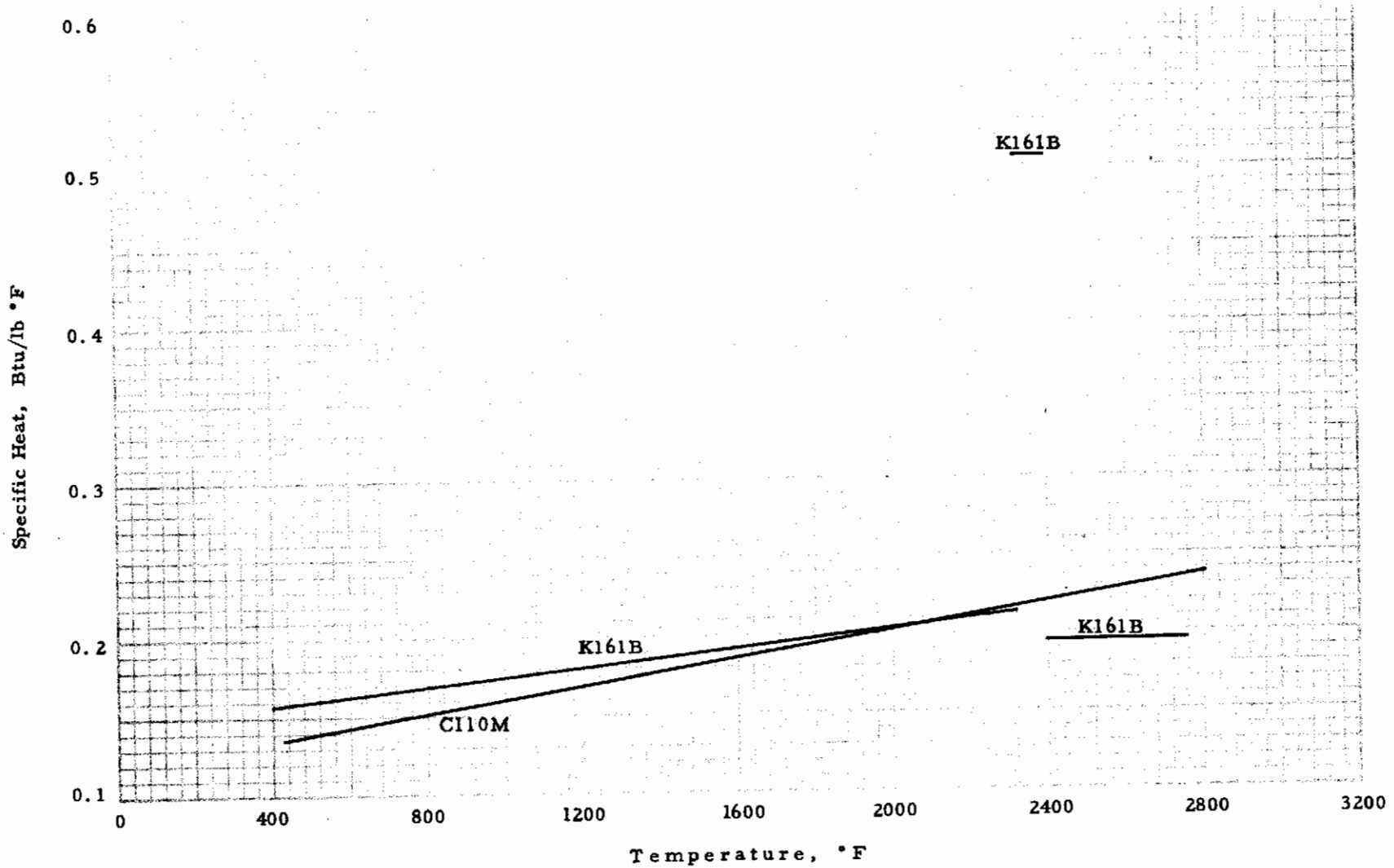

Figure 36 SPECIFIC HEATS OF KENNAMETAL K161B AND TITANIUM C110M

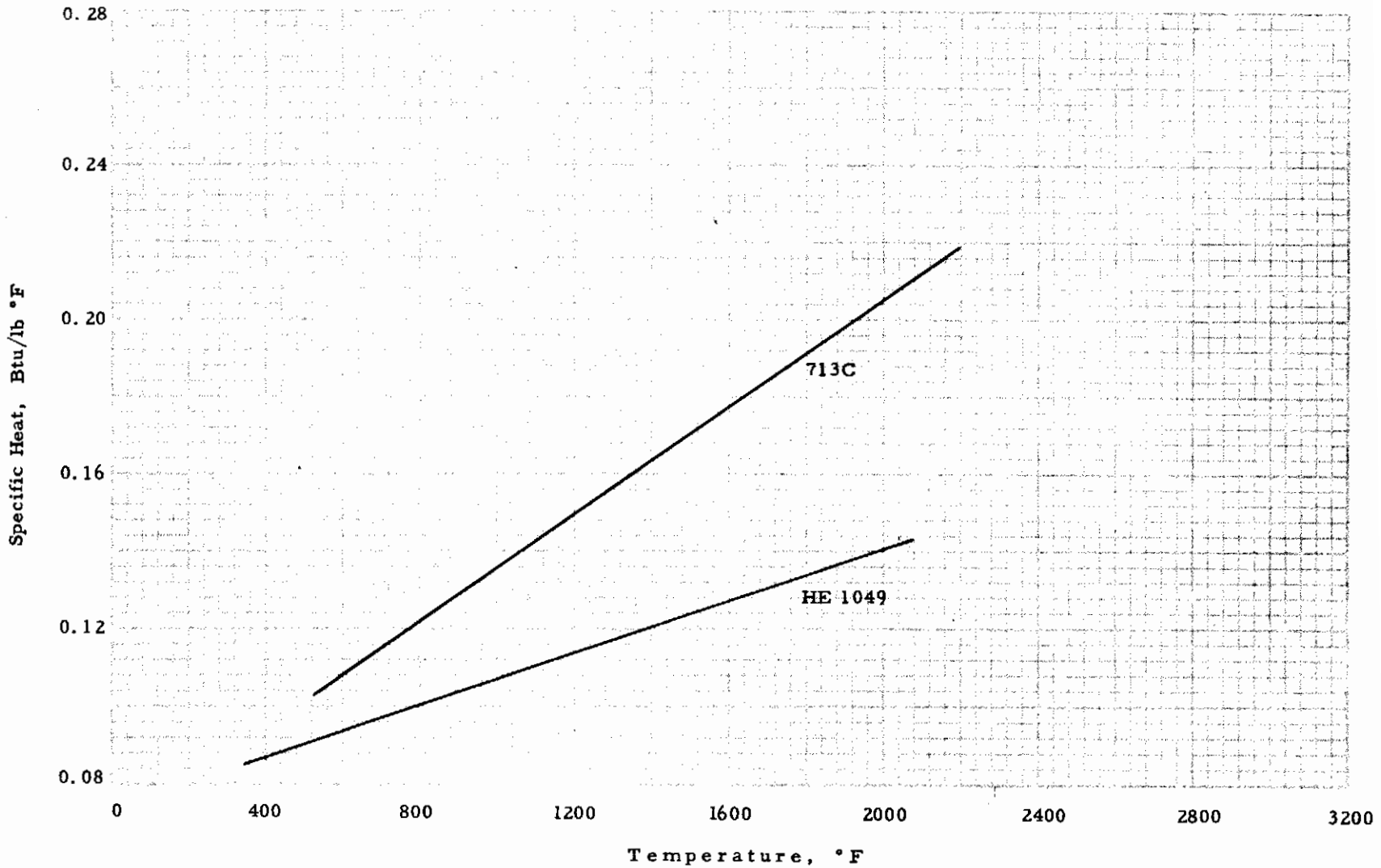

Figure 37 SPECIFIC HEATS OF INCO 713C AND HAYNES STELLITE HE 1049

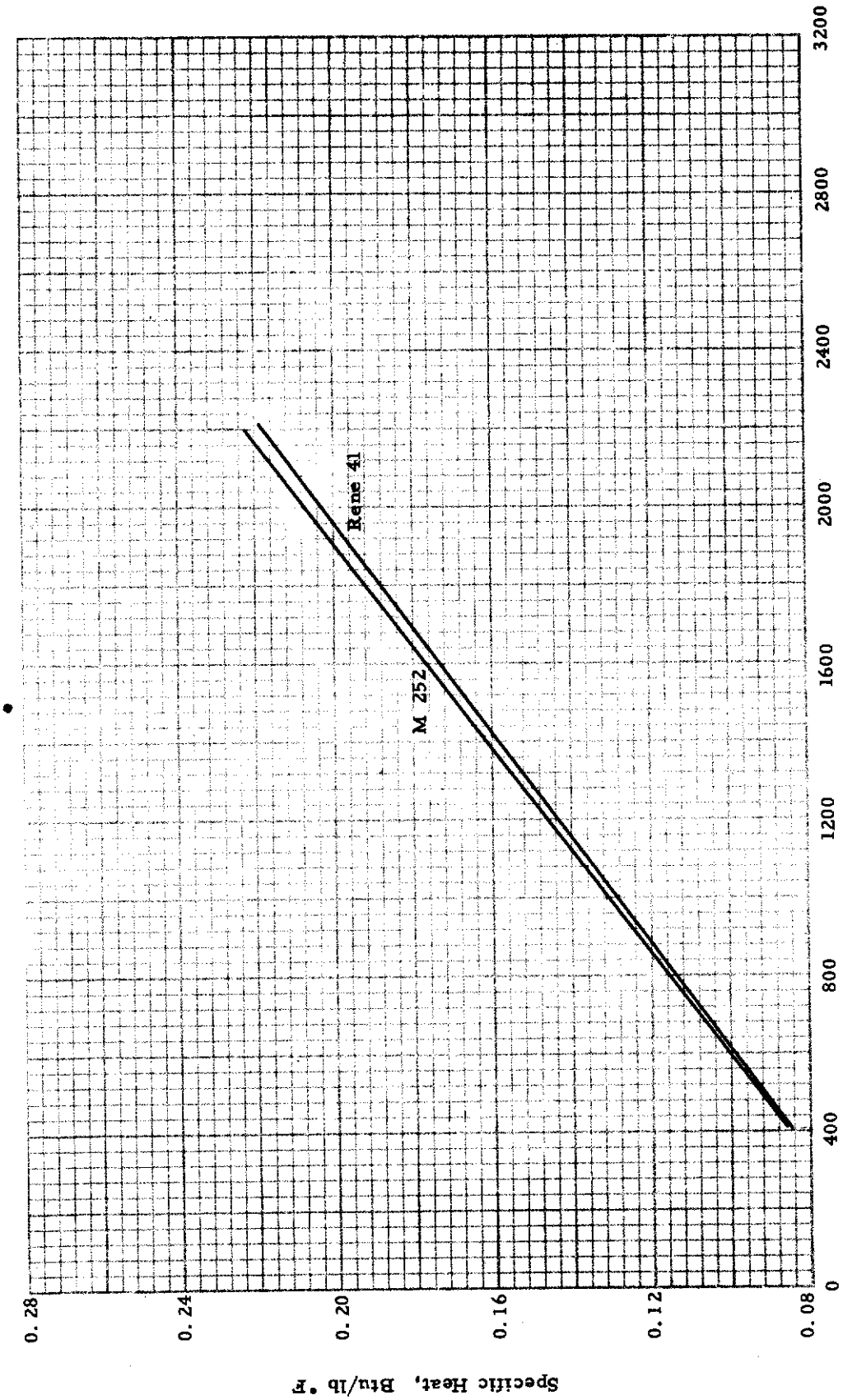

Figure 38 SPECIFIC HEATS OF M 252 AND RENE 41

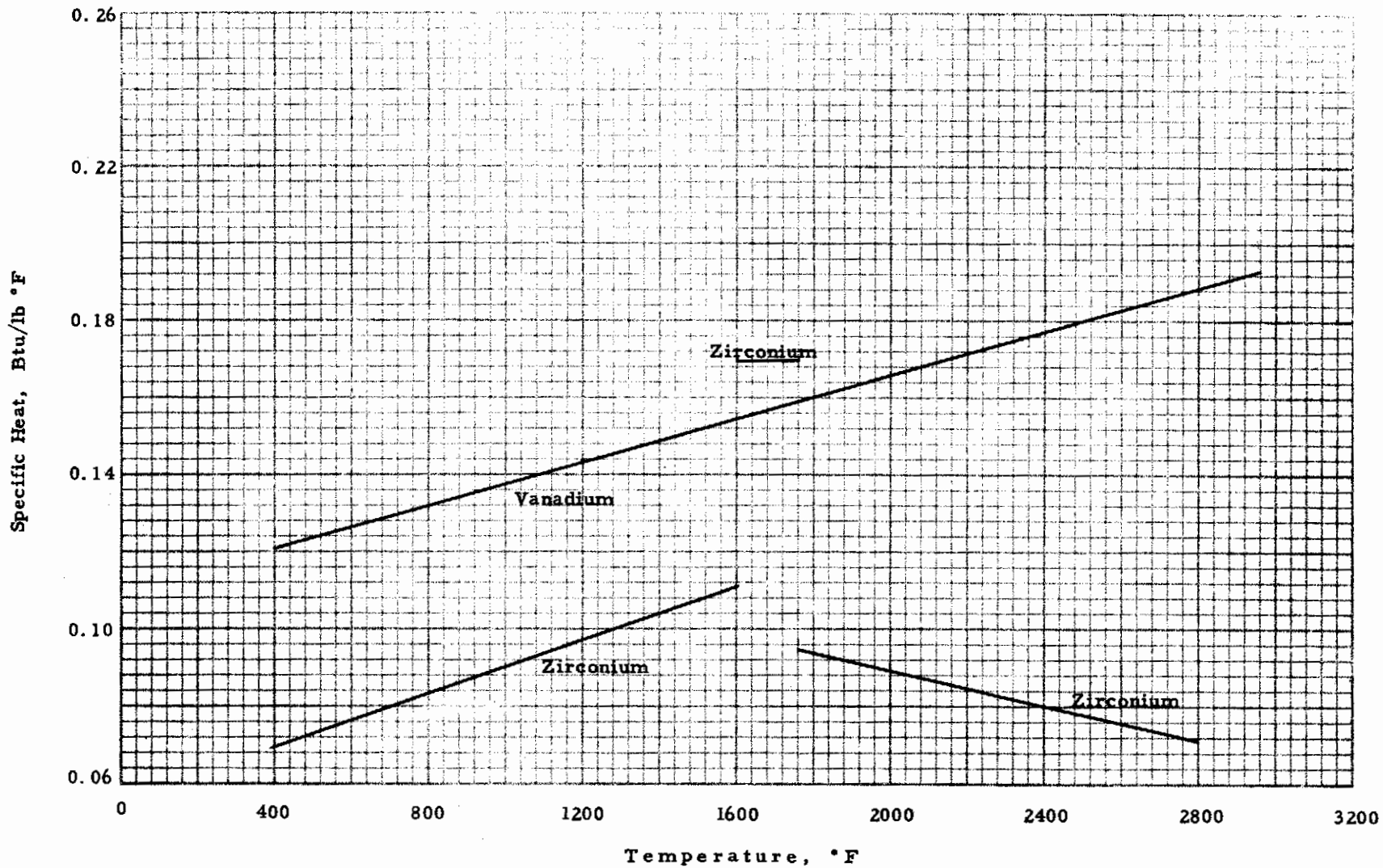

Figure 39 SPECIFIC HEATS OF VANADIUM AND ZIRCONIUM

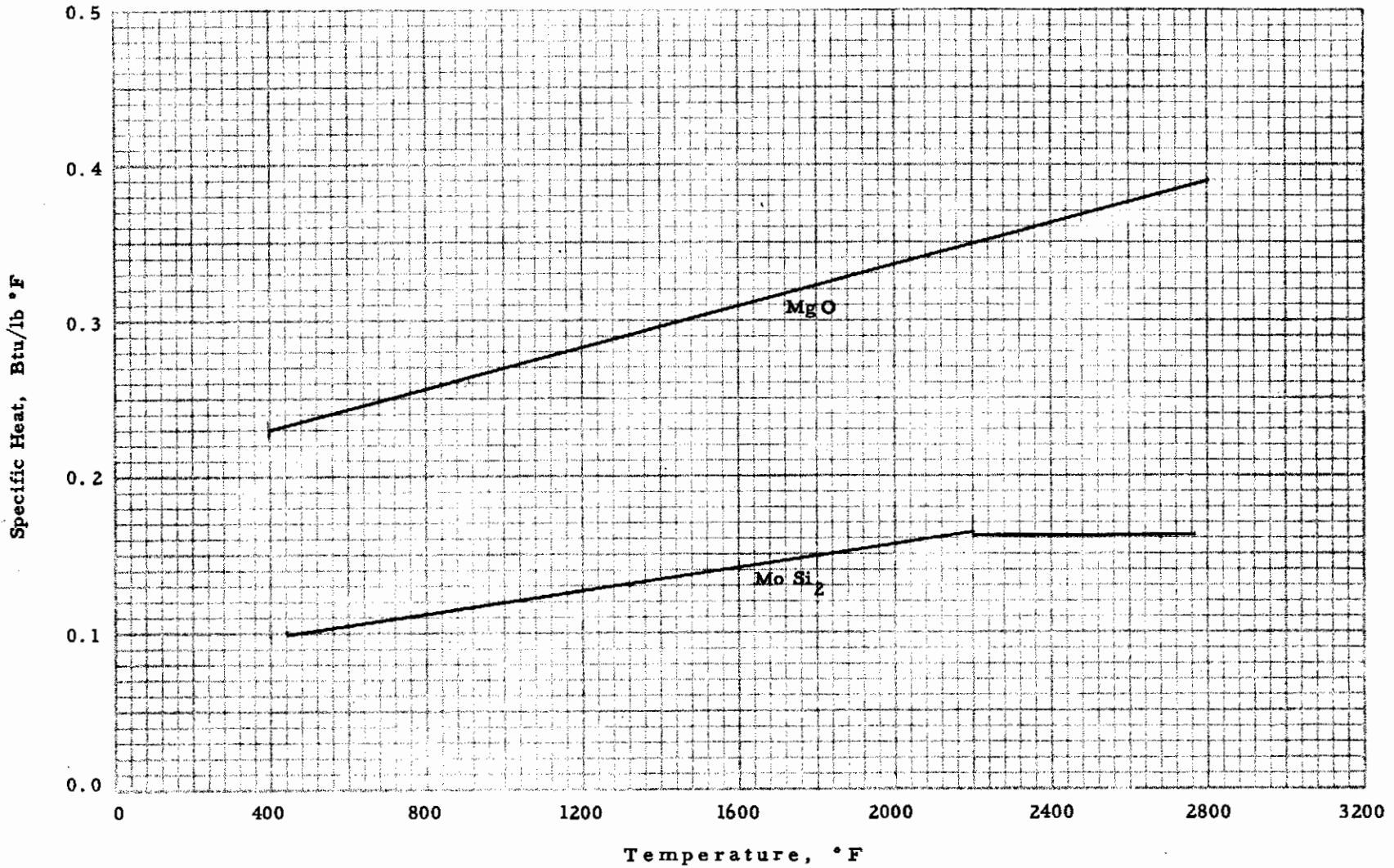

Figure 40 SPECIFIC HEATS OF MOLYBDENUM DISILICIDE AND MAGNESIUM OXIDE

Figure 41 SPECIFIC HEAT OF HAFNIUM

LINEAR THERMAL EXPANSION

APPARATUS

A schematic diagram of the apparatus is shown in Figure 42. The furnace is heated by three banks of globar elements at the front, middle and rear of the furnace. Each bank of globar elements may be heated independently so as to insure a uniform temperature along the middle of the furnace. Preliminary tests indicated that the variation of temperature of the specimens along their length was within 5°F. The furnace temperature was measured by platinum, platinum-10% rhodium thermocouples located one inch from either end of the sample and the sample temperature was measured by a thermocouple located in one end of the specimen.

The specimen is mounted in a ceramic tube in the center of the furnace, with the ceramic pins pointing upward. In this position the line-up is such that the pins may be seen from outside the furnace and the distance between them is measured directly with the telemicroscopes. During the lower temperature portions of each run, the pins are silhouetted against a lighted white background behind the furnace. Once the interior of the furnace begins to get cherry red, the lights are turned off and the red pins are easily seen against the now dark background. A slow stream of helium is maintained into the ceramic tube supporting the sample to protect the sample from oxidation.

The telemicroscopes are mounted on an Invar bar which has a very low coefficient of thermal expansion and the displacements of the pins are read by means of a micrometer to an accuracy of 0.0001 inch. The complete assembly is shock mounted to minimize vibrations.

OPERATING PROCEDURE

The procedure for operation of the apparatus is outlined below. The outline is presented in chronological order.

1. Two holes are drilled 10 inches apart through a rod of the specimen 1/2 inch in diameter and 11 inches long.

2. A thermocouple is located in a 0.020 inch hole at one end of the specimen.

3. Two ceramic pins are mounted in the holes in the specimen and project out about 1/8 inch from them.

4. The specimen is mounted in the ceramic tube in the furnace with the pins pointing up.

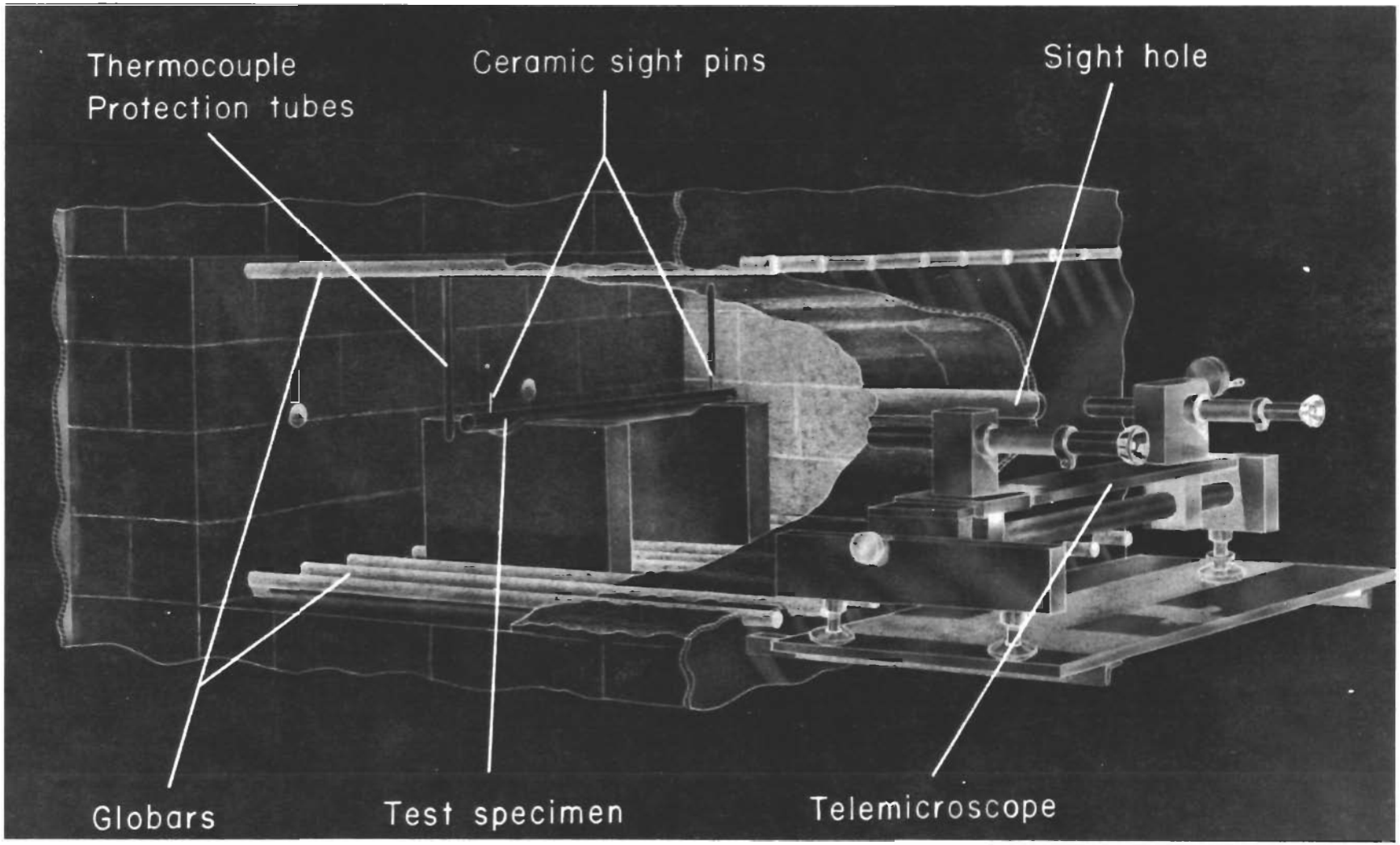

Figure 42 APPARATUS FOR MEASURING LINEAR THERMAL EXPANSION

5. The end cap on the furnace is then closed, and helium gas fed to the ceramic tube supporting the sample.

6. Heat is supplied to the furnace, and temperature and pin displacement measurements are made at regular time intervals. The rate of heating may be varied from 0 to 300°F per hour and still give consistent test results.

7. During the test the optical system is checked by a standard 10 inch Invar bar at room temperature.

The telemicroscope calibration was checked by measurement of the length of standard gage bars. This measurement was conducted by the Gage Laboratory of the Armour Research Foundation. The results of these measurements are presented below.

Table 36

CALIBRATION OF OPTICAL SYSTEM

Gage Bar Length, inches	Telemicroscope Length, inches
9.9000	9.9002
9.9500	9.9505
10.0000	10.0000
10.1000	10.1000
10.2000	10.1995
10.3000	10.2999

RESULTS

The thermal expansion of 15 materials was measured from 80°F to slightly below their melting point, or to 3000°F.

The fractional increases of the sample length, i.e., $\Delta L/L$, are given in Tables 37 to 51 as a function of temperature. These data are plotted in Figures 43 to 57, and the curves drawn through the points. ΔL is the fractional increase in sample length, and L is the sample length at 80°F.

DISCUSSION OF EXPERIMENTAL ERRORS

The measurement of thermal expansion is an absolute measurement and hence all errors are inherent in the apparatus and observer, such as incorrect temperature measurements or variations in the optical system. These sources of error are considered to be relatively small and of a random nature.

Table 37

LINEAR THERMAL EXPANSION
MEASUREMENTS FOR STAINLESS STEEL TYPE 420

Temperature, °F	ΔL/L, %
297	0.022
402	.068
464	.139
502	.195
658	.369
797	.492
907	.574
1058	.666
1201	.772
1350	.897
1386	.940
1416	.953
1467	.979
1517	.873
1554	.803
1595	.869
1705	1.024
1805	1.166
1854	1.235
1895	1.319
1992	1.500
2062	1.595
2102	1.647
2148	1.705

Table 38

LINEAR THERMAL EXPANSION
MEASUREMENTS FOR PH 17-4 (H900)

Temperature, °F	ΔL/L, %
70	0.00
128	0.05
209	0.05
282	0.12
356	0.13
447	0.20
506	0.26
562	0.29
598	0.32
678	0.35
744	0.42
833	0.44
877	0.48
935	0.50
1055	0.59
1171	0.62
1214	0.68
1335	0.66
1396	0.72
1510	0.82
1582	0.92
1645	1.02
1717	1.10
1773	1.19
1797	1.21
1890	1.35
2003	1.44
2088	1.57
2170	1.76
2261	1.86
2309	2.01
2349	2.09

Table 39

LINEAR THERMAL EXPANSION MEASUREMENTS FOR AM 355

Temperature, °F	ΔL/L, %
232	0.024
296	0.054
374	0.085
550	0.172
655	0.258
733	0.322
806	0.394
901	0.506
967	0.559
1044	0.612
1102	0.659
1146	0.678
1198	0.703
1249	0.716
1302	0.683
1335	0.644
1355	0.639
1398	0.634
1431	0.655
1450	0.666
1549	0.746
1651	0.849
1750	0.947
1801	1.007
1908	1.150
1983	1.284
2104	1.430
2201	1.559
2304	1.692
2391	1.819

Table 40

LINEAR THERMAL EXPANSION MEASUREMENTS FOR CRUCIBLE HNM

Temperature, °F	ΔL/L, %
70	0.00
128	0.04
209	0.14
282	0.19
356	0.25
447	0.32
506	0.42
562	0.44
598	0.50
678	0.61
744	0.68
833	0.80
877	0.82
935	0.84
1055	0.97
1171	1.13
1214	1.19
1335	1.33
1396	1.37
1510	1.49
1582	1.58
1645	1.66
1717	1.77
1773	1.85
1797	1.89
1890	1.94
2003	2.13
2088	2.30
2170	2.49
2261	2.65
2309	2.75

Table 41

THERMAL LINEAR EXPANSION MEASUREMENTS FOR TITANIUM C110M

Temperature, °F	ΔL/L, %
200	0.061
356	0.124
472	0.161
600	0.243
748	0.363
869	0.446
1001	0.531
1095	0.635
1203	0.864
1342	1.238
1449	1.280
1582	1.411
1683	1.520
1801	1.803
1891	1.976
2016	2.221
2114	2.605
2241	2.852
2363	3.177
2502	3.485
2598	3.770
2687	3.992

Table 42

LINEAR THERMAL EXPANSION MEASUREMENTS FOR INCO 713C

Temperature, °F	ΔL/L, %
204	0.041
351	0.126
443	0.207
560	0.307
646	0.389
750	0.482
850	0.570
905	0.609
1002	0.680
1100	0.769
1197	0.863
1301	0.975
1362	1.046
1501	1.180
1556	1.236
1661	1.385
1755	1.517
1872	1.673
1994	1.917
2110	2.114
2161	2.216
2247	2.358
2352	2.578

Table 43

LINEAR THERMAL EXPANSION MEASUREMENTS FOR HE 1049

Temperature, °F	ΔL/L, %
80	0
299	0.040
378	0.067
498	0.135
700	0.283
799	0.431
897	0.565
997	0.660
1103	0.848
1292	0.983
1394	1.144
1598	1.494
1700	1.602
1913	1.939
2051	2.100

Table 44

LINEAR THERMAL EXPANSION
MEASUREMENTS FOR KENNAMETAL K161B

Temperature, °F	ΔL/L, %
195	0.018
271	.042
368	.073
468	.112
755	.197
673	.223
778	.226
870	.337
983	.395
1083	.444
1178	.509
1290	.601
1448	.634
1600	.744
1727	.824
1829	.863
1979	.946
2134	1.019
2252	1.116
2326	1.149
2400	1.371
2466	1.502
2526	1.689
2582	1.858
2645	1.978
2763	2.283

Table 45

LINEAR THERMAL EXPANSION
MEASUREMENTS FOR M252 (GE J1500)

Temperature, °F	ΔL/L, %
70	0.00
153	0.09
233	0.14
287	0.18
341	0.25
487	0.41
529	0.43
578	0.48
626	0.51
669	0.54
763	0.66
816	0.67
970	0.79
1115	0.88
1192	0.93
1266	0.97
1314	1.04
1386	1.08
1527	1.24
1577	1.33
1649	1.42
1727	1.53
1818	1.67
1887	1.78
2044	1.94
2169	2.13
2256	2.26
2312	2.46
2333	2.54

Table 46

LINEAR THERMAL EXPANSION MEASUREMENTS FOR RENE 41

Temperature, °F	ΔL/L, %
70	0.00
153	0.07
233	0.14
287	0.22
341	0.25
487	0.38
529	0.42
578	0.47
626	0.49
669	0.50
763	0.64
816	0.65
970	0.78
1115	0.89
1192	0.94
1266	1.00
1314	1.04
1386	1.10
1527	1.24
1577	1.31
1649	1.40
1727	1.52
1818	1.68
1887	1.76
2044	1.92
2169	2.12
2256	2.25
2312	2.42
2333	2.54

Table 47

LINEAR THERMAL EXPANSION MEASUREMENTS FOR VANADIUM

Temperature, °F	ΔL/L, %
70	0.0
152	0.04
188	0.06
276	0.09
603	0.27
734	0.37
825	0.36
978	0.45
1159	0.57
1263	0.63
1414	0.74
1460	0.77
1658	0.92
1793	1.04
1904	1.12
1992	1.16
2060	1.24
2253	1.37
2359	1.48
2436	1.58
2501	1.73
2557	1.88
2614	2.10
2672	2.37
2701	2.50
2748	2.71
2776	2.94
2665	2.94

Table 48

LINEAR THERMAL EXPANSION MEASUREMENTS FOR ZIRCONIUM

Temperature, °F	ΔL/L, %
70	0.00
160	0.04
294	0.05
379	0.12
457	0.13
524	0.14
590	0.16
637	0.15
746	0.18
915	0.21
1045	0.33
1129	0.30
1196	0.35
1309	0.31
1297	0.31
1410	0.32
1499	0.34
1572	0.37
1629	0.40
1703	0.50
1751	0.55
1831	0.62
1972	0.65
2069	0.75
2133	0.74
2206	0.86
2249	0.89
2295	0.98
2341	1.05
2670	1.23
2660	1.24
2670	1.30
2860	1.53
2960	1.56

Table 49

LINEAR THERMAL EXPANSION
MEASUREMENTS FOR MOLYBDENUM DISILICIDE

Temperature, °F	ΔL/L, %
80	0.0
176	0.009
250	0.029
418	0.041
495	0.060
595	0.112
717	0.168
812	0.200
902	0.274
994	0.300
1096	0.397
1197	0.454
1424	0.594
1499	0.622
1597	0.672
1695	0.762
1793	0.791
1897	0.887
1991	0.950
2098	1.04
2233	1.13
2298	1.17
2397	1.20
2509	1.25
2592	1.29
2696	1.38

Table 50

LINEAR THERMAL EXPANSION MEASUREMENTS FOR MAGNESIUM OXIDE

Temperature, °F	ΔL/L, %
70	0.00
290	0.16
335	0.19
420	0.22
550	0.33
587	0.37
633	0.43
735	0.46
834	0.54
892	0.59
941	0.61
989	0.65
1176	0.75
1328	0.86
1390	0.94
1454	1.00
1514	1.05
1569	1.11
1655	1.17
1757	1.25
1818	1.34
1886	1.42
1924	1.48
1971	1.52
2110	1.60
2195	1.73
2277	1.79
2368	1.86
2428	1.91
2516	1.97
2709	2.11
2785	2.20
2855	2.26
2934	2.30
2975	2.34

Table 51

LINEAR THERMAL EXPANSION MEASUREMENTS FOR HAFNIUM

Temperature, °F	ΔL/L, %
70	0.000
289	0.105
378	0.162
385	0.165
450	0.227
500	0.260
550	0.277
616	0.315
672	0.350
750	0.370
800	0.382
912	0.440
970	0.487
1056	0.505
1117	0.545
1150	0.612
1218	0.622
1253	0.625
1304	0.635
1407	0.680
1459	0.705
1500	0.742
1570	0.807
1629	0.858
1800	0.902
1872	0.927
1940	1.010
2040	1.07
2140	1.15
2240	1.18
2340	1.26
2490	1.34
2690	1.38
2840	1.46

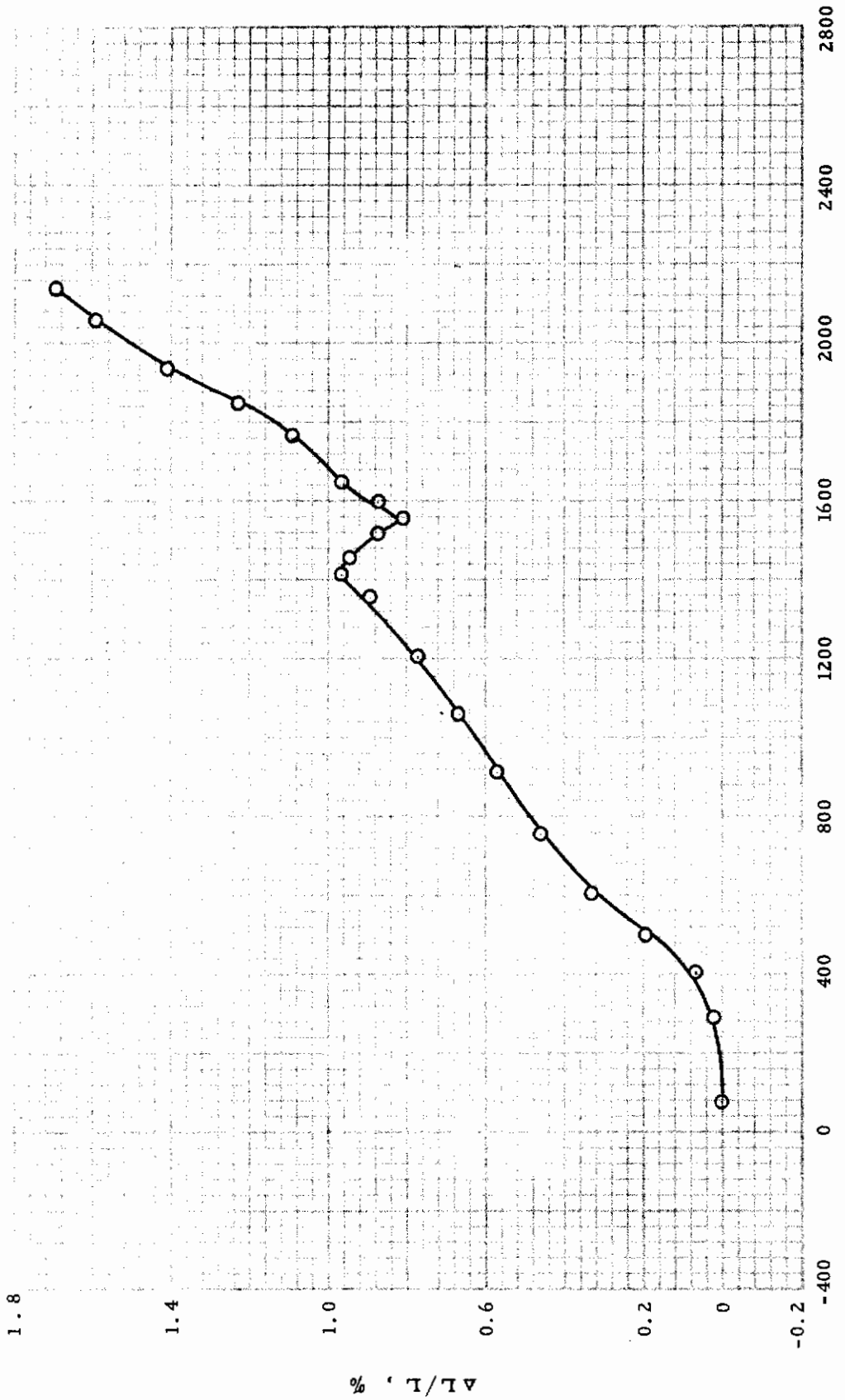

Figure 43 LINEAR THERMAL EXPANSION OF STAINLESS STEEL TYPE 420

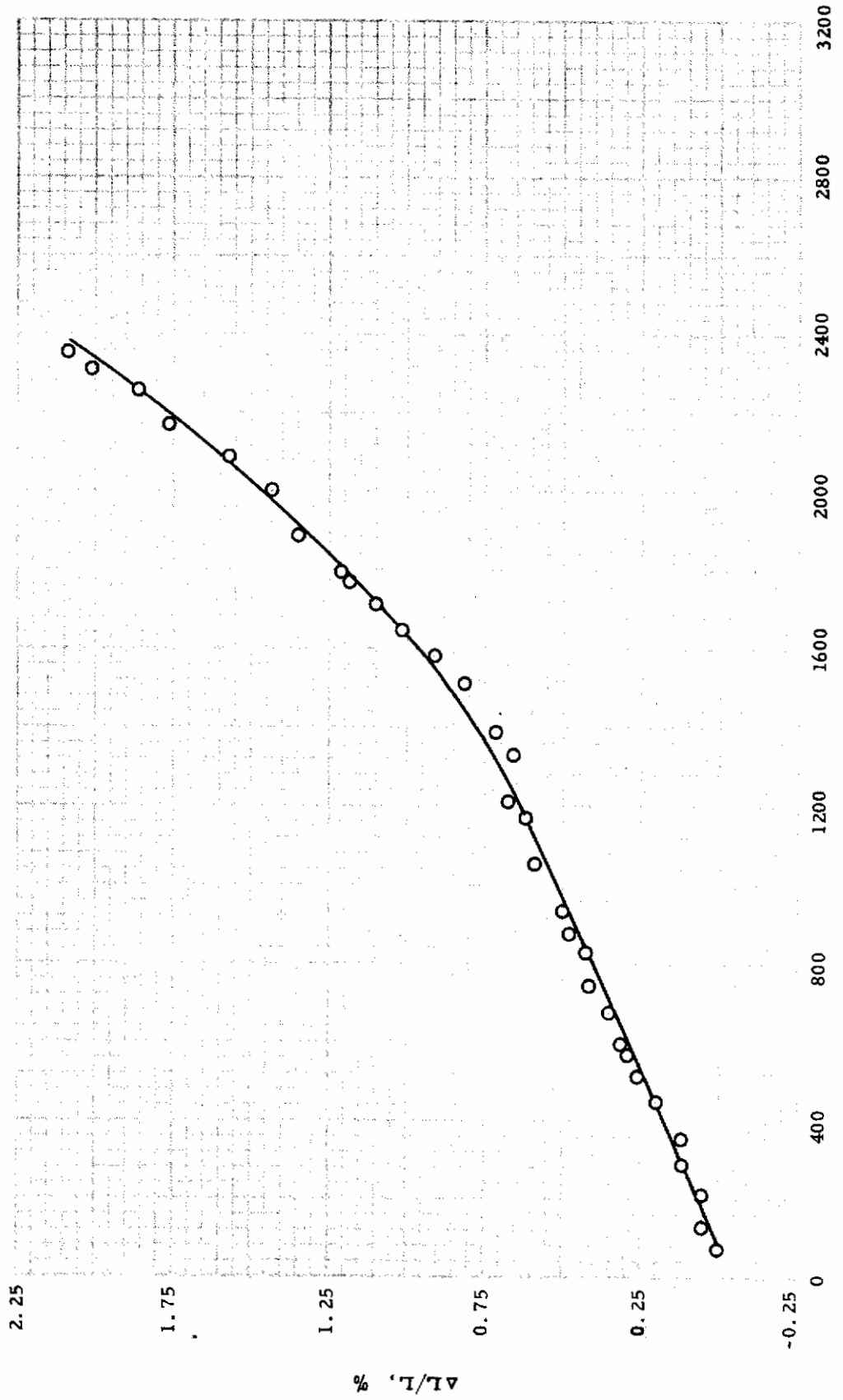

Figure 44 LINEAR THERMAL EXPANSION OF STAINLESS STEEL TYPE PH 17-4

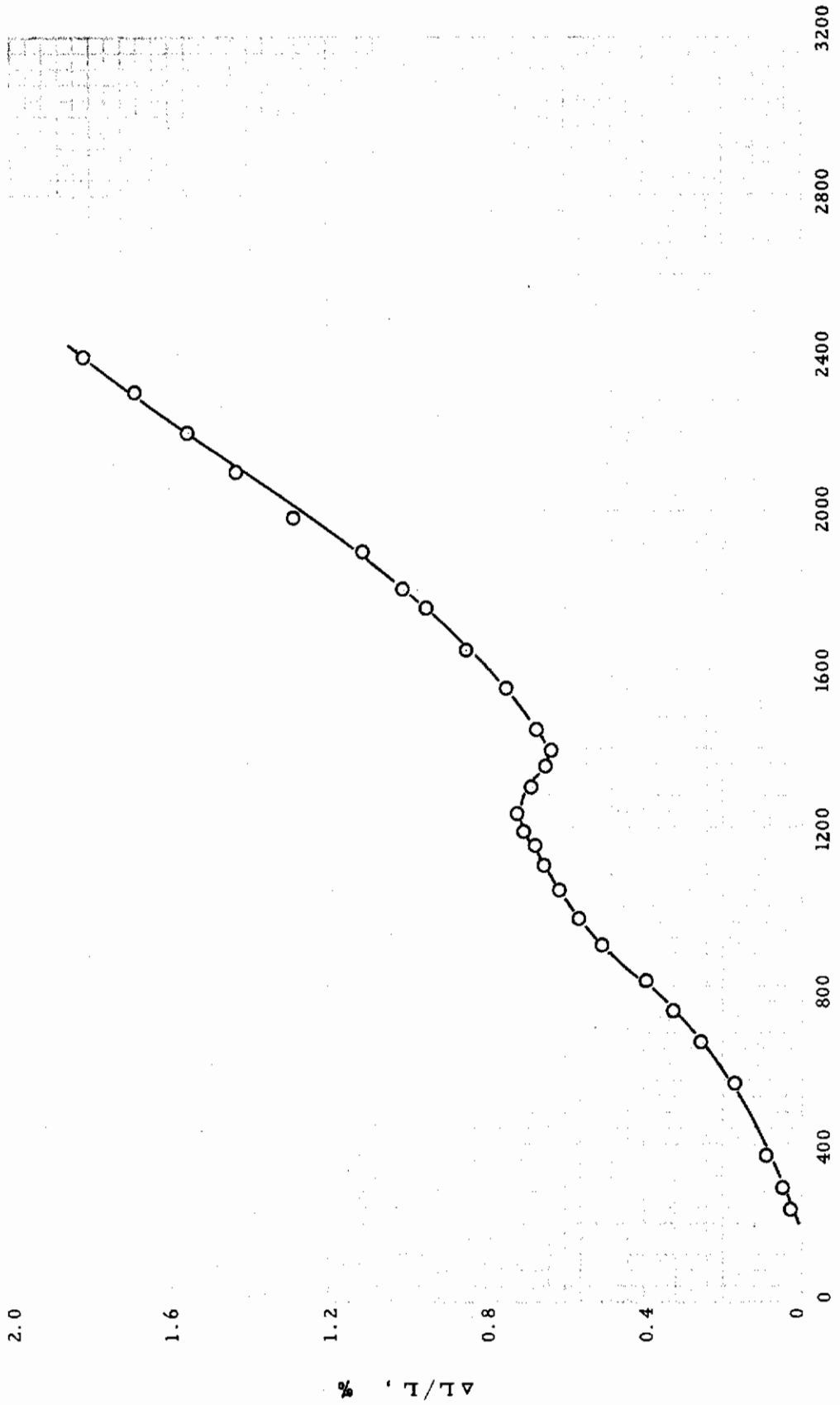

Figure 45 LINEAR THERMAL EXPANSION OF AM 355

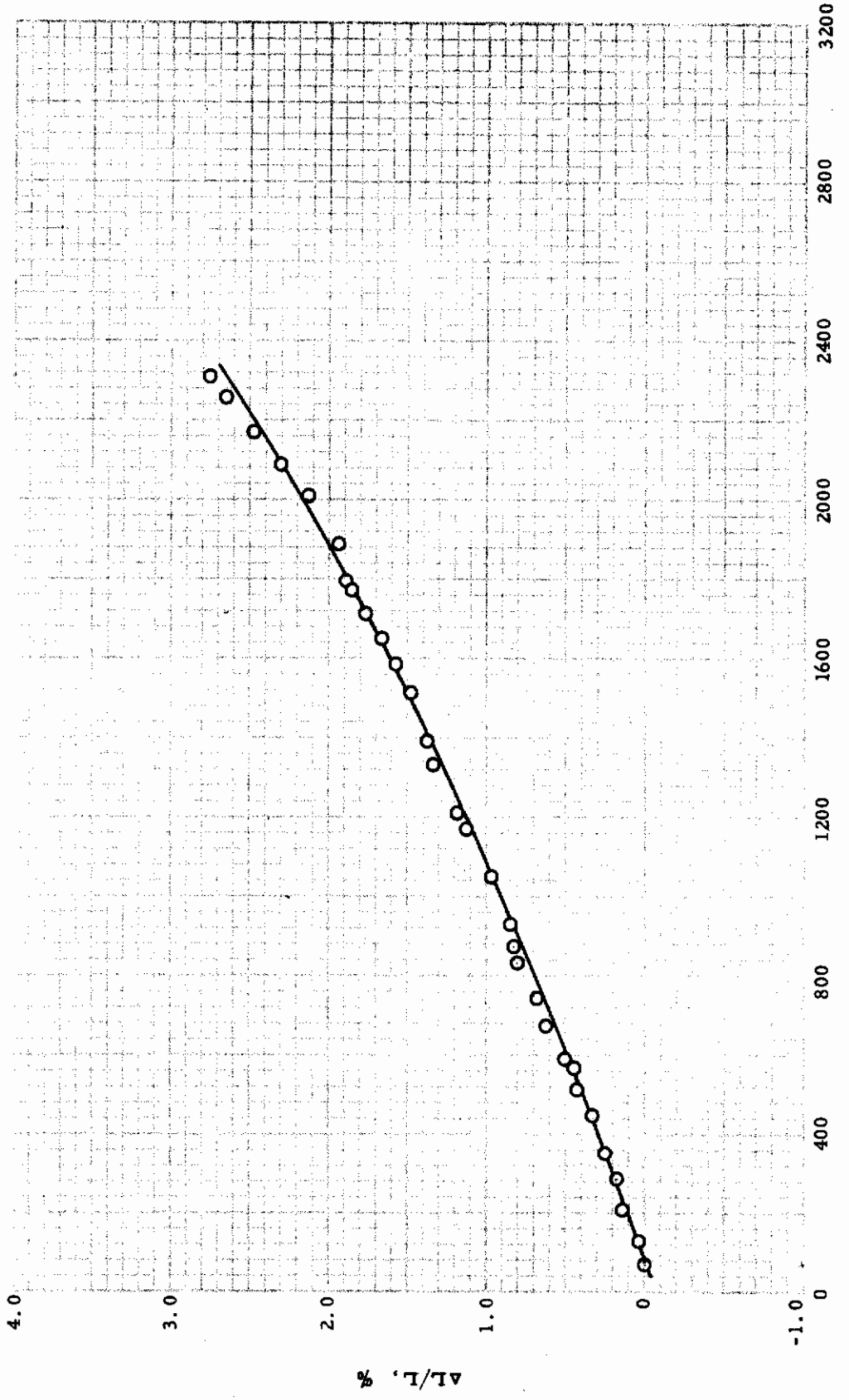

Figure 46 LINEAR THERMAL EXPANSION OF CRUCIBLE HNM

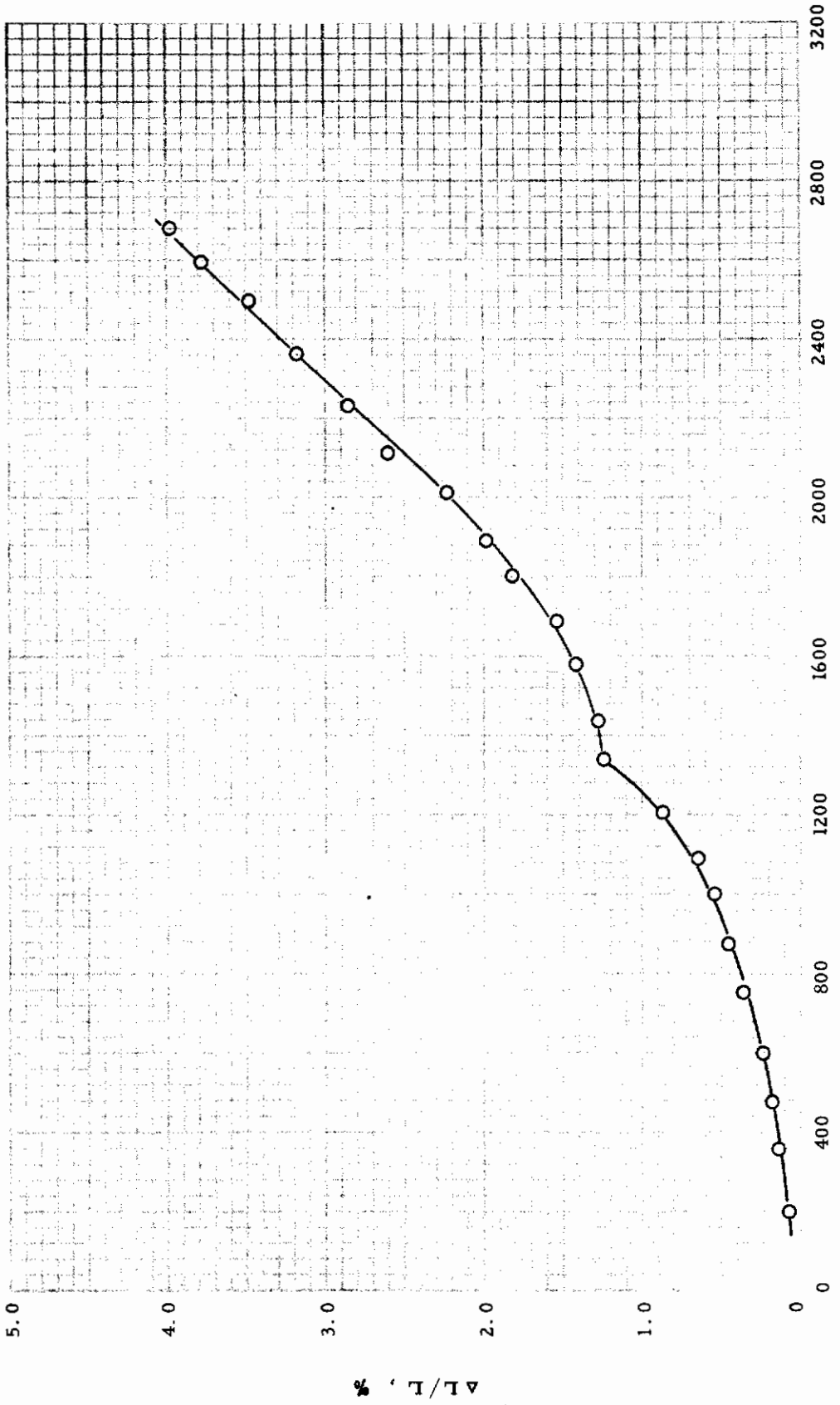

Figure 47 LINEAR THERMAL EXPANSION OF TITANIUM C110M

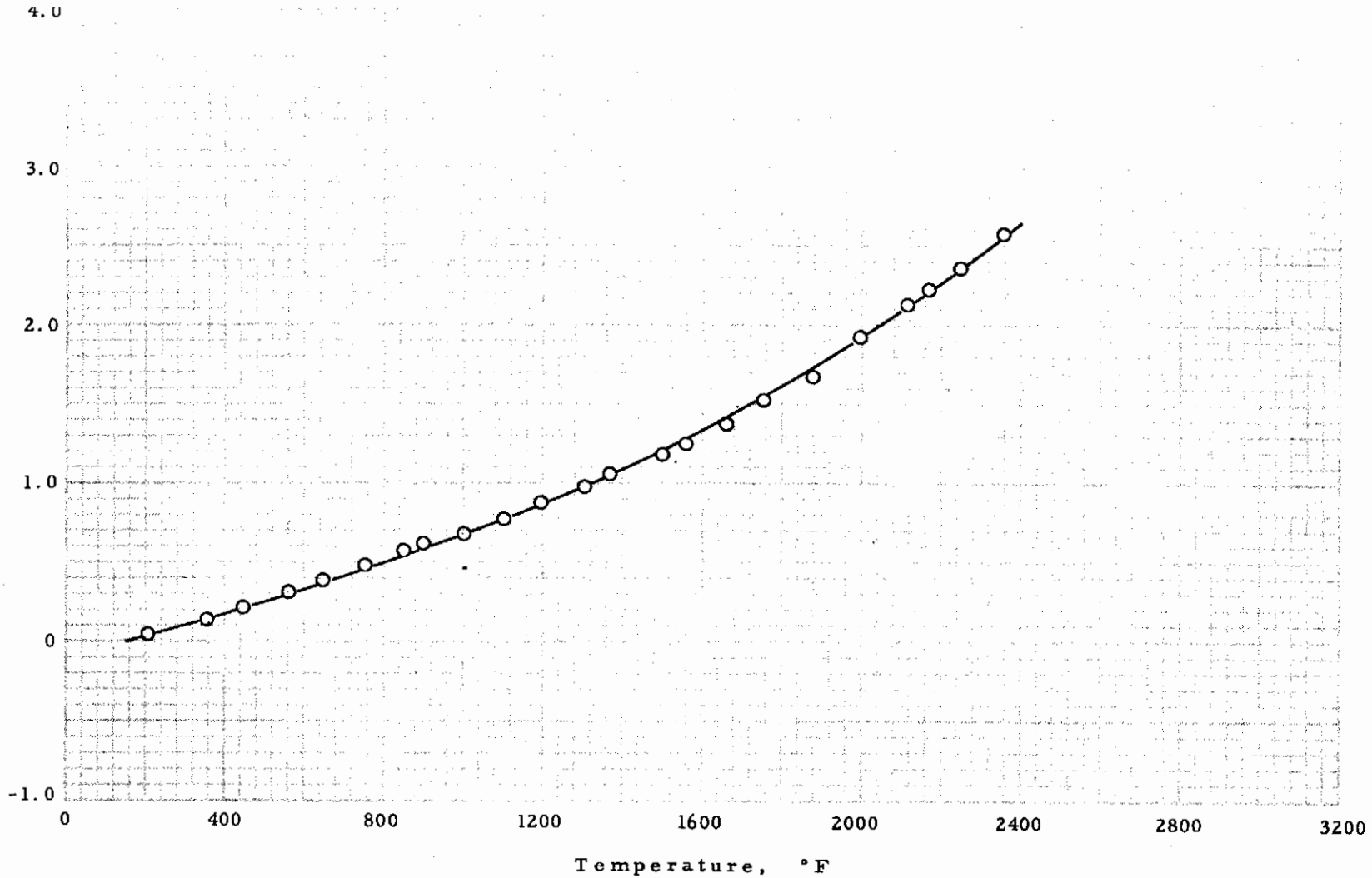

Figure 48 LINEAR THERMAL EXPANSION OF INCO 713C

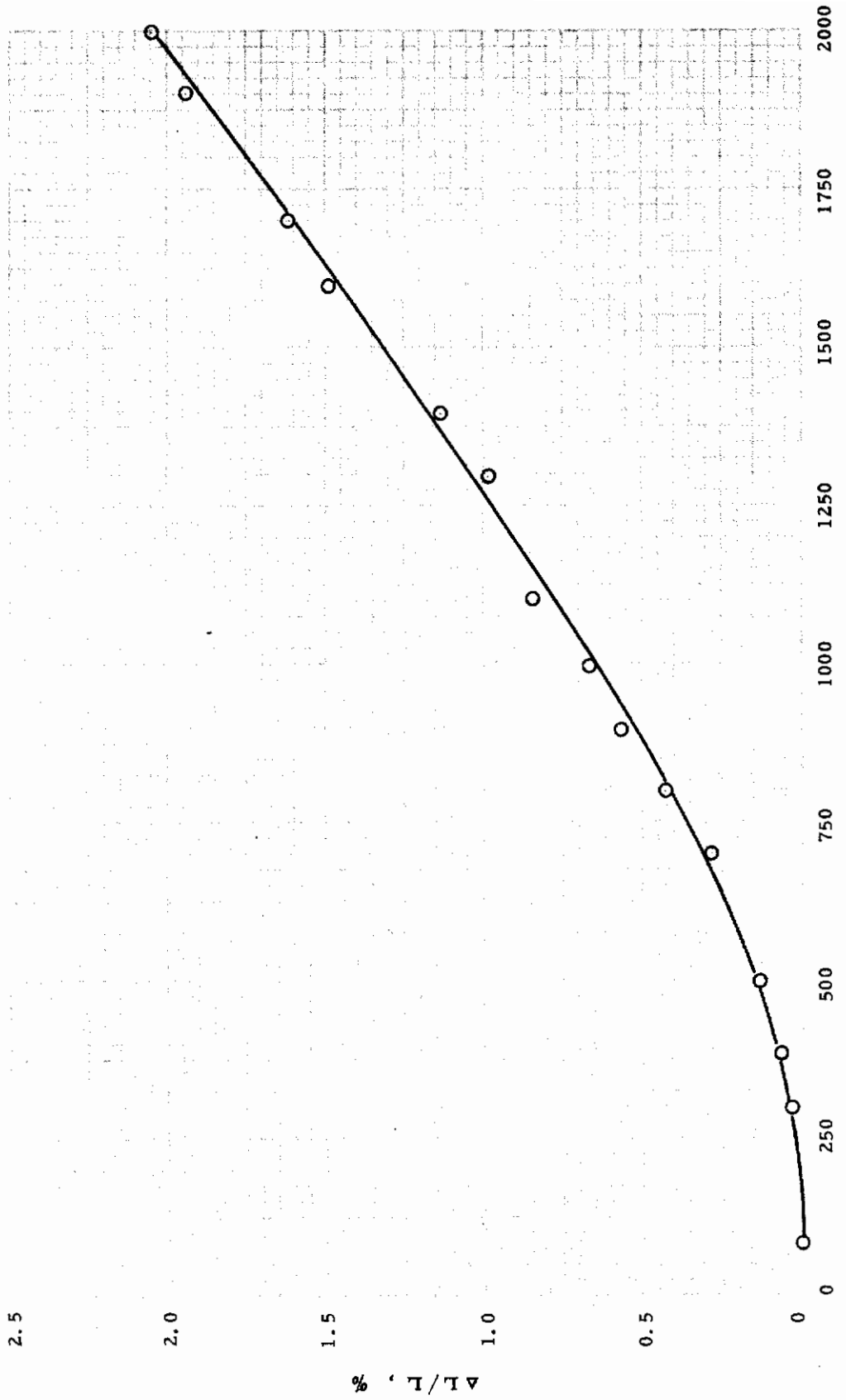

Figure 49 LINEAR THERMAL EXPANSION OF HE 1049

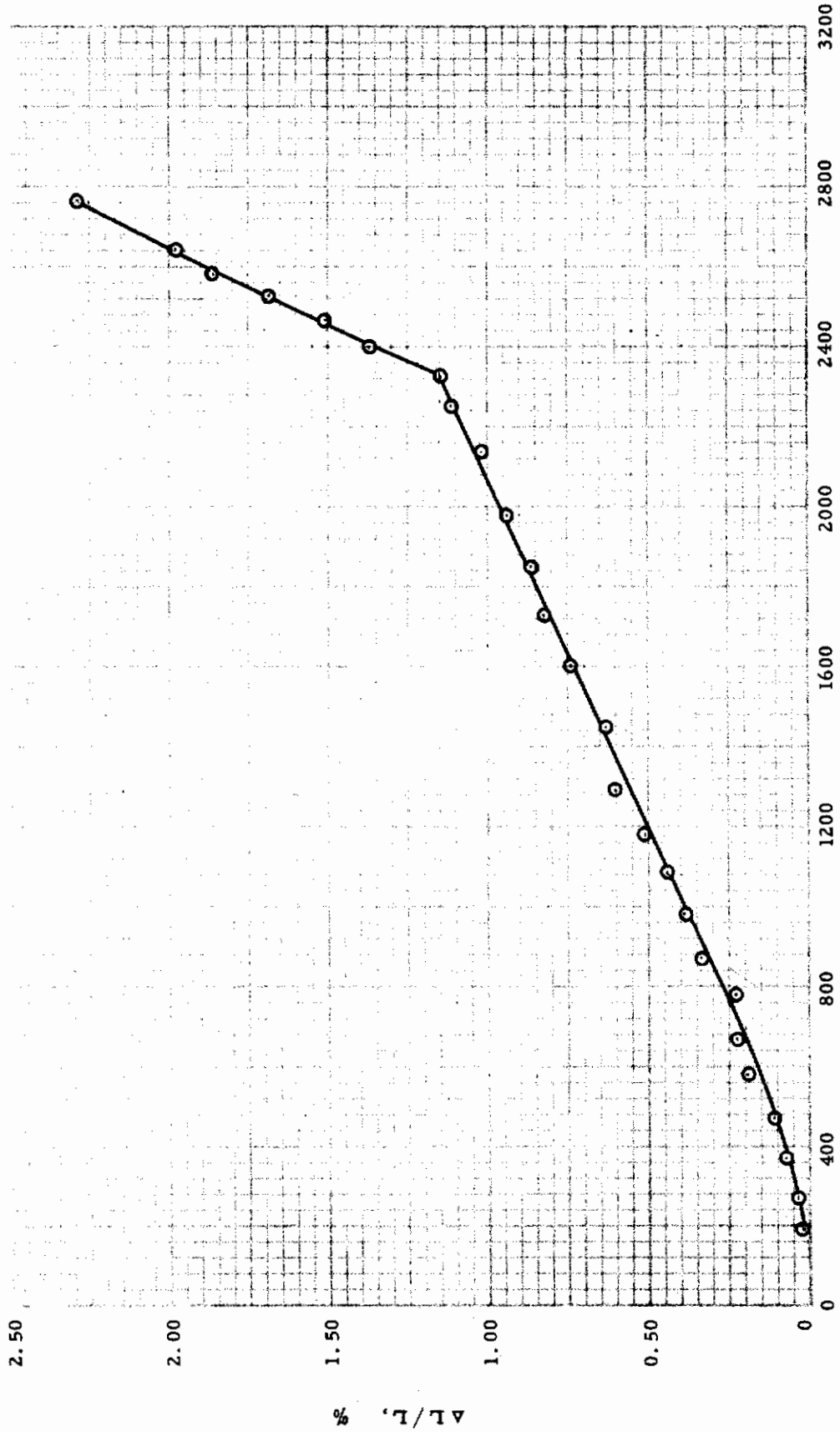

Figure 50 LINEAR THERMAL EXPANSION OF KENNAMETAL K161B

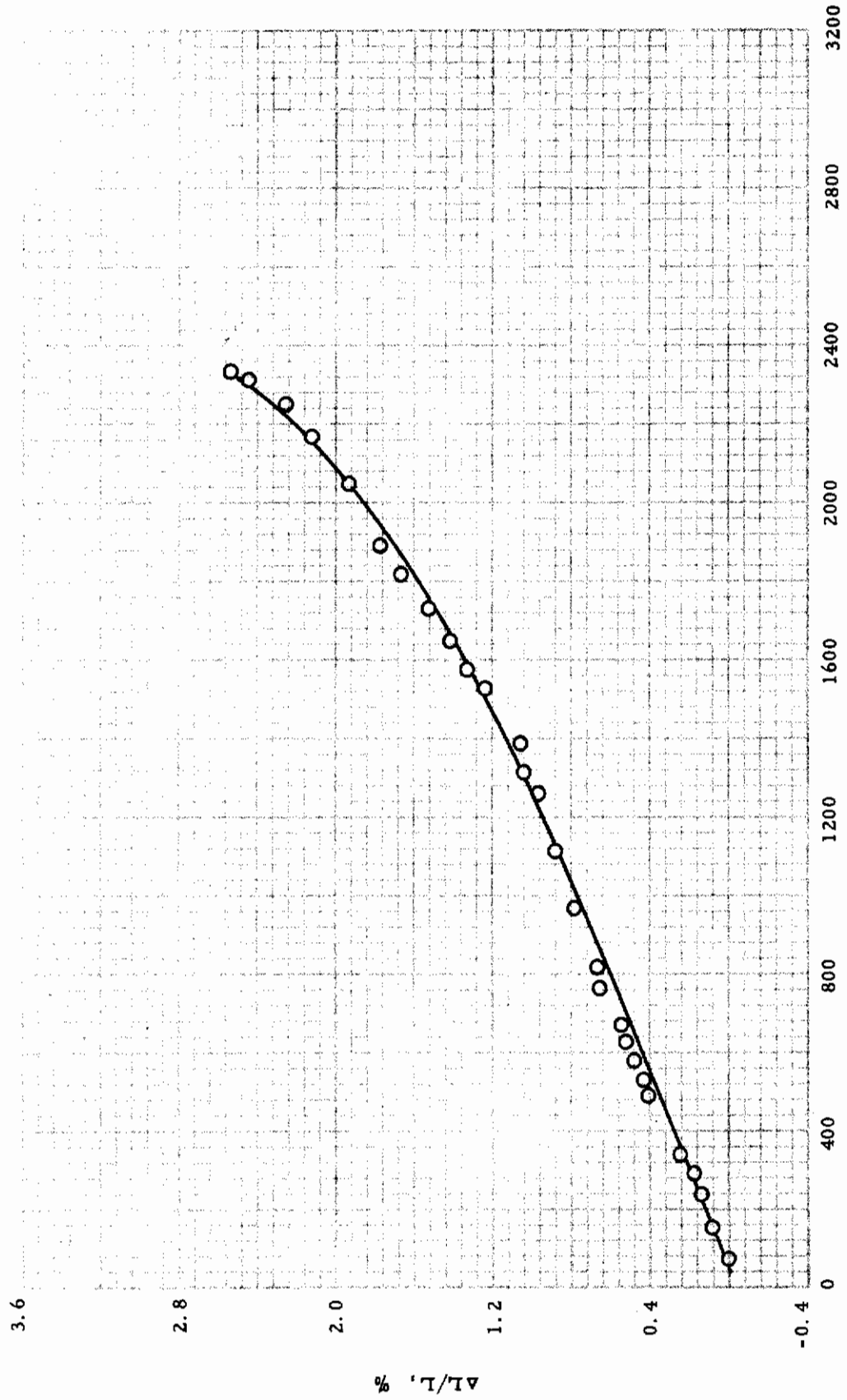

Figure 51 LINEAR THERMAL EXPANSION OF M252

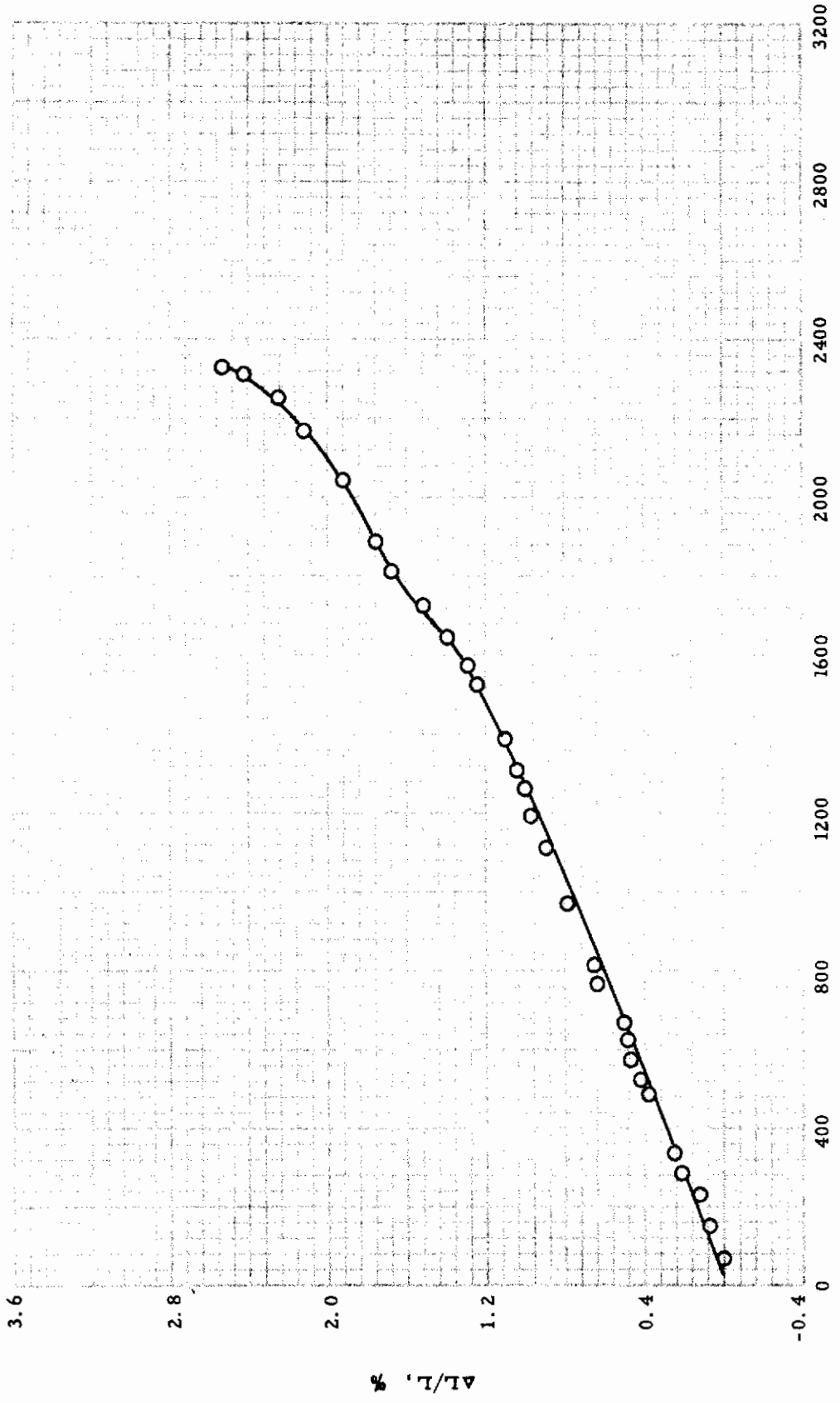

Figure 52 LINEAR THERMAL EXPANSION OF RENE 41

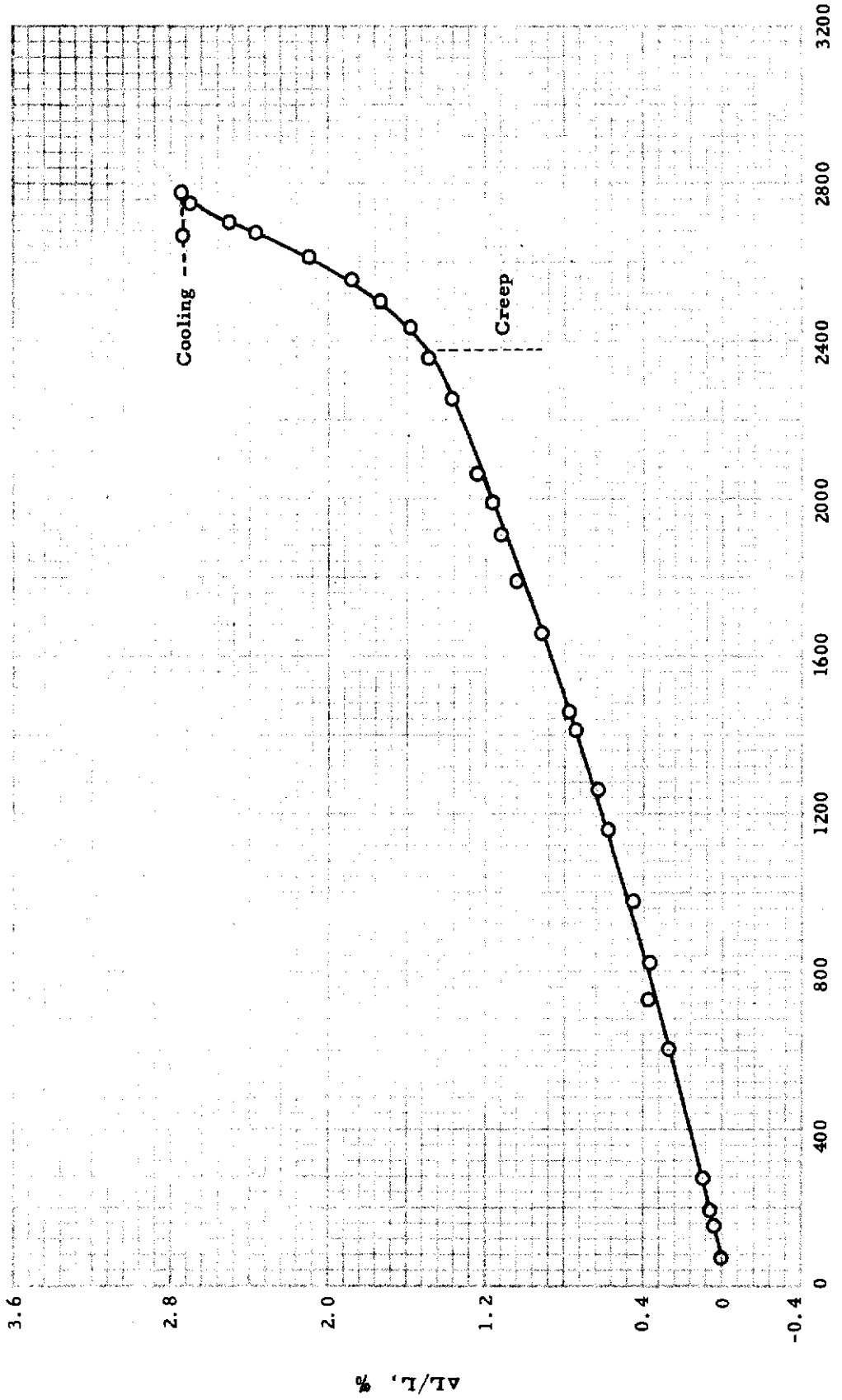

Figure 53 LINEAR THERMAL EXPANSION OF VANADIUM

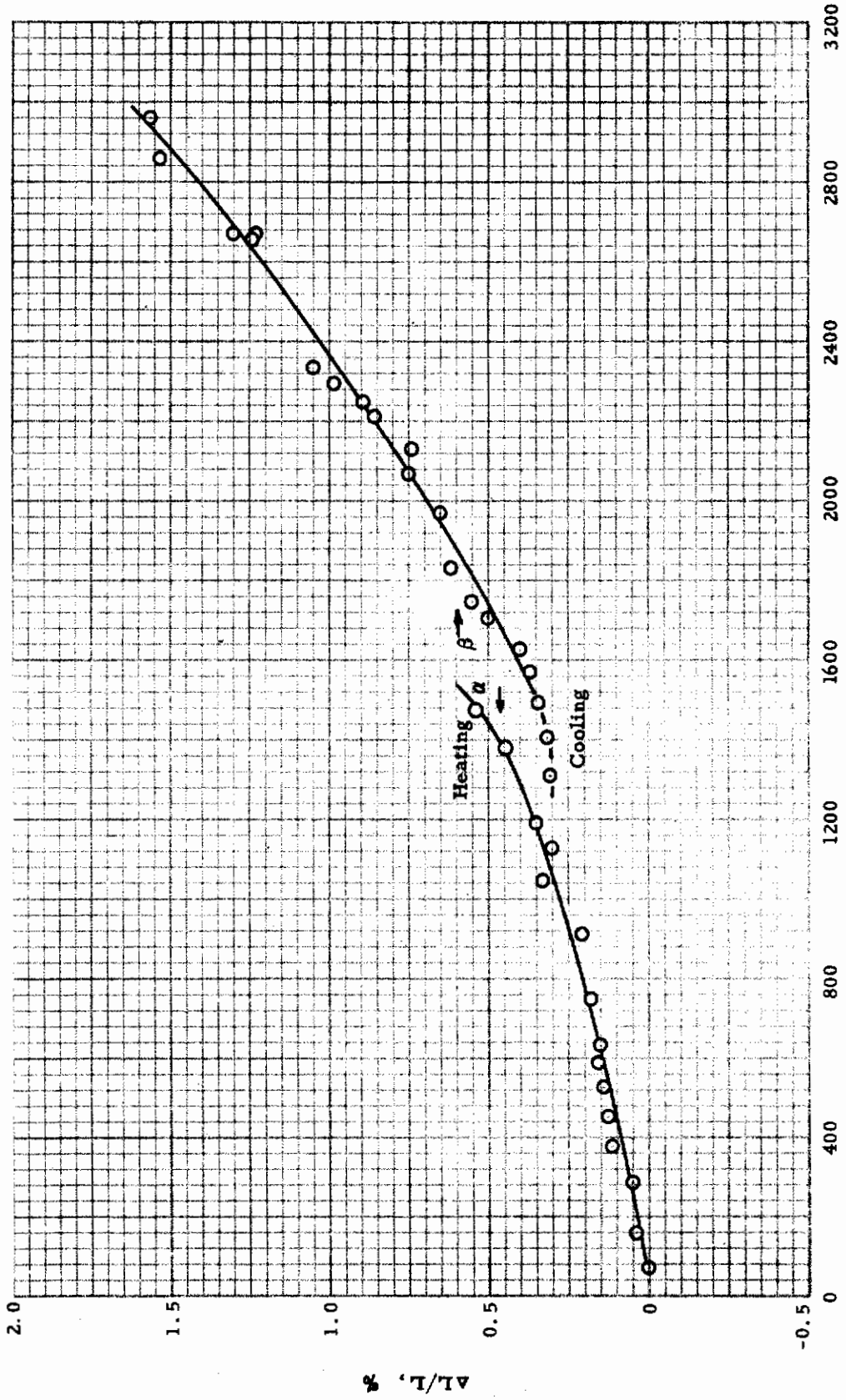

Figure 54 LINEAR THERMAL EXPANSION OF ZIRCONIUM

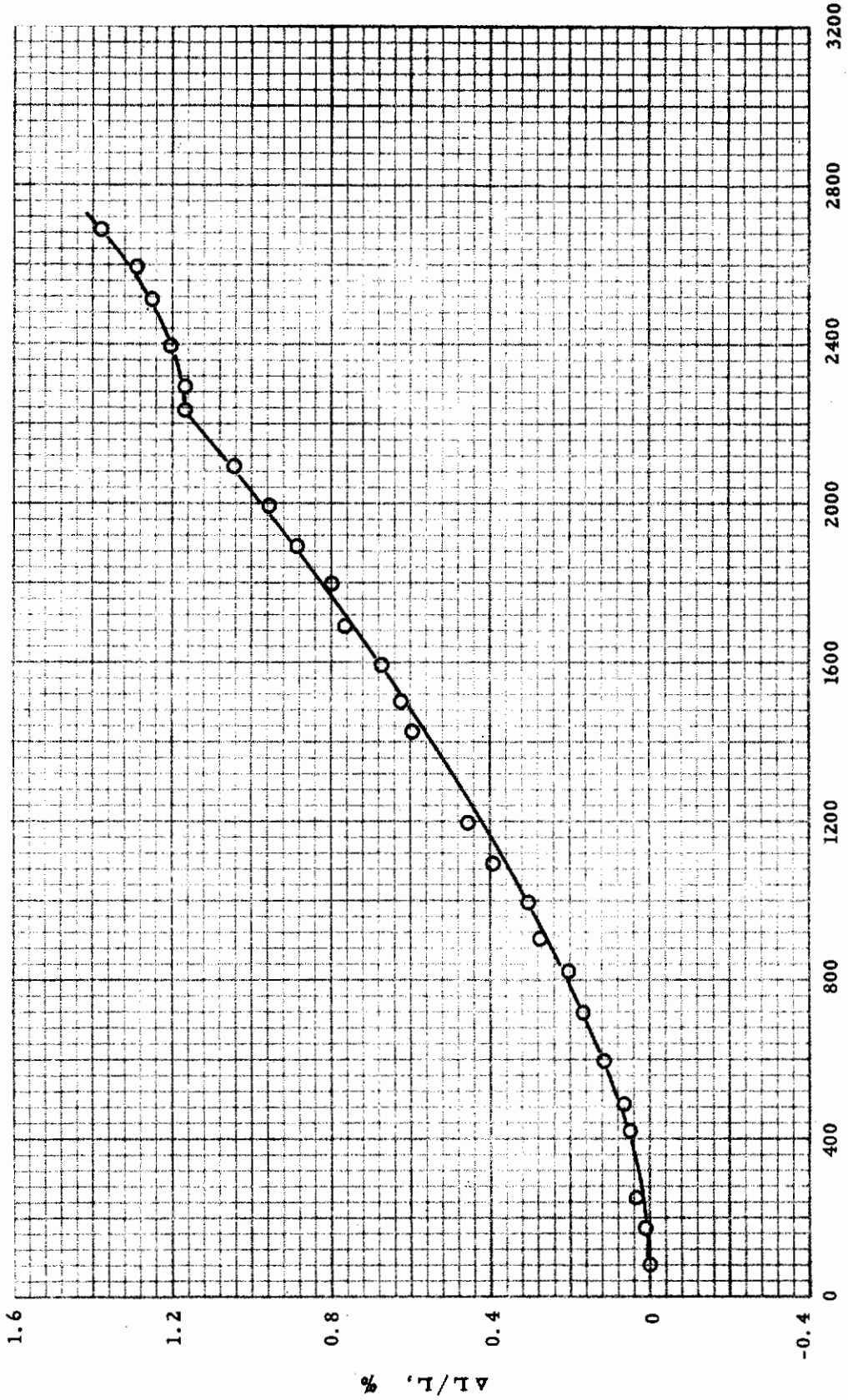

Figure 55 LINEAR THERMAL EXPANSION OF MOLYBDENUM DISILICIDE

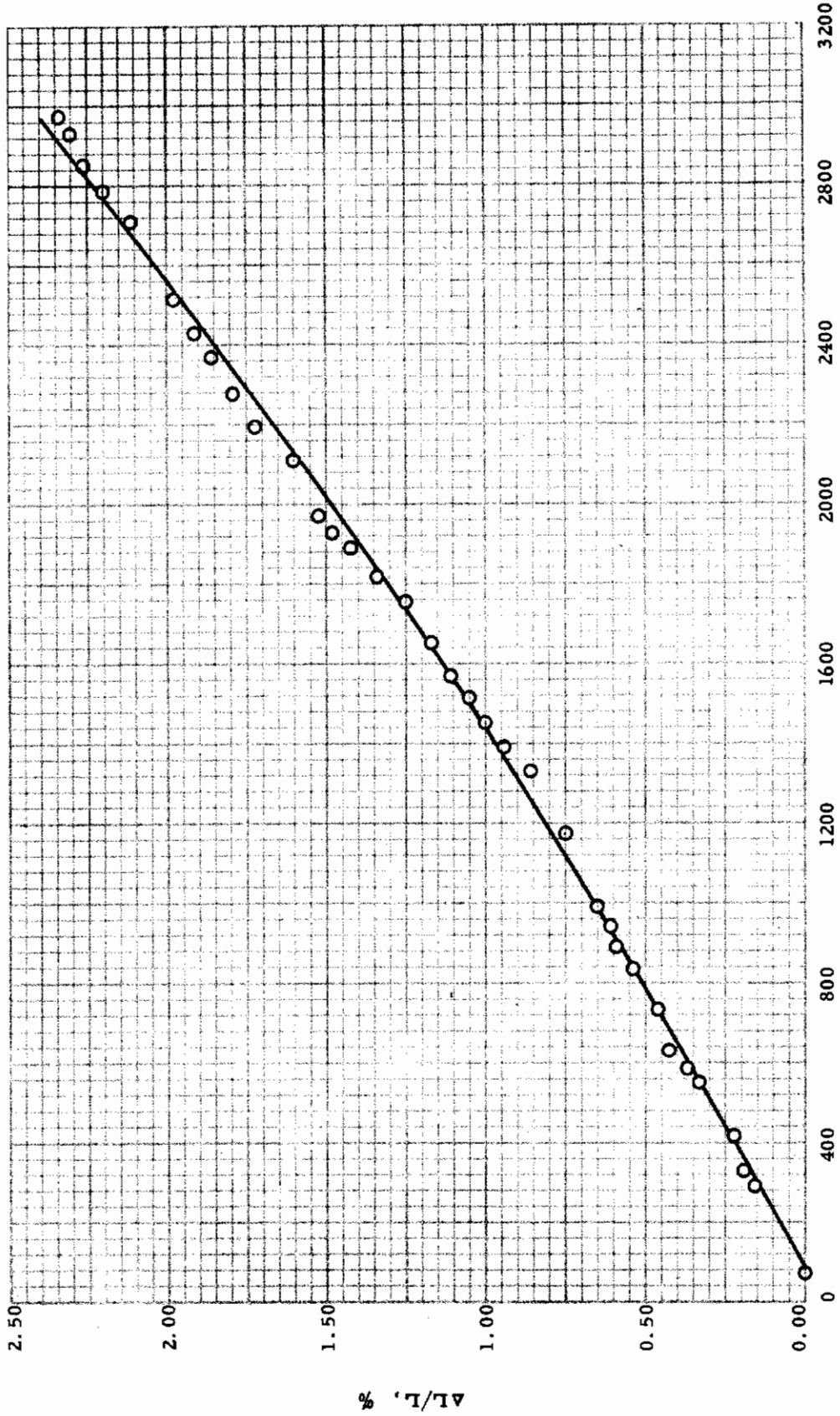

Figure 56 LINEAR THERMAL EXPANSION OF MAGNESIUM OXIDE

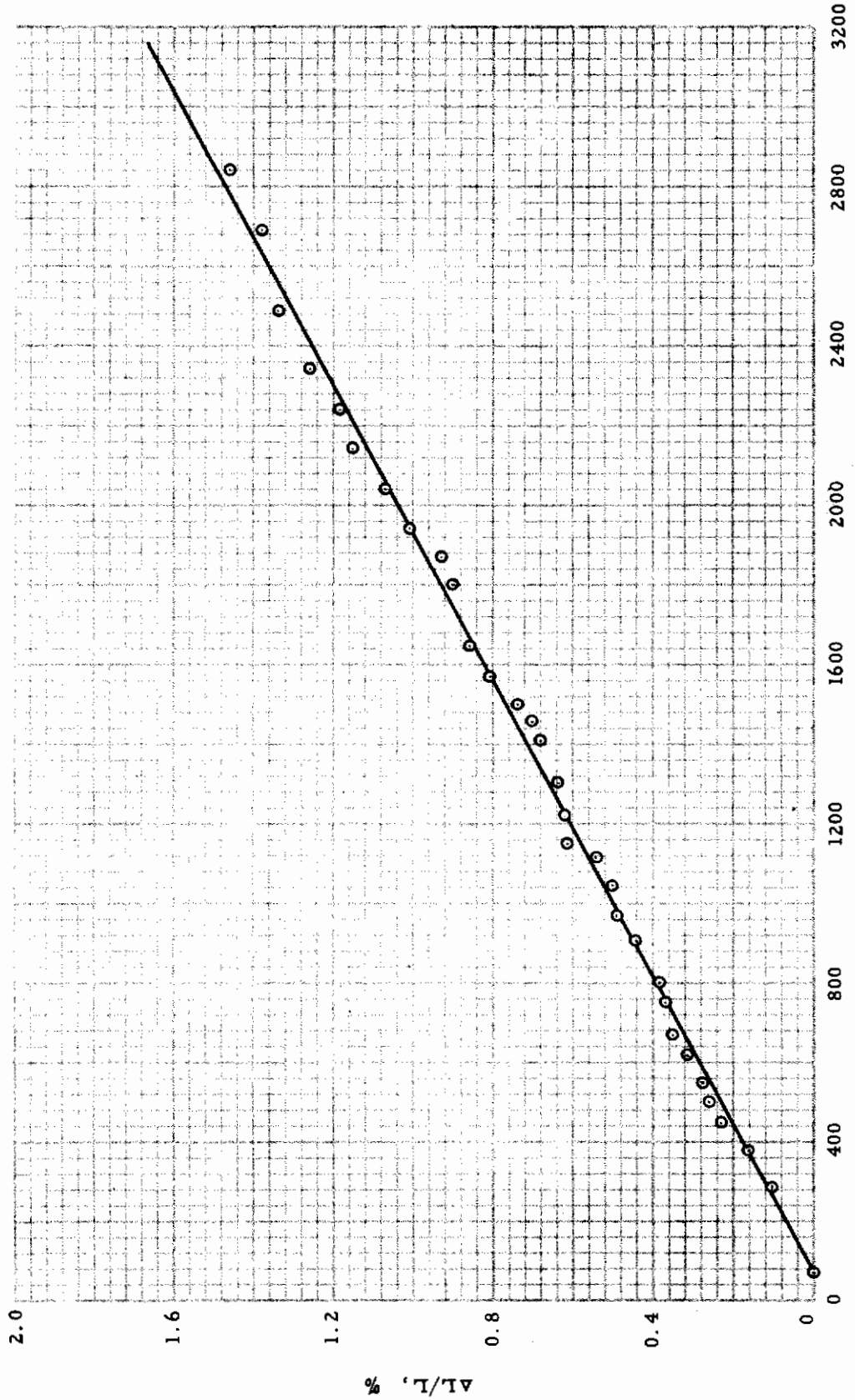

Figure 57 LINEAR THERMAL EXPANSION OF HAFNIUM